Canadian Powder Diffraction Workshop
October 11 – 14, 2022

In-situ diffraction

beatriz.moreno@lightsource.ca

In-situ diffraction motivation

Studying material under working conditions:

1. temperature
2. gas atmosphere
3. pressure
4. stress/strain
5. voltage/current
6. Light
7. …

Provides information on the chemical and physical properties of materials and devices under realistic processing conditions

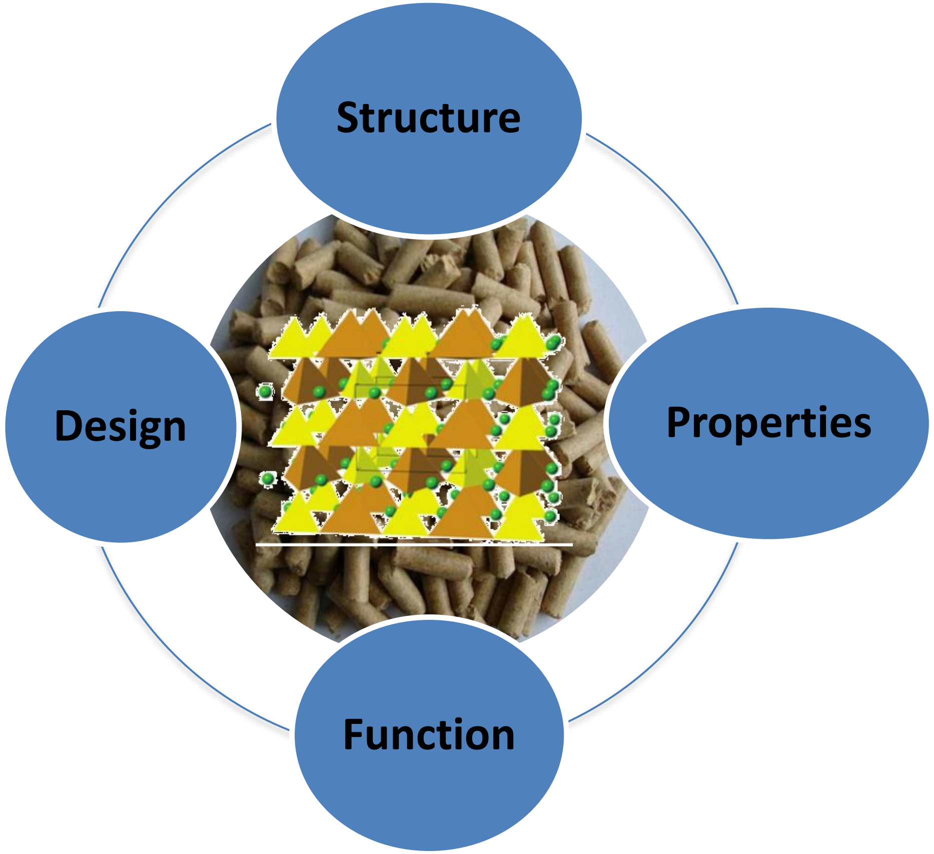

Applications:

- Microelectronics
- batteries and fuel cells
- catalysis
- solar cells
- materials under extreme conditions
- cement
- and many others!

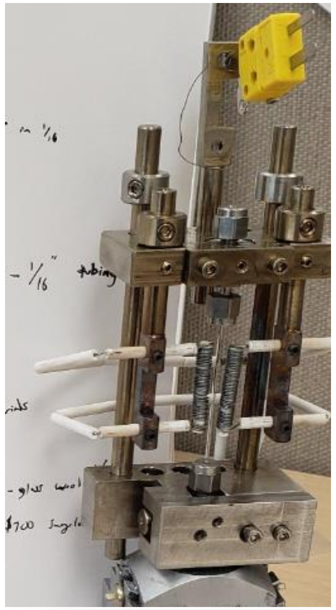

(e)

Sample environments

Sample environments seek to mimic the operation conditions of the materials or devices being tested

- Furnaces with controlled atmosphere and temperature
- Tensile rigs
- Temperature/humidity light chambers
- in situ cycling / temperature control for battery studies
- Customized setups

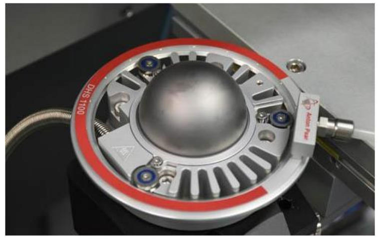

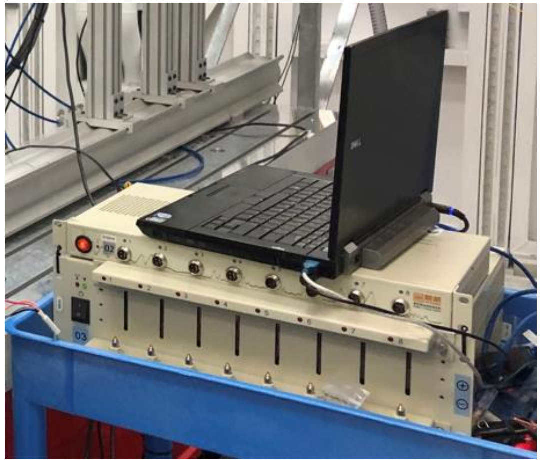

beatriz.moreno@lightsource.ca

Contents:

1. Phase transitions
2. Microelectronics
3. Batteries
4. Solar cells
5. Mechanical rigs
6. Catalysts
7. Corrosion
8. High pressure

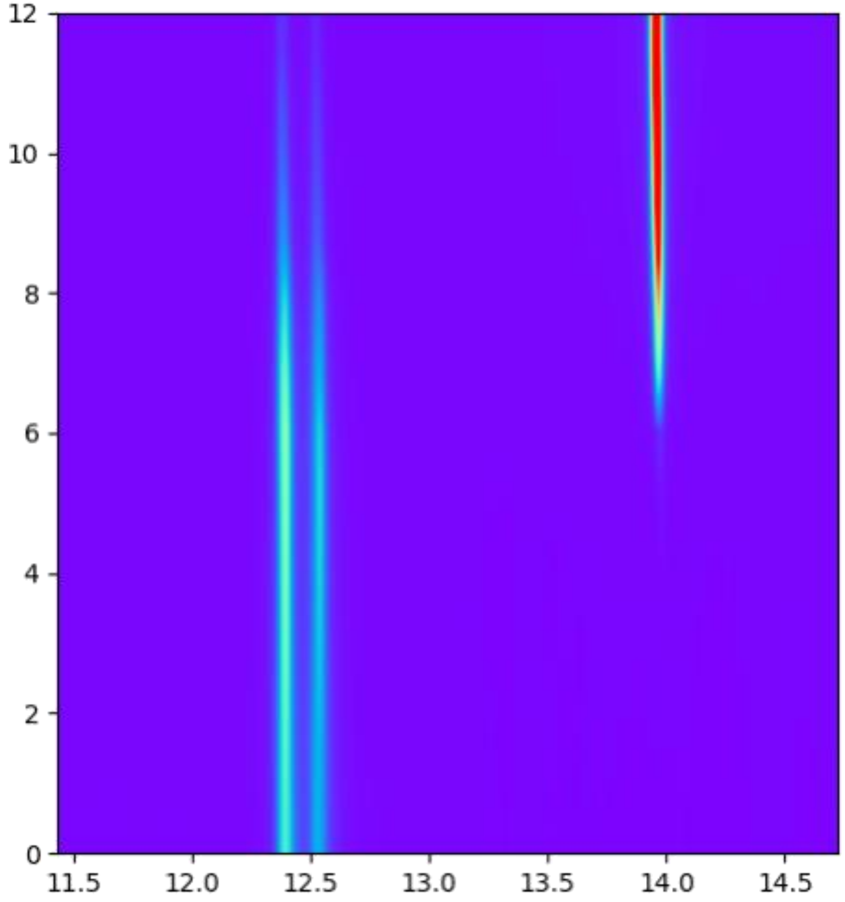

beatriz.moreno@lightsource.ca

Applications – Structural phase transitions

Orthorhombic α – *KNO_3* to trigonal β - *KNO_3 phase transition*

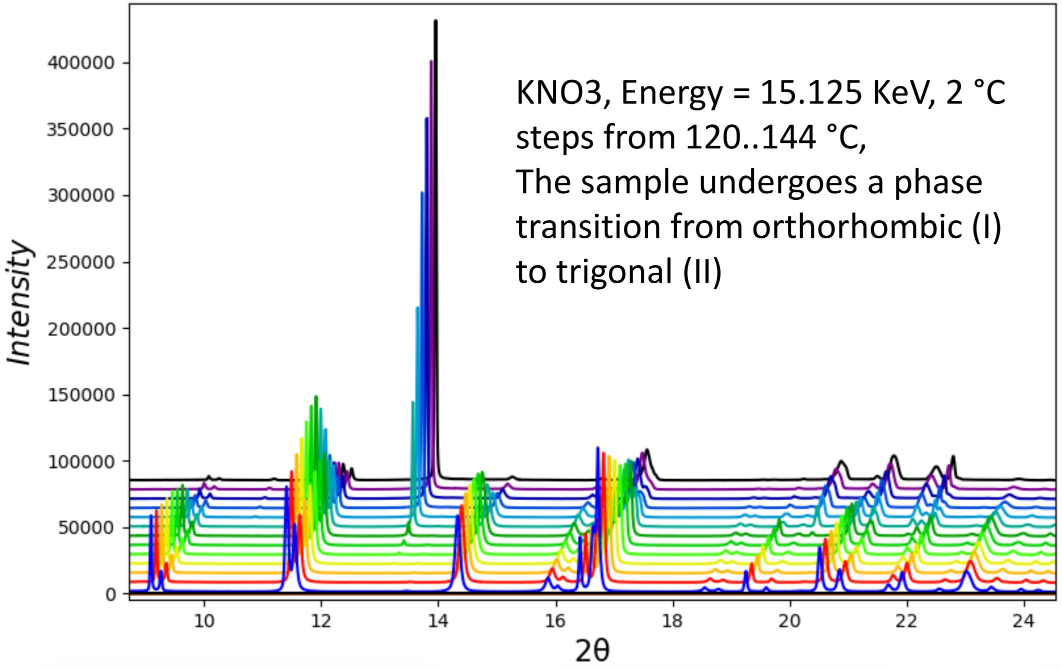

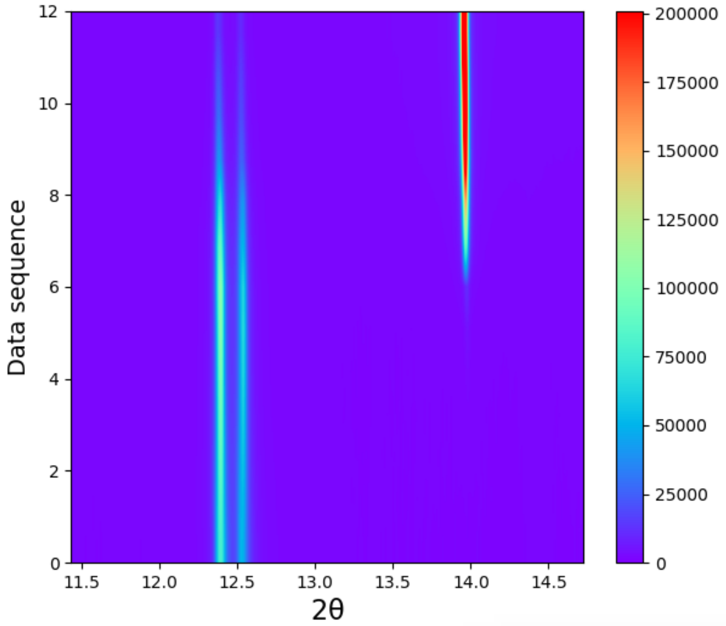

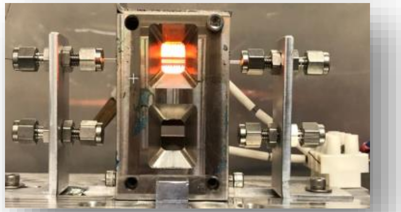

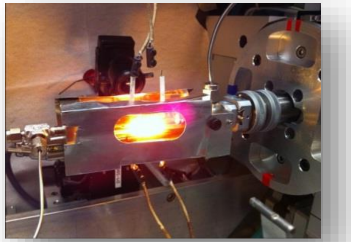

High entropy alloys phase transitions

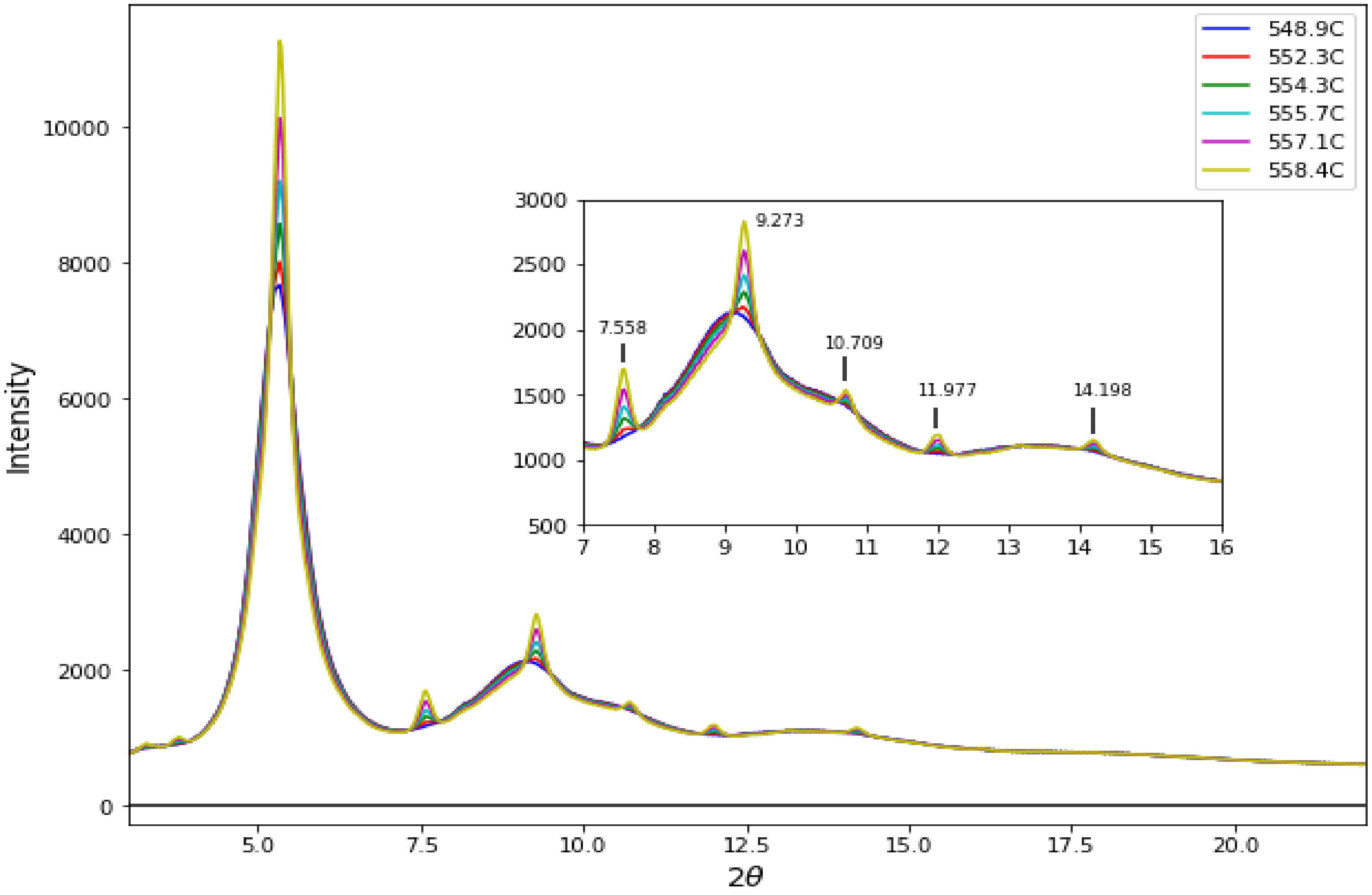

Applications to Microelectronics

beatriz.moreno@lightsource.ca

IBM end-station

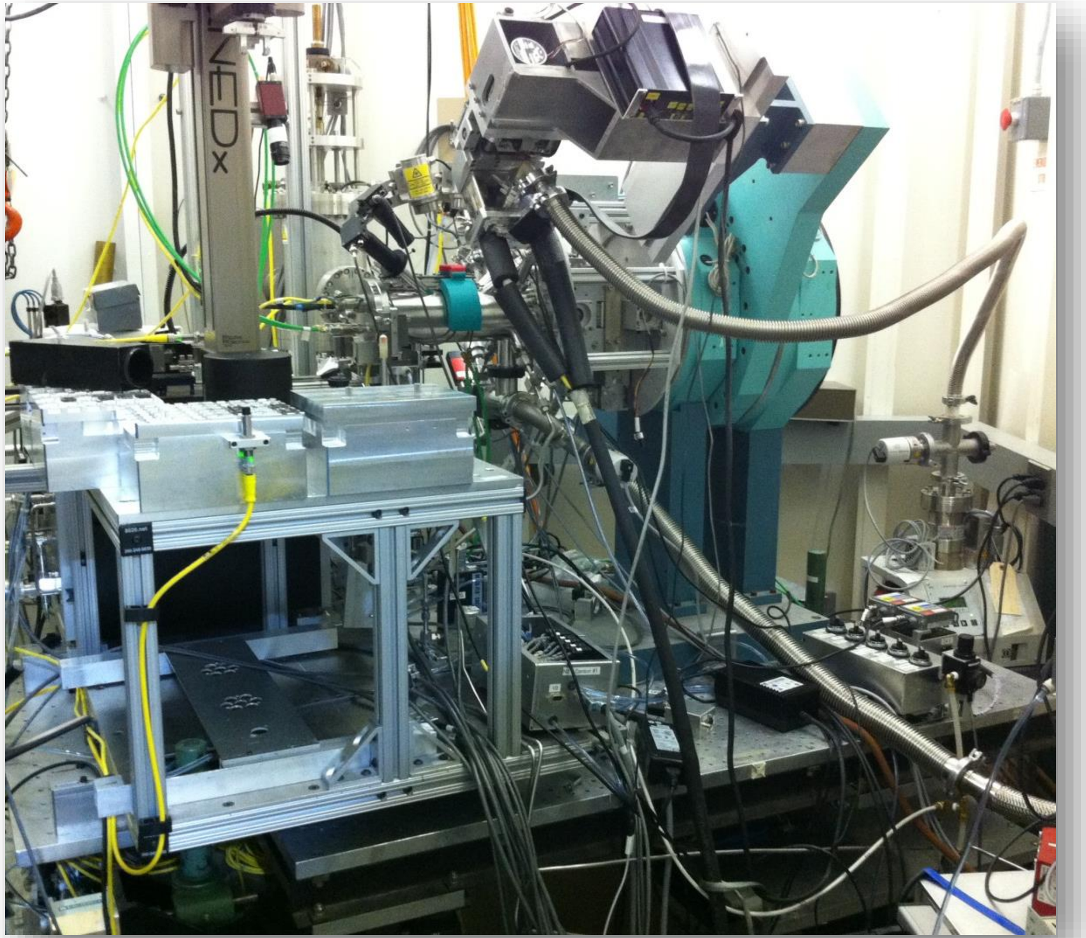

- **In-situ characterization**
  - thin films
  - microelectronic materials
  - semiconductors
- **Rapid thermal annealing (up to ~ 1100ºC)**

Techniques

✓ X-Ray diffraction

✓ Four point probe to measure film resistivity

✓ Optical light scattering to measure surface morphology

beatriz.moreno@lightsource.ca

IBM end-station

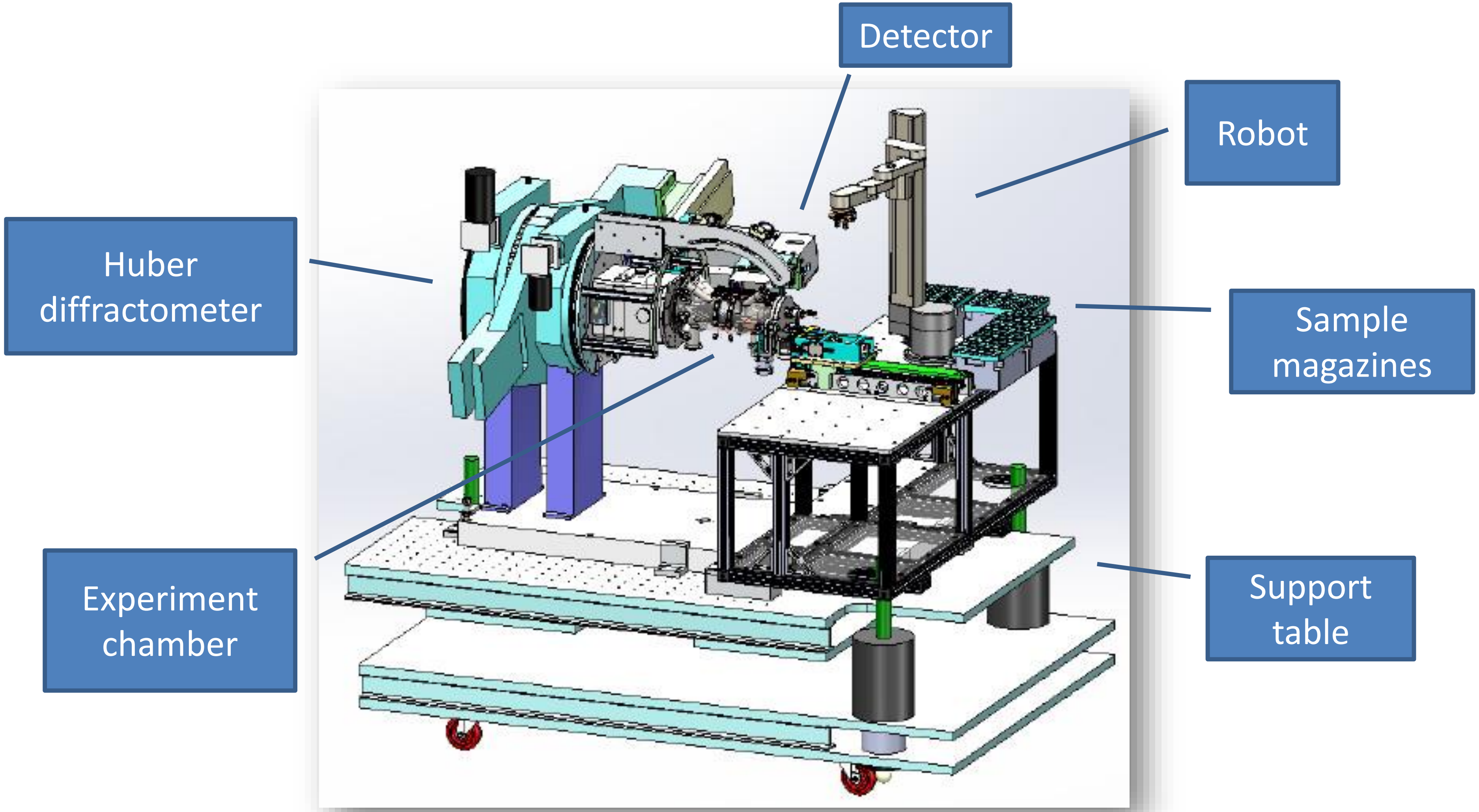

beatriz.moreno@lightsource.ca

Experiment chamber

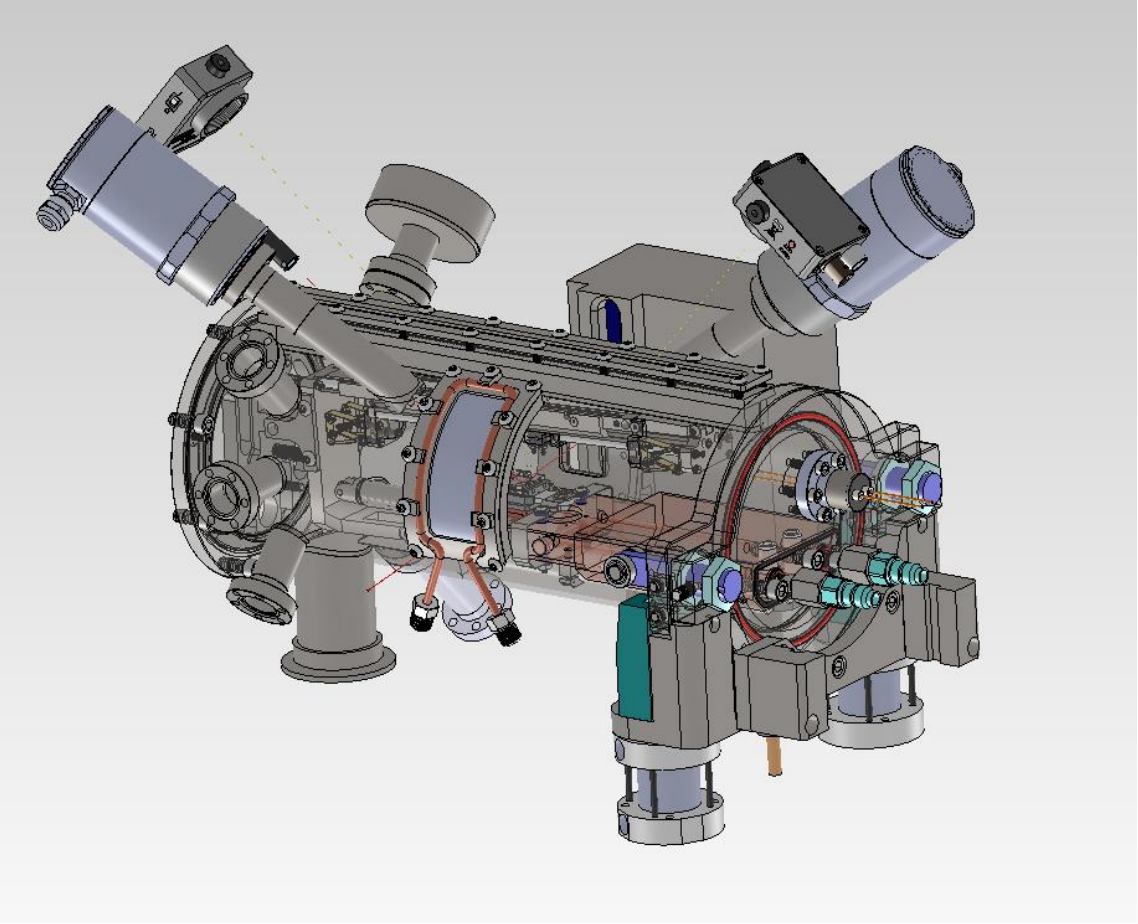

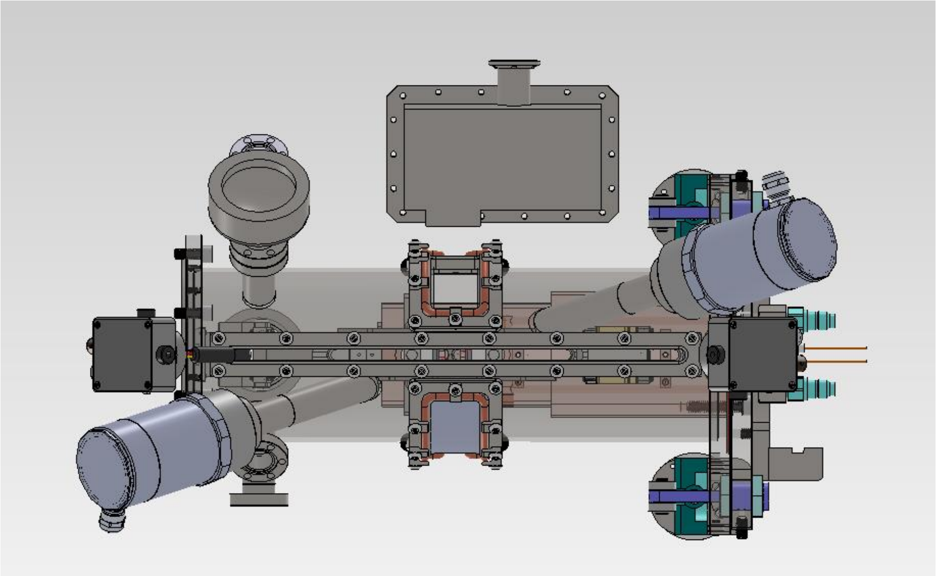

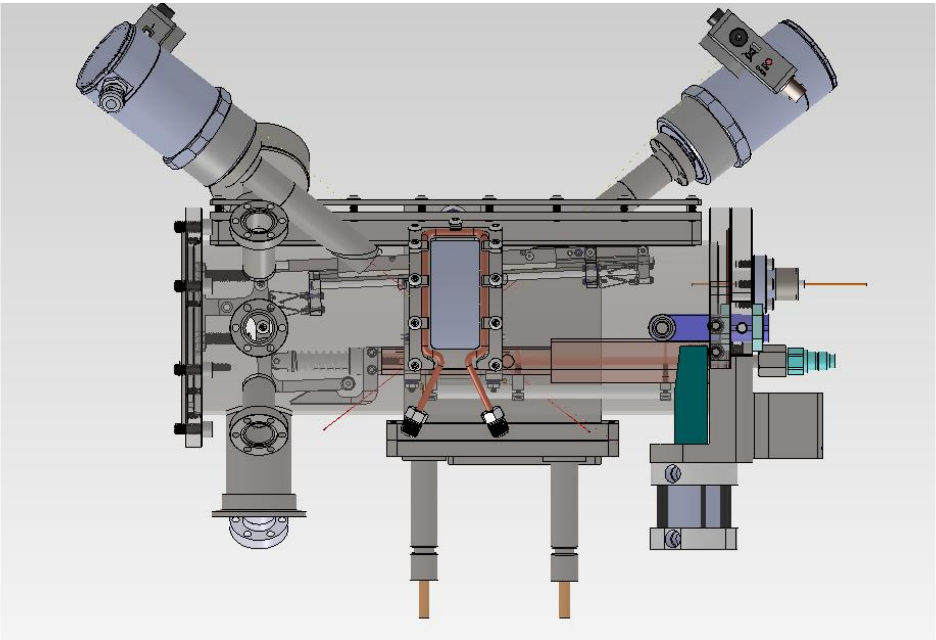

Experiment chamber

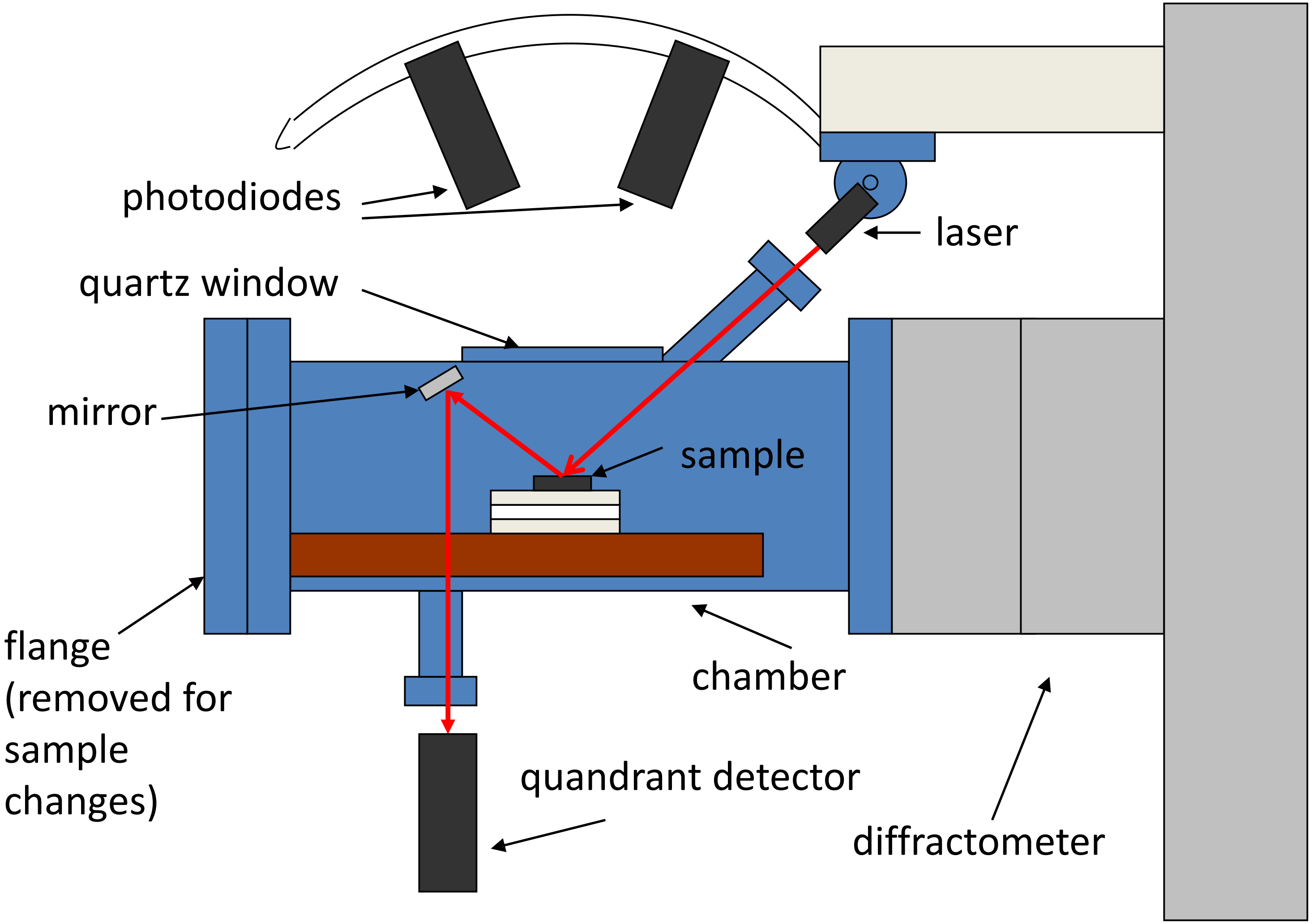

beatriz.moreno@lightsource.ca

Sample size and format

IBM end-station

Thin films studies

Combined diffraction,
resistivity and roughness measurements
under ultra high purity N_2 or He.
Temperature up to 1100 ºC.

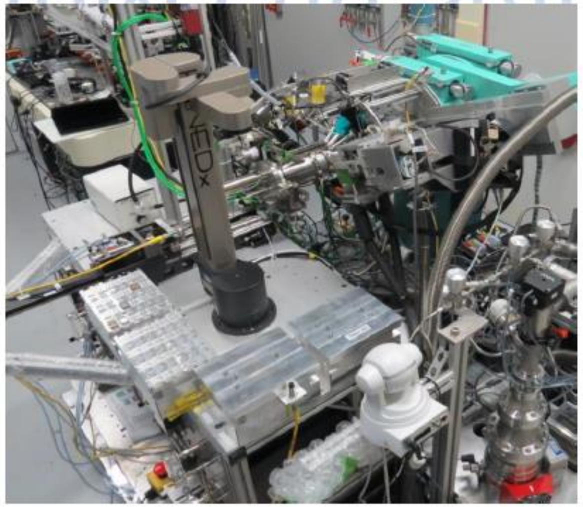

Molybdenum sample holder

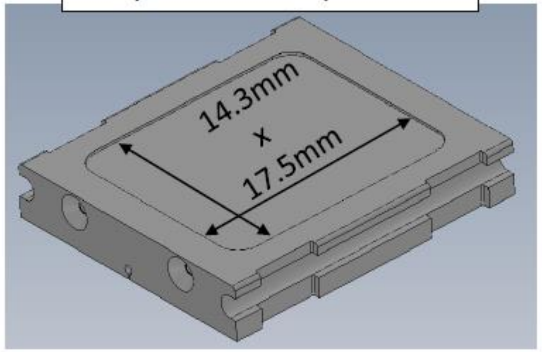

Sample size should be
approximately 12mm x 15 mm

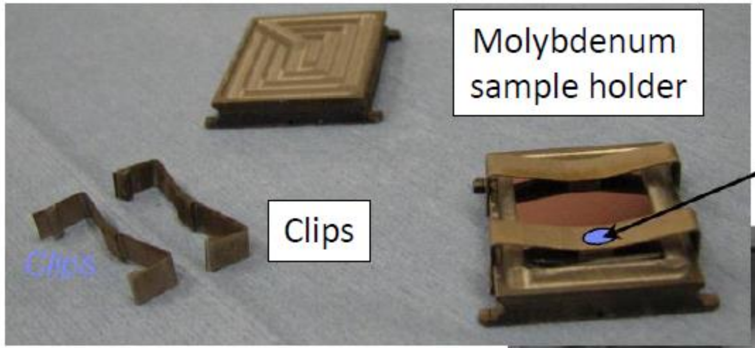

Molybdenum
sample holder

Clips

Pyrometer reads
from here

Sample holder on top of the heater

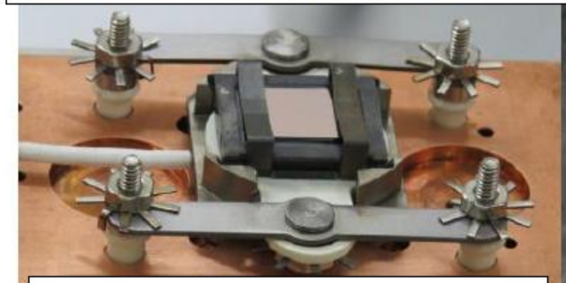

Maximum temperature: 1100ºC

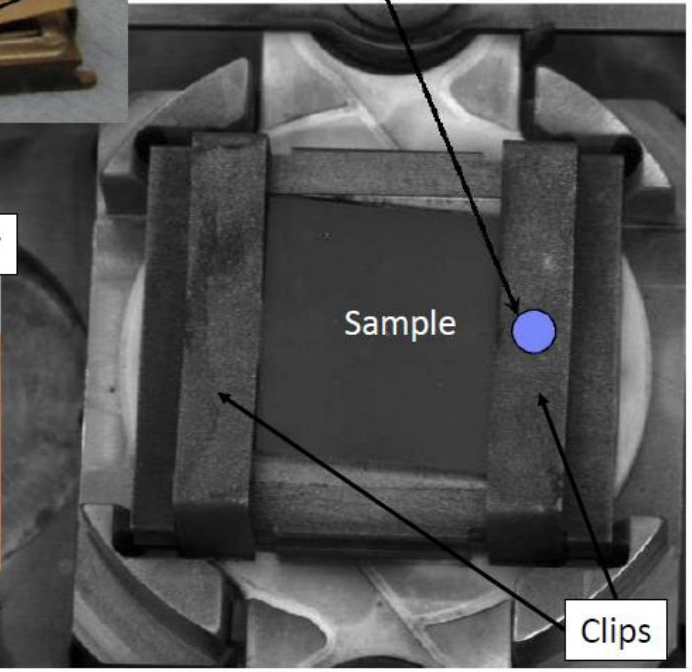

Clips

IBM end-station in action

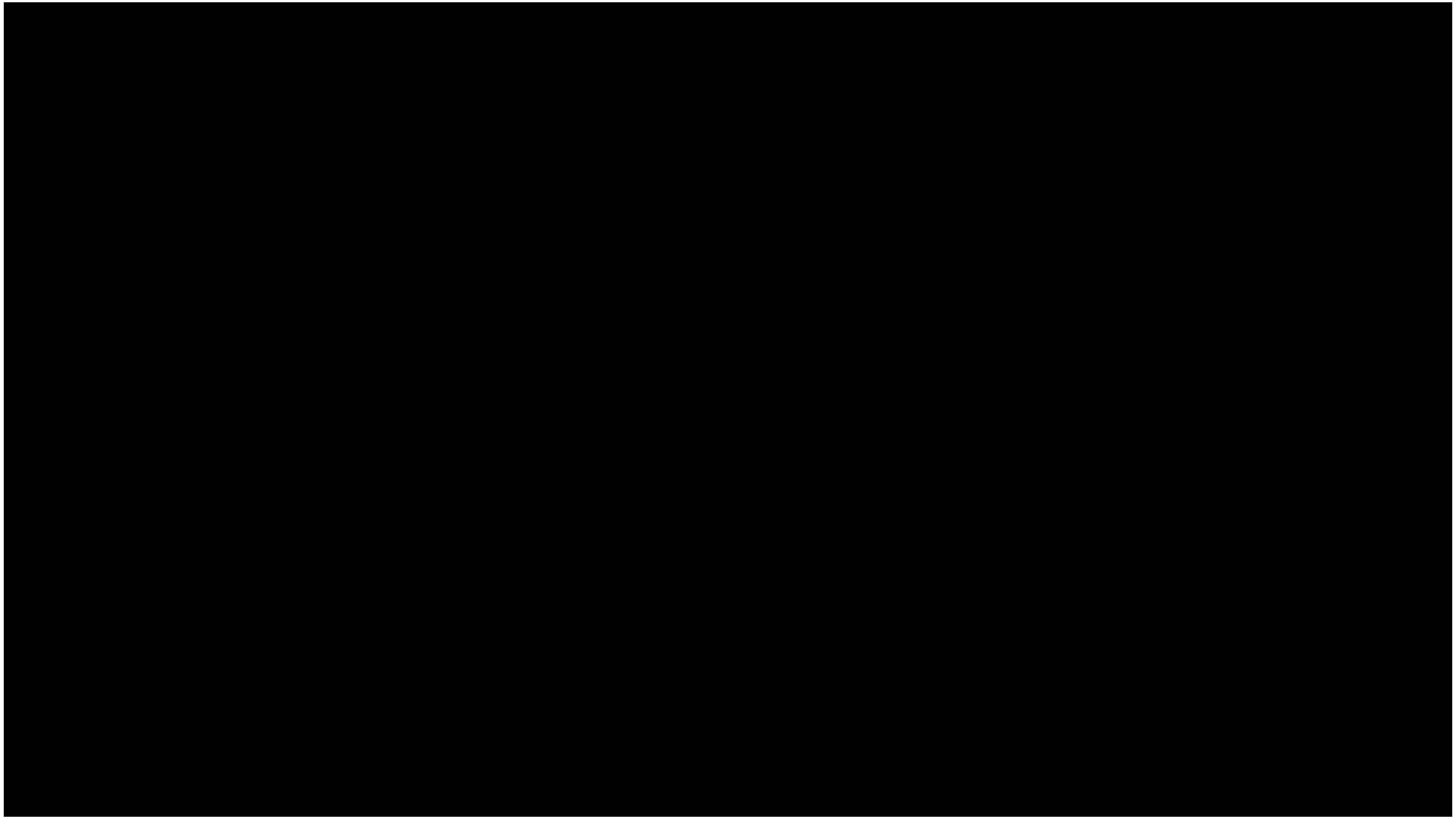

beatriz.moreno@lightsource.ca

Atomic layer deposited ultrathin metal nitride barrier layers for ruthenium interconnect applications. Sonal Dey et al.

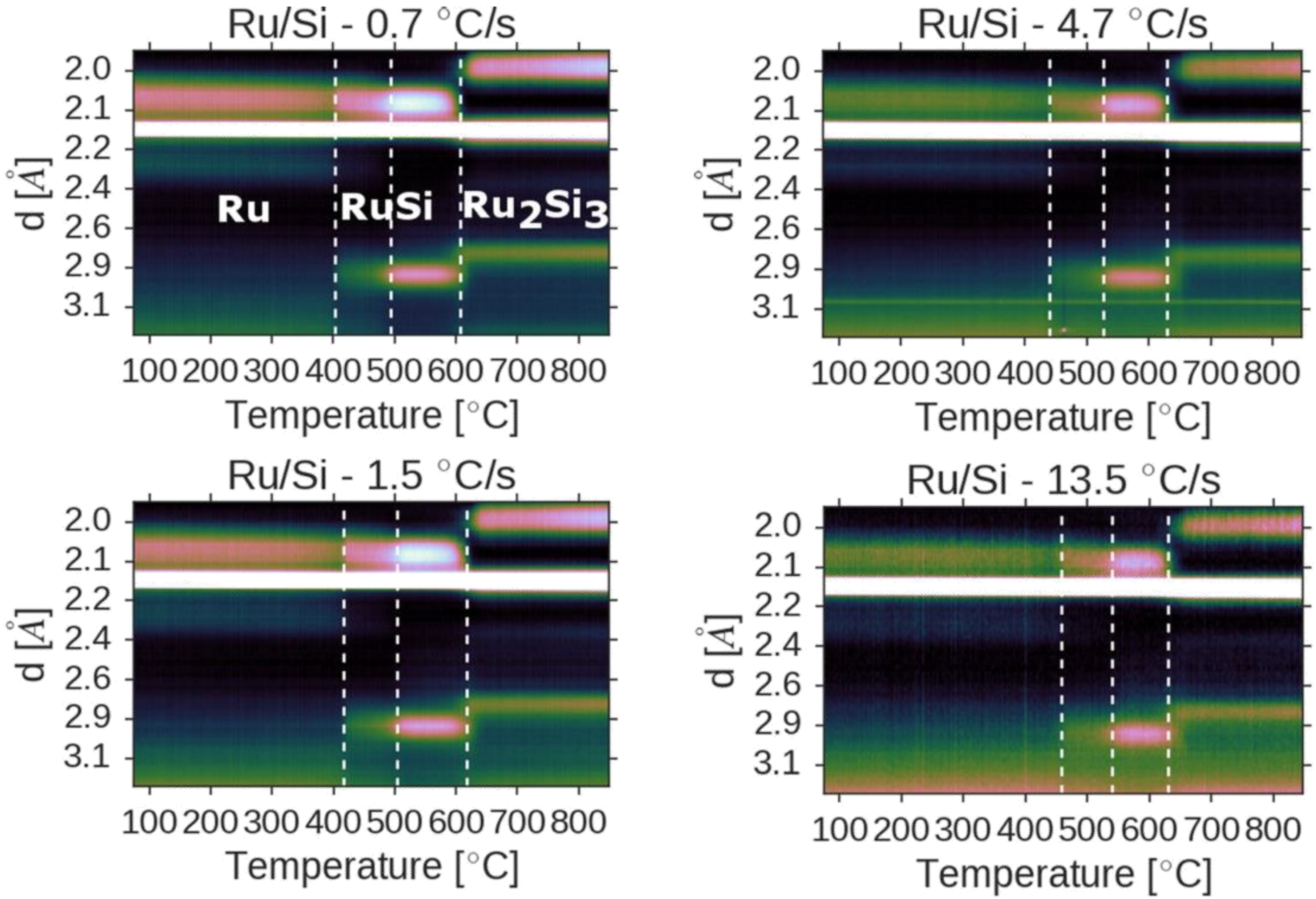

Journal of Vacuum Science & Technology A **35**, 03E109 (2017)

IBM end-station

- ✓ Quick investigation of different growth conditions
- ✓ Better nucleation processes
- ✓ Improved film stability at higher temperatures
- ✓ Lower interface roughness

Effects of additive elements on the phase formation and morphological stability of nickel monosilicide films

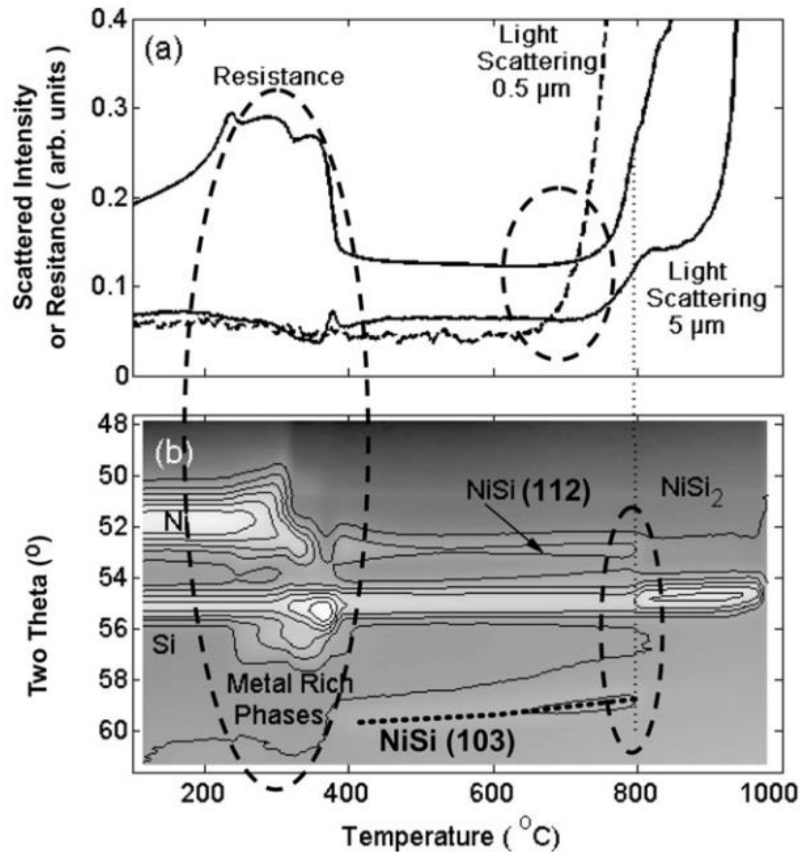

Fig. 4. (a) Elastic light scattering at 0.5 μm and 5 μm length scales and resistance measurements together with (b) X-ray diffraction measurements performed *in situ* during annealing in purified He of a 15 nm Ni layer deposited on a 100 nm poly-Si film (3 °C /s). The three ellipse also refer to the challenges discussed using the phase diagram in Fig. 1.

Microelectronic Engineering **83**, 2042-2054 (2006)
C. Lavoie et al.

IBM end-station

Crystallization properties of materials along the pseudo-binary line between GeTe and Sb

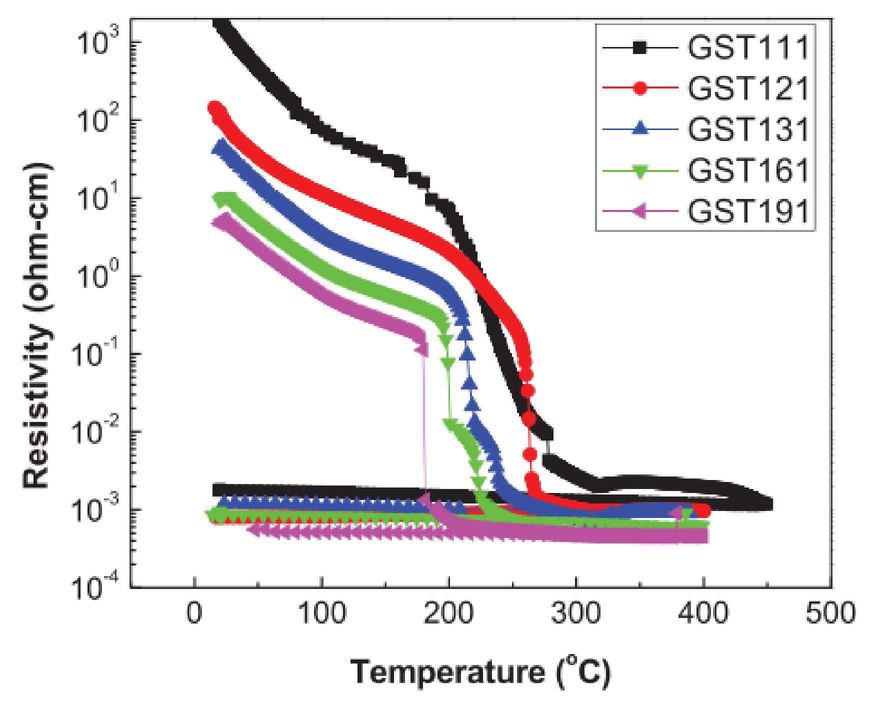

Resistivity as a function of temperature for $Ge_1Sb_xTe_1$ films for $x > 1$ during a heating ramp to 300–450 °C at 5 °C/min and subsequent cooling back to room temperature.

Journal of Applied Physics **115**, 093101 (2014)
Huai-Yu Cheng et al.

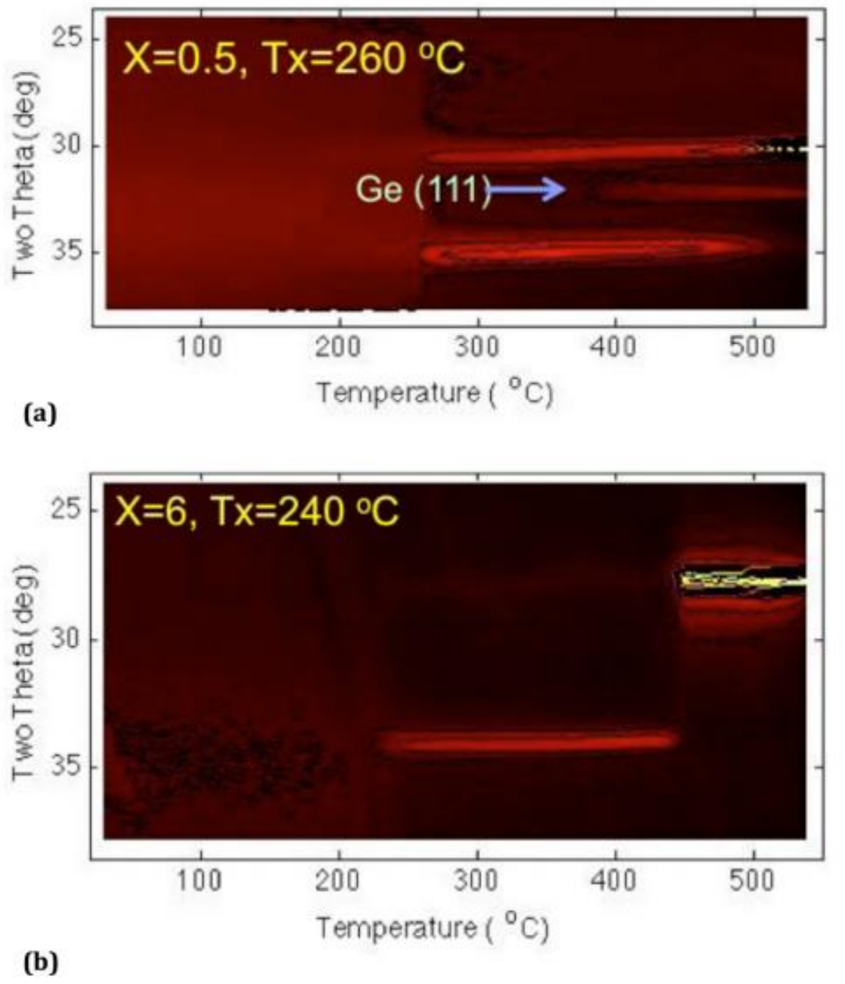

FIG. 2. XRD peak intensity as a function of temperature T during heating at 3 °C/s to 550 °C of a $Ge_1Sb_xTe_1$ film with (a) $x = 0.5$ and (b) $x = 6$, respectively.

IBM end-station

Crystallization properties of materials along the pseudo-binary line between GeTe and Sb

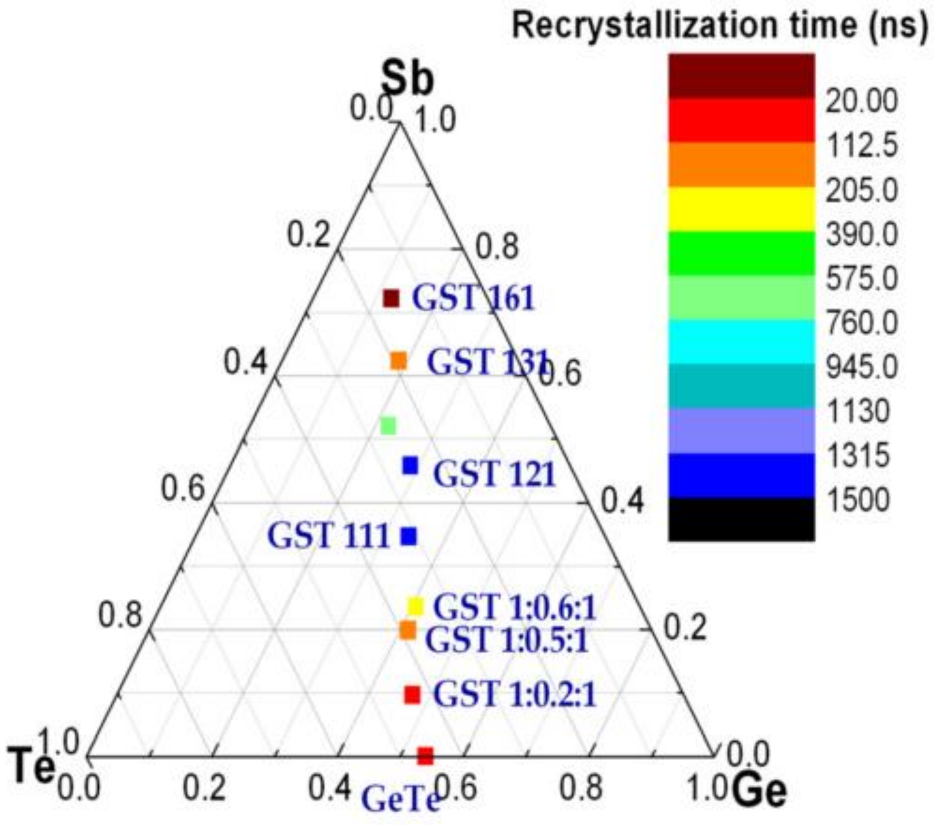

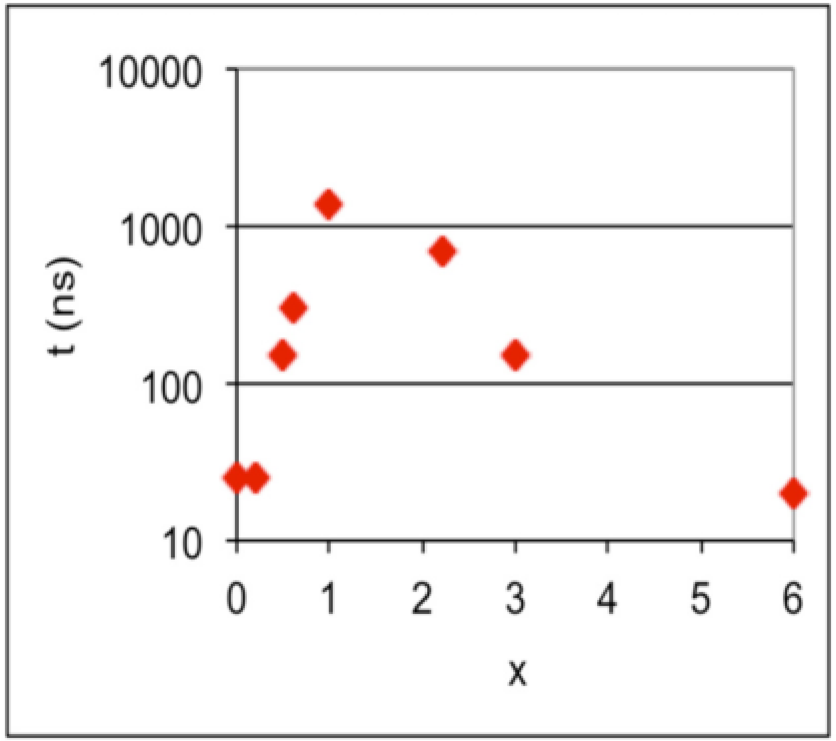

Journal of Applied Physics **115**, 093101 (2014)
Huai-Yu Cheng et al.

Battery experiments

In-situ battery research

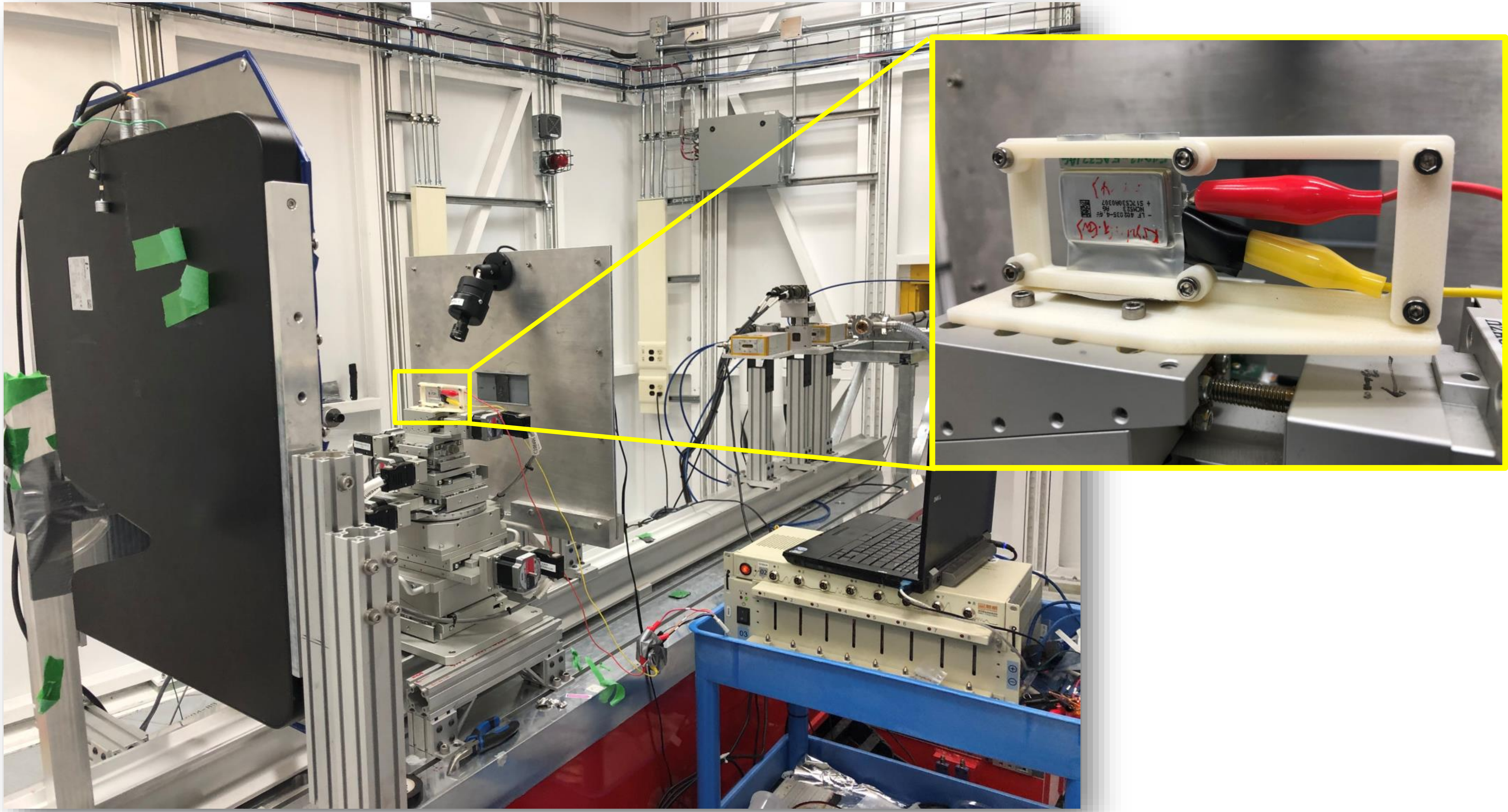

beatriz.moreno@lightsource.ca

In-situ battery research

Anode (Graphite)

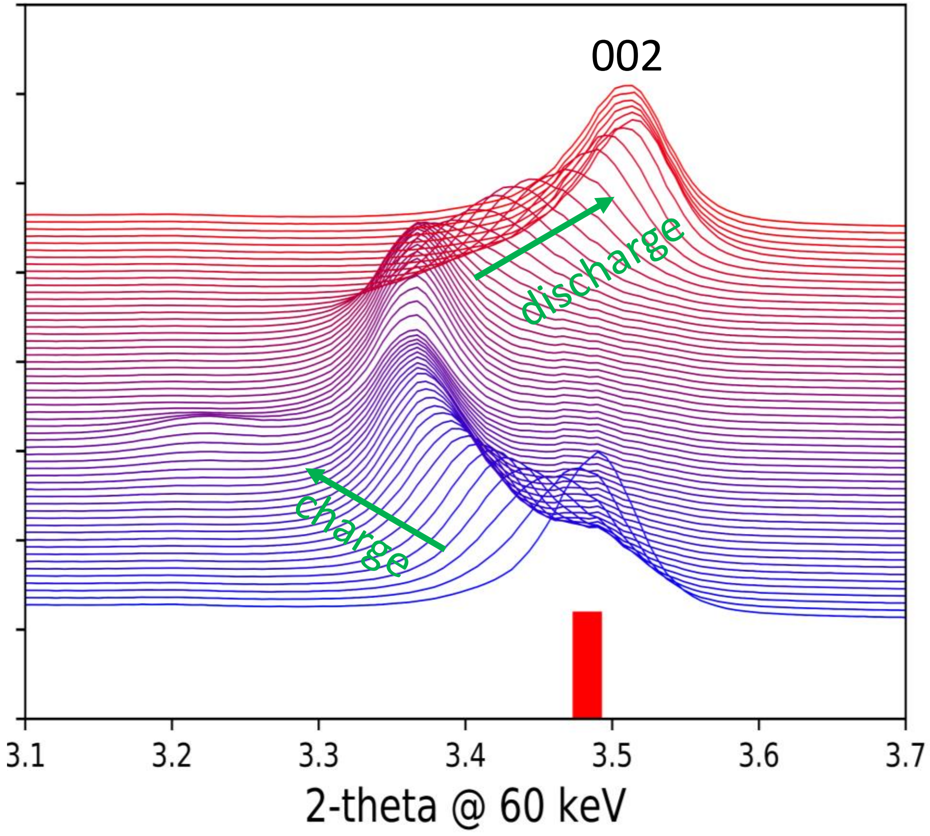

Cathode (Transition Metal Oxide)

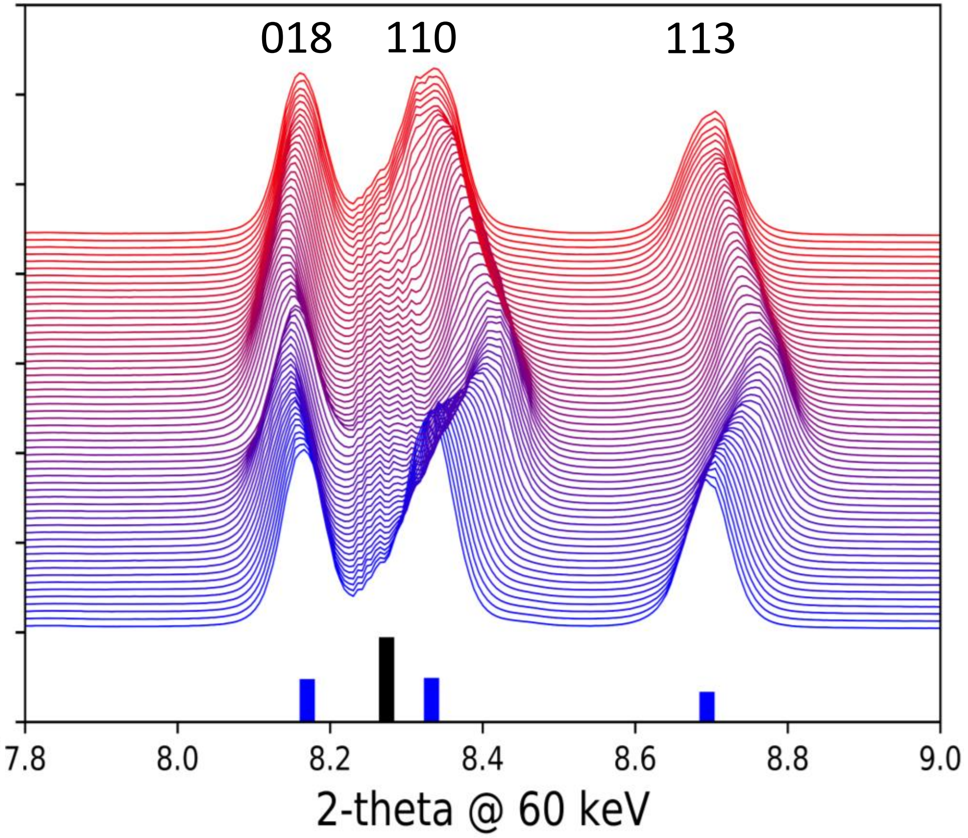

beatriz.moreno@lightsource.ca

In-situ battery research

High Temperature Compatible Conflat Cell with Adjustable Stack Pressure for In-Situ and Operando X-Ray Studies of Lithium-Ion Battery Materials

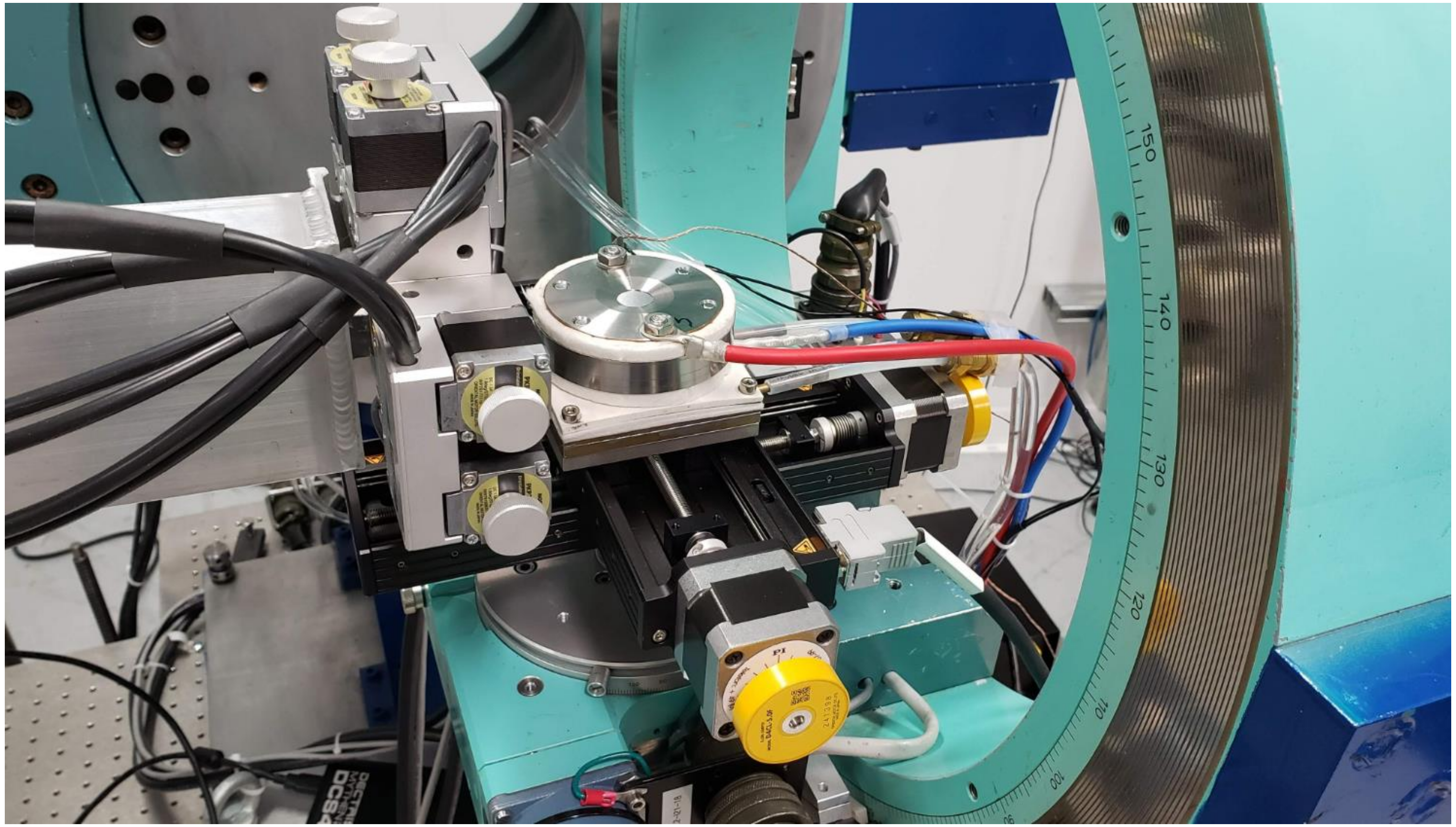

Michael Fleischauer - NRC / University of Alberta

In-situ battery research

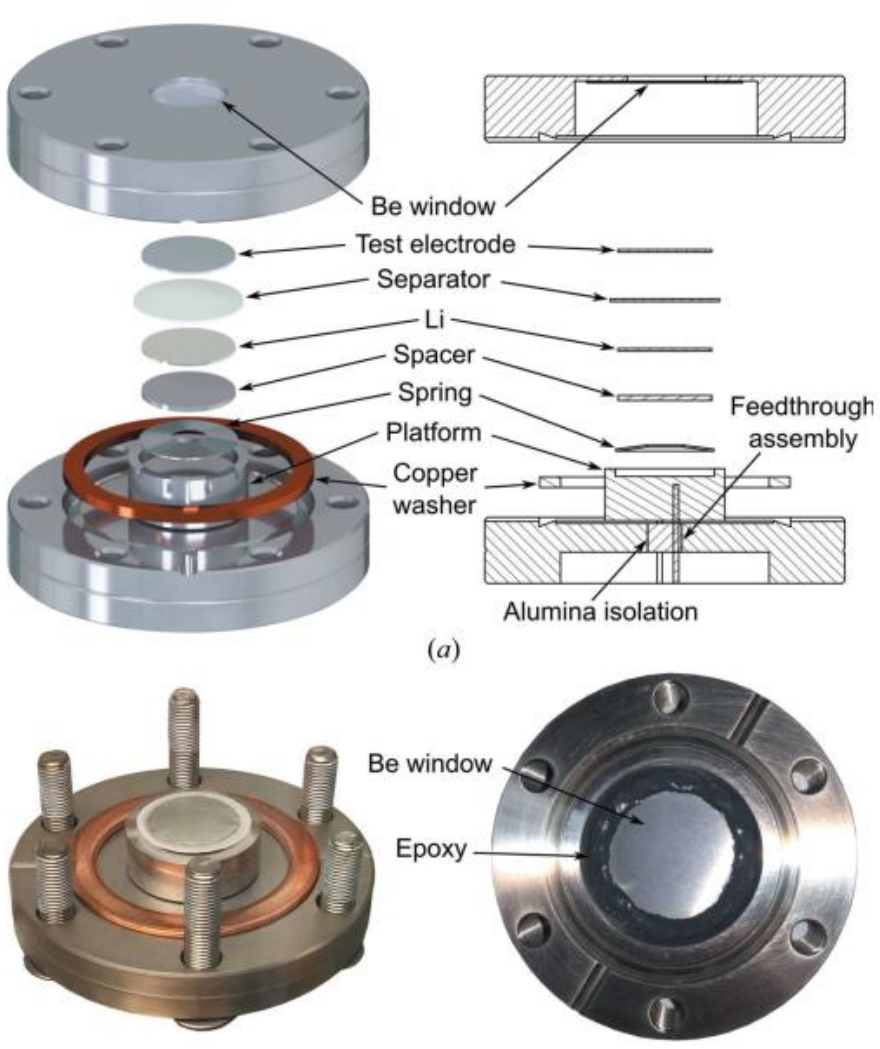

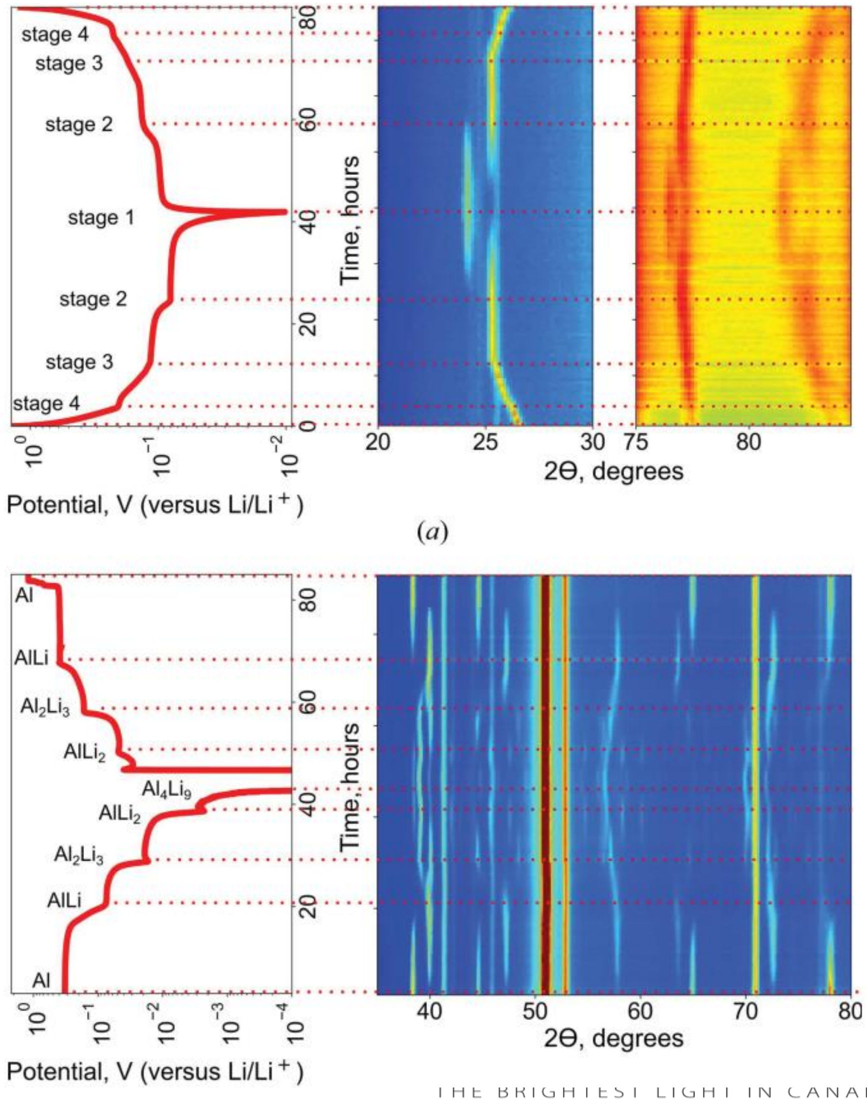

Capturing metastable structures during high-rate cycling of $LiFePO_4$ nanoparticle electrodes

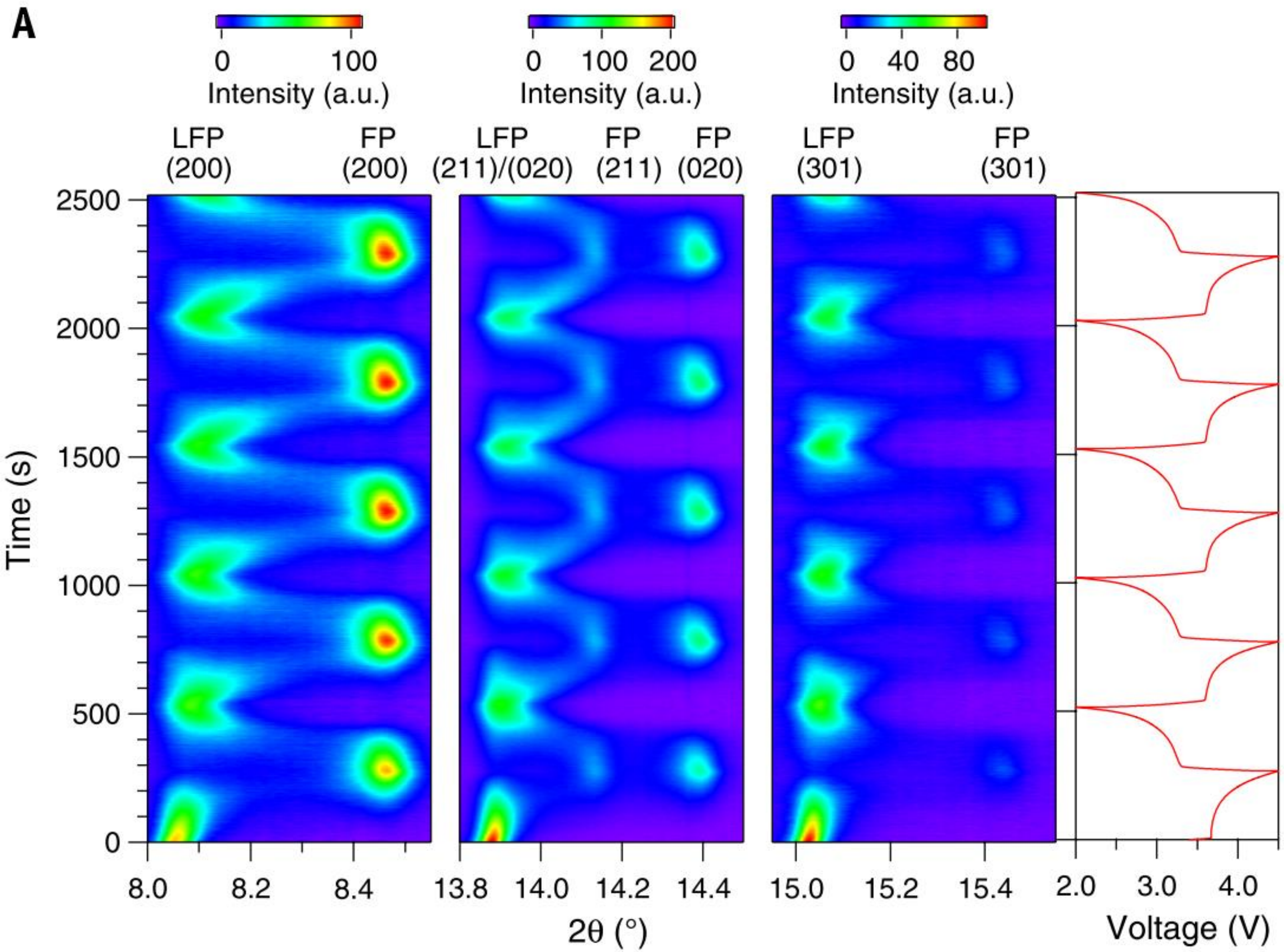

Liu et al.
Science **344**(6191): 1252817

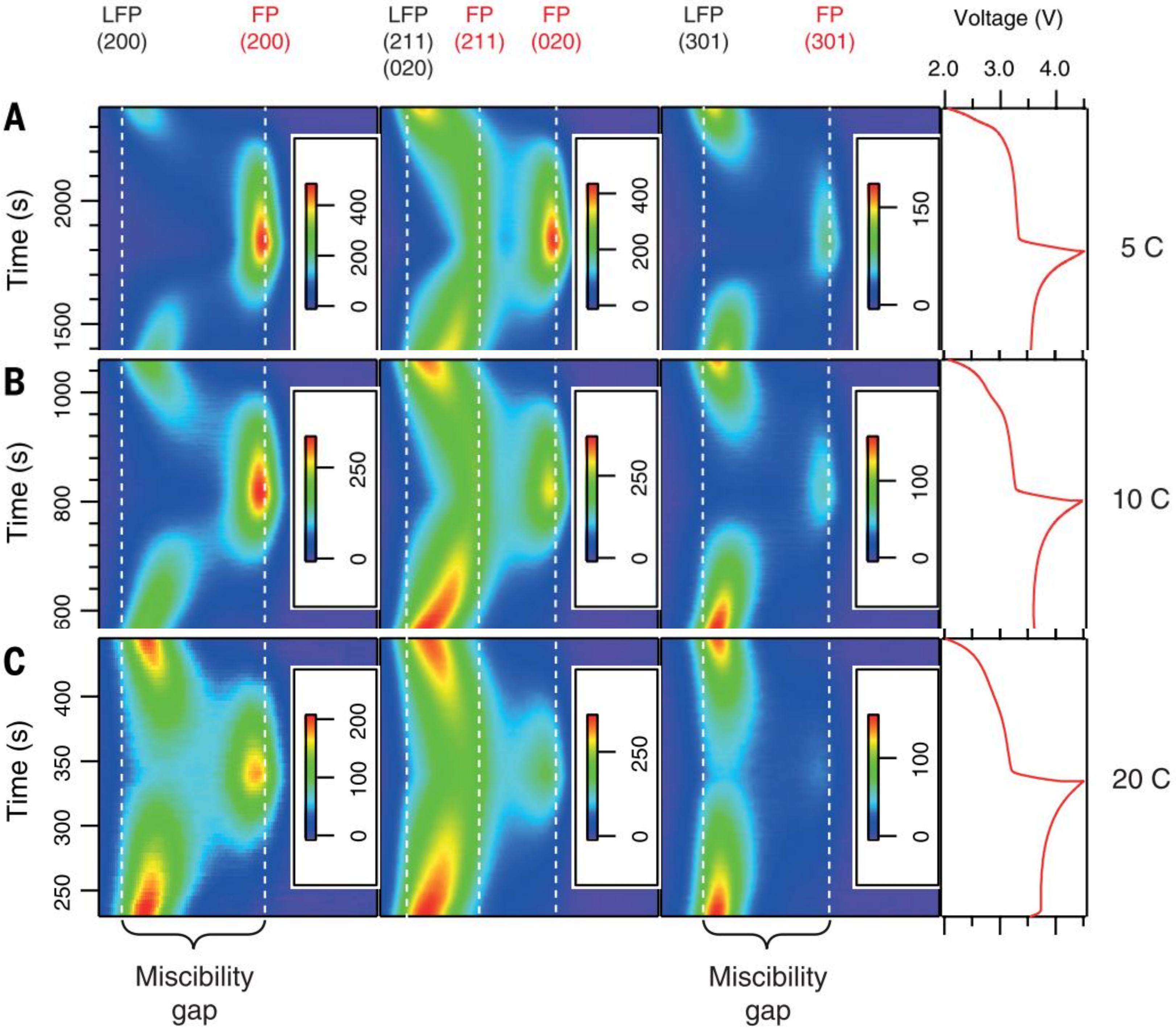

LFP (200)
FP (200)
LFP (211) (020)
FP (211)
FP (020)
LFP (301)
FP (301)
Voltage (V)
2.0 3.0 4.0
A
B
C
Time (s)
5 C
10 C
20 C
Miscibility gap
Miscibility gap

Capturing metastable structures during high-rate cycling of $LiFePO_4$ nanoparticle electrodes

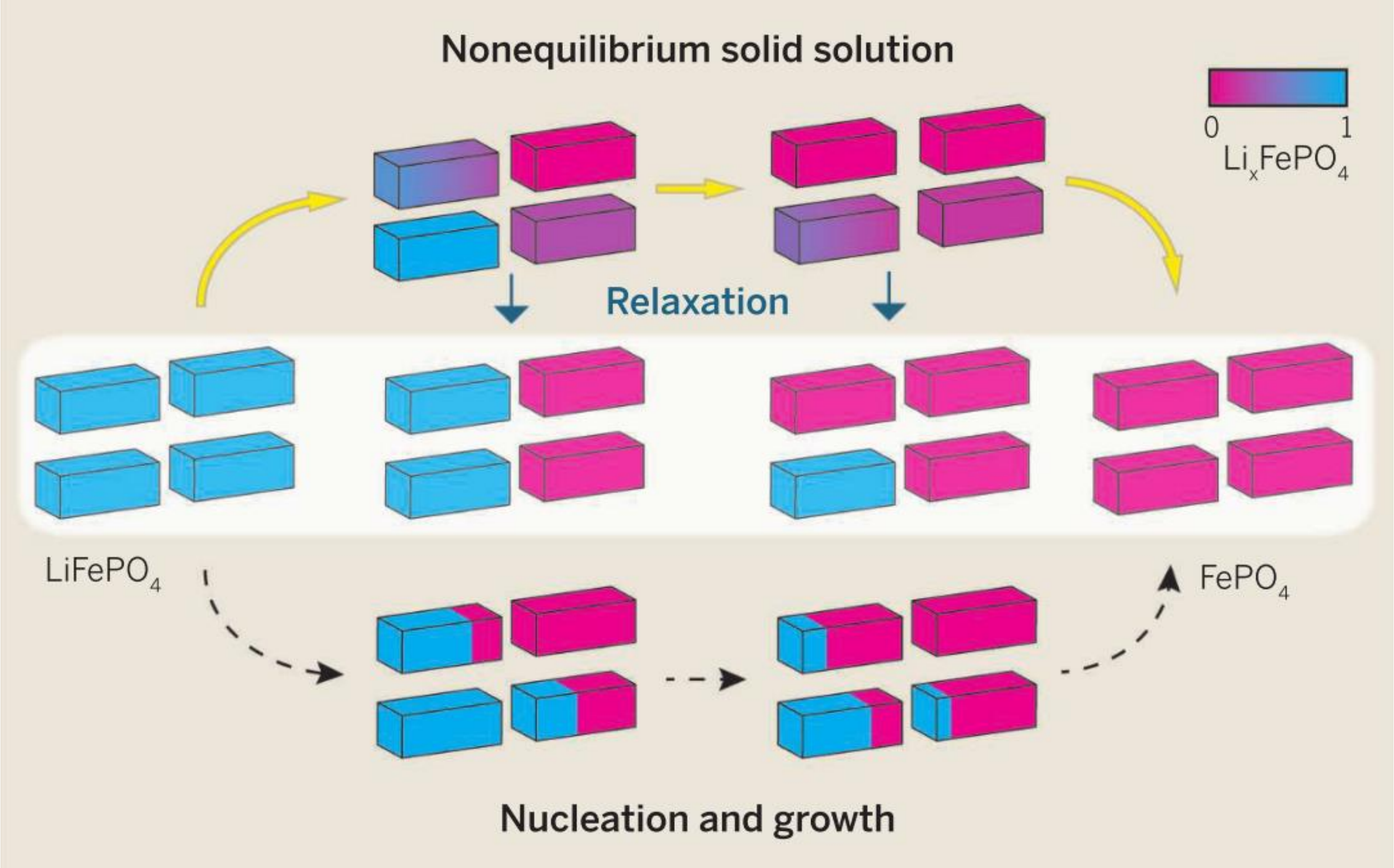

Liu et al. Science **344**(6191): 1252817

Solar cell research

In situ studies of the degradation mechanisms of perovskite solar cells

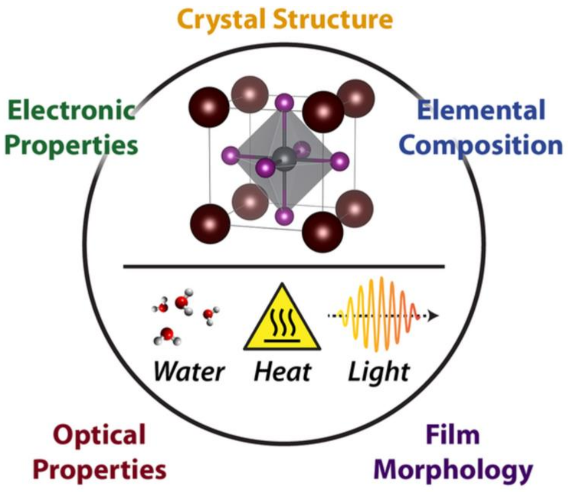

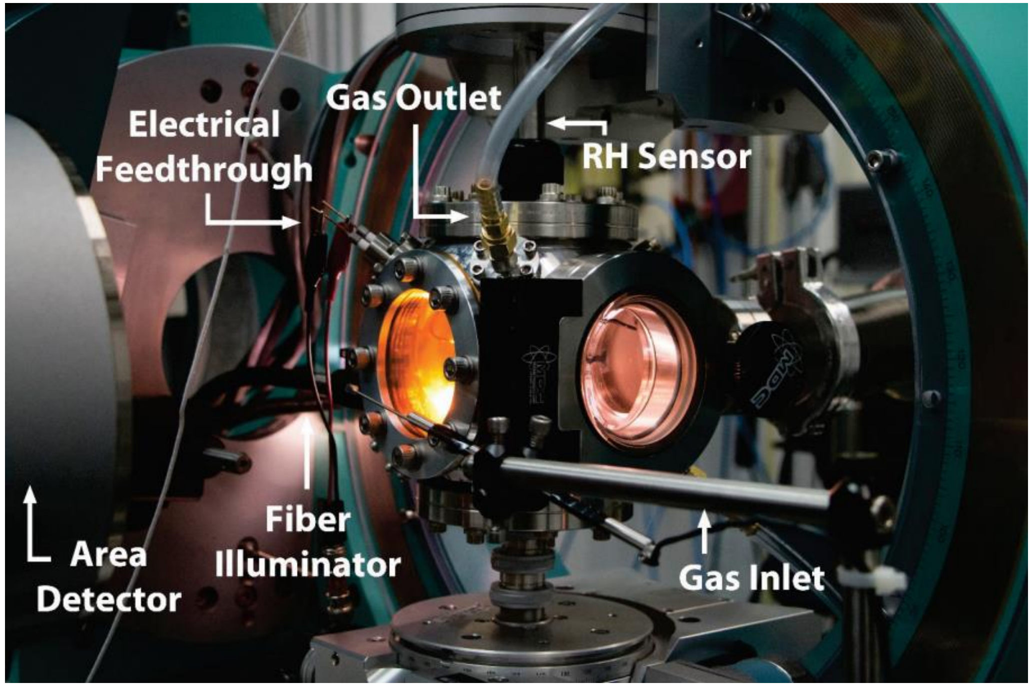

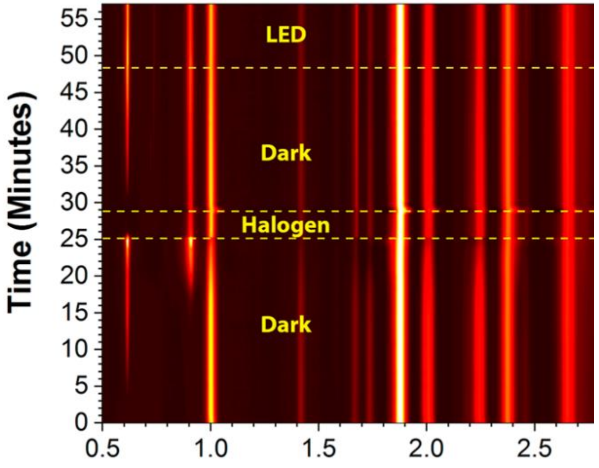

GIWAXS pattern of an ITO/ZnO/$CH_3NH_3PbI_3$/P3HT/Ag device exposed to a nitrogen atmosphere with RH ≈ 90%.

Elucidating the Failure Mechanisms of Perovskite Solar Cells in Humid Environments Using In Situ GI-WAXS

Tim Kelly - USASK

Corrosion studies

Corrosion can lead to failure involving personal injuries, fatalities, unscheduled shutdowns and environmental contamination

- One 2003 study estimated that the total annual direct and indirect **impact of corrosion** on the Canadian economy had a staggering $46.4 billion price tag.
- That's roughly 2.5 % of Canada's gross domestic product.

In situ studies of breakaway oxidation in type 430 stainless steel

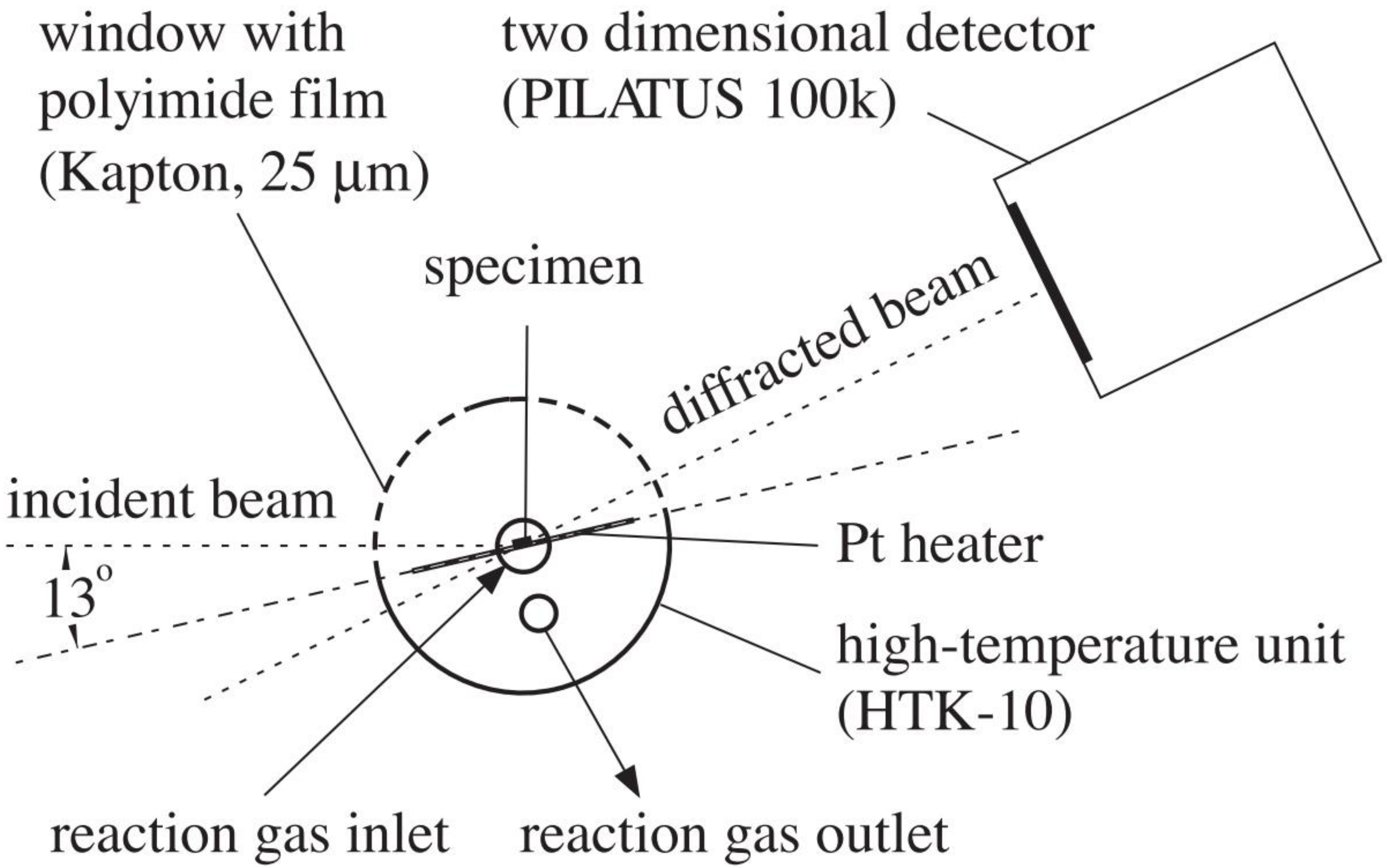

BL-46XU in SPring-8

Saeki et al. Corrosion Science ***55****, 219, 2012*

In situ studies of breakaway oxidation in type 430 stainless steel

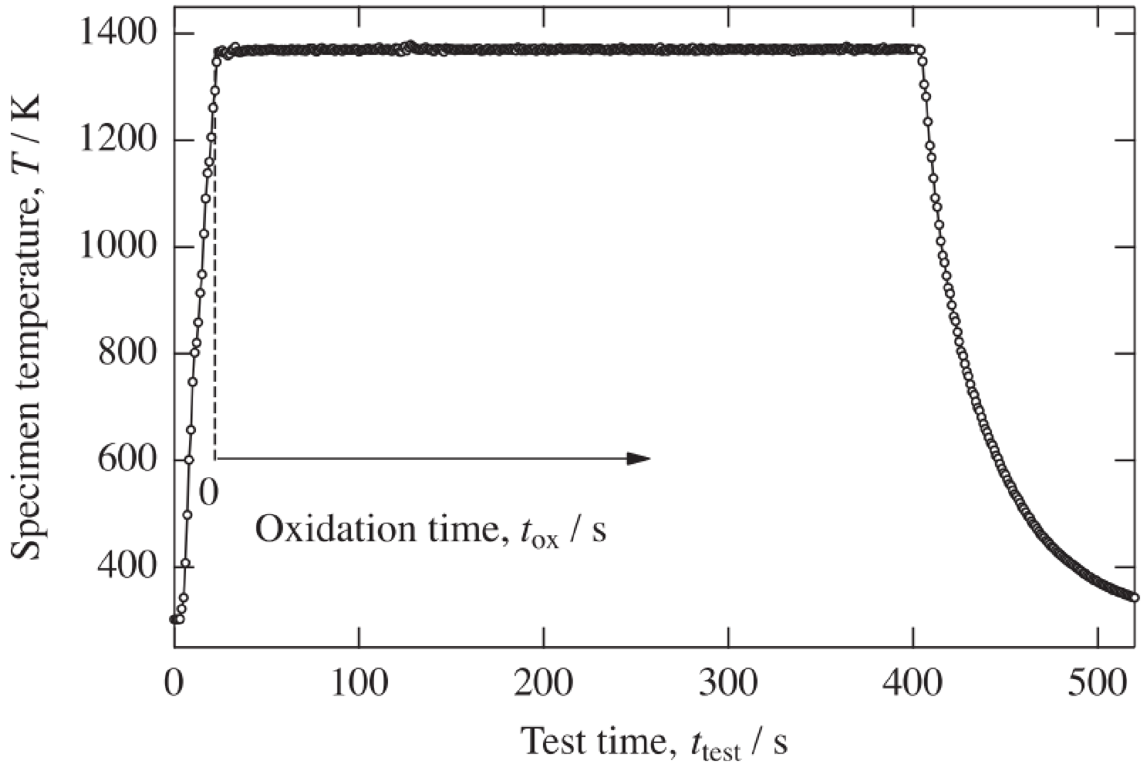

These specimens were heated at a rate of 50 K/s and
kept at 1373 K for ~400 s;

They were then cooled in the high-temperature unit.

Gas mixture:

- 17 vol.% O2
- 20 vol.% H2O
- N2 gas

Rate of 8.3 cm^3/s

In situ studies of breakaway oxidation in type 430 stainless steel

Commercial type 430 stainless steel was used.
The composition of the steel was:

- 0.054 mass% C,
- 0.55 mass% Si,
- 0.09 mass% Mn,
- 0.004 mass% S,
- 0.13 mass% Ni,
- 16.1 mass% Cr,
- and Fe

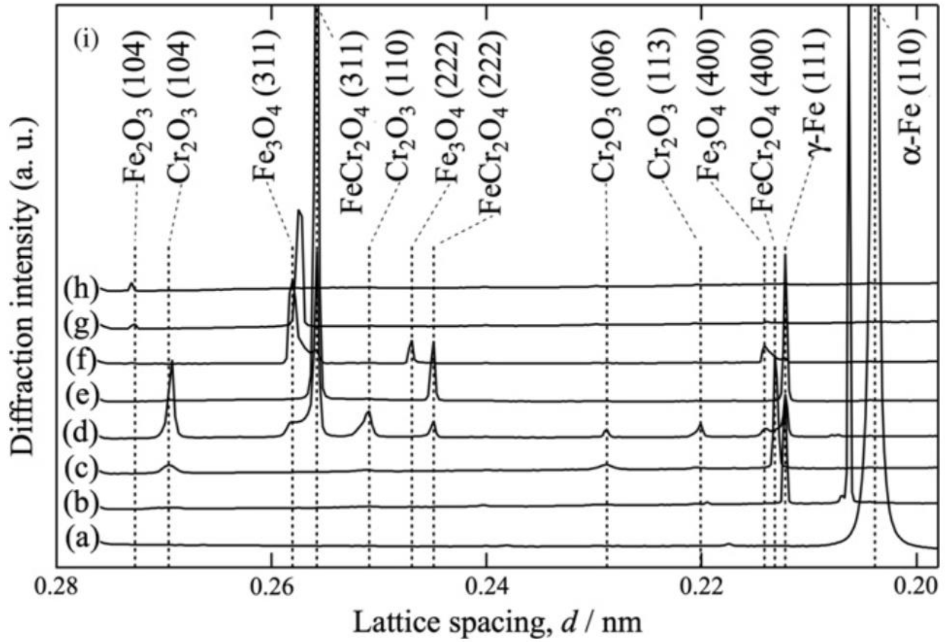

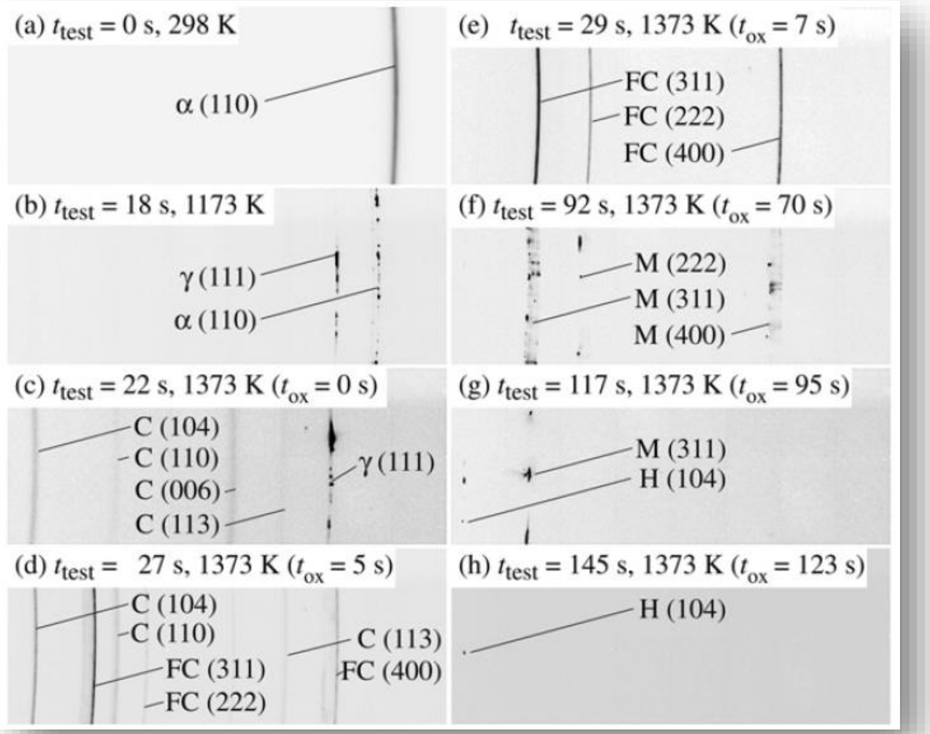

Saeki et al. Corrosion Science ***55****, 219, 2012*

In situ studies of breakaway oxidation in type 430 stainless steel

Commercial type 430 stainless steel was used.
The composition of the steel was:

- 0.054 mass% C,
- 0.55 mass% Si,
- 0.09 mass% Mn,
- 0.004 mass% S,
- 0.13 mass% Ni,
- 16.1 mass% Cr,
- and Fe

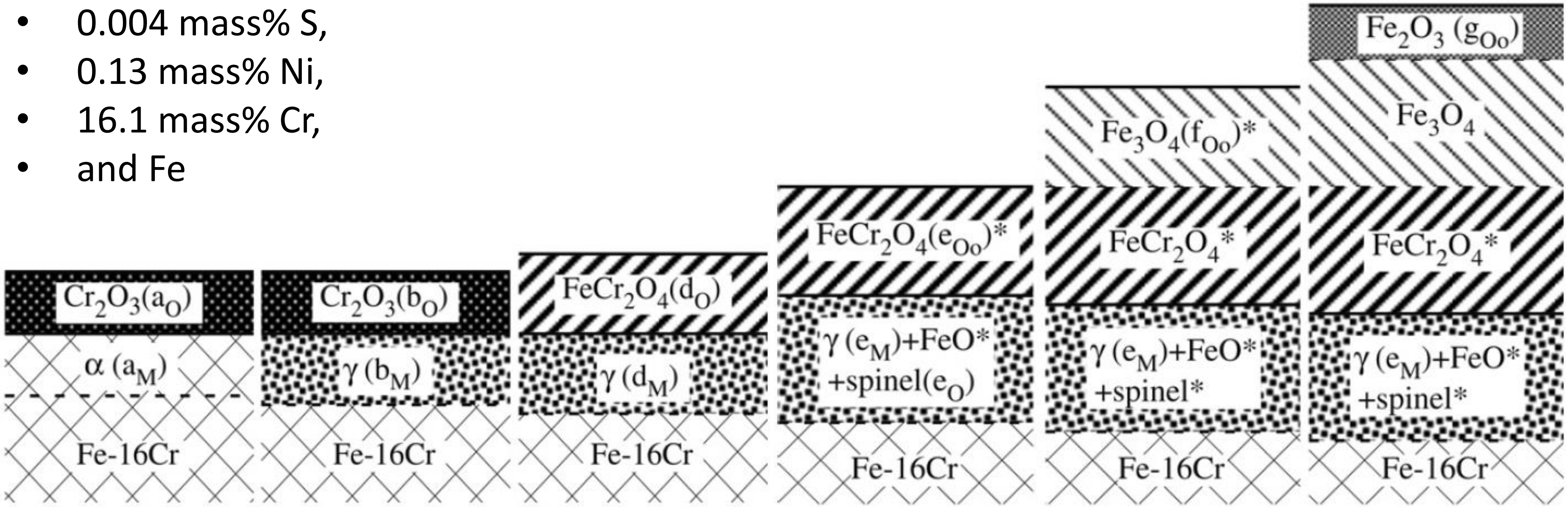

*Saeki et al. Corrosion Science **55**, 219, 2012*

In situ mechanical testing

beatriz.moreno@lightsource.ca

Gleeble 3S50

Gleeble®Synchrotron

Allows the material of interest to be subject to a wide range of thermo-mechanical conditions

<u>Applications</u>:

- ✓ Phase transformations
- ✓ Residual stress evolution
- ✓ Corrosion
- ✓ Oxidation

Razorbill strain cell

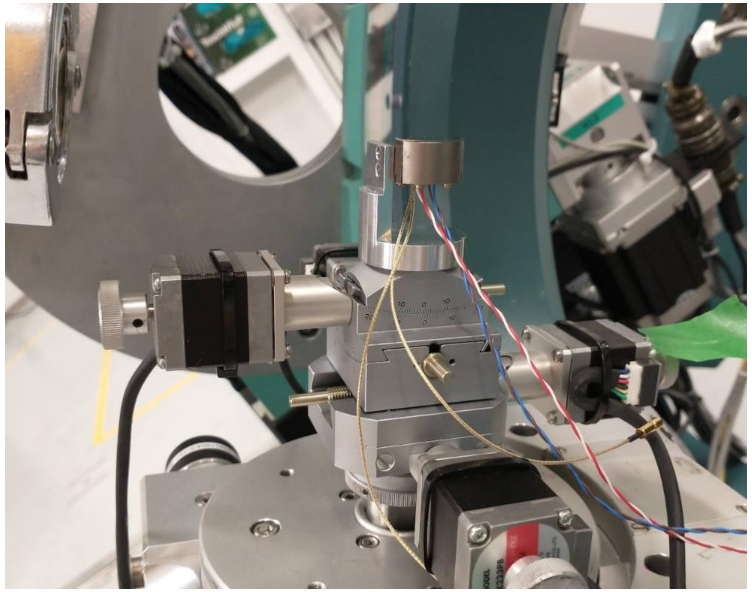

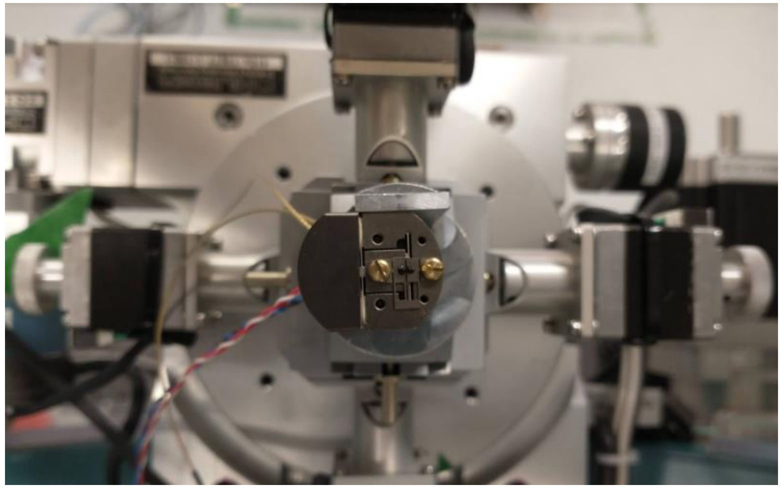

https://razorbillinstruments.com/uniaxial-strain-cell/

Deben 20kN stress rig at Diamond

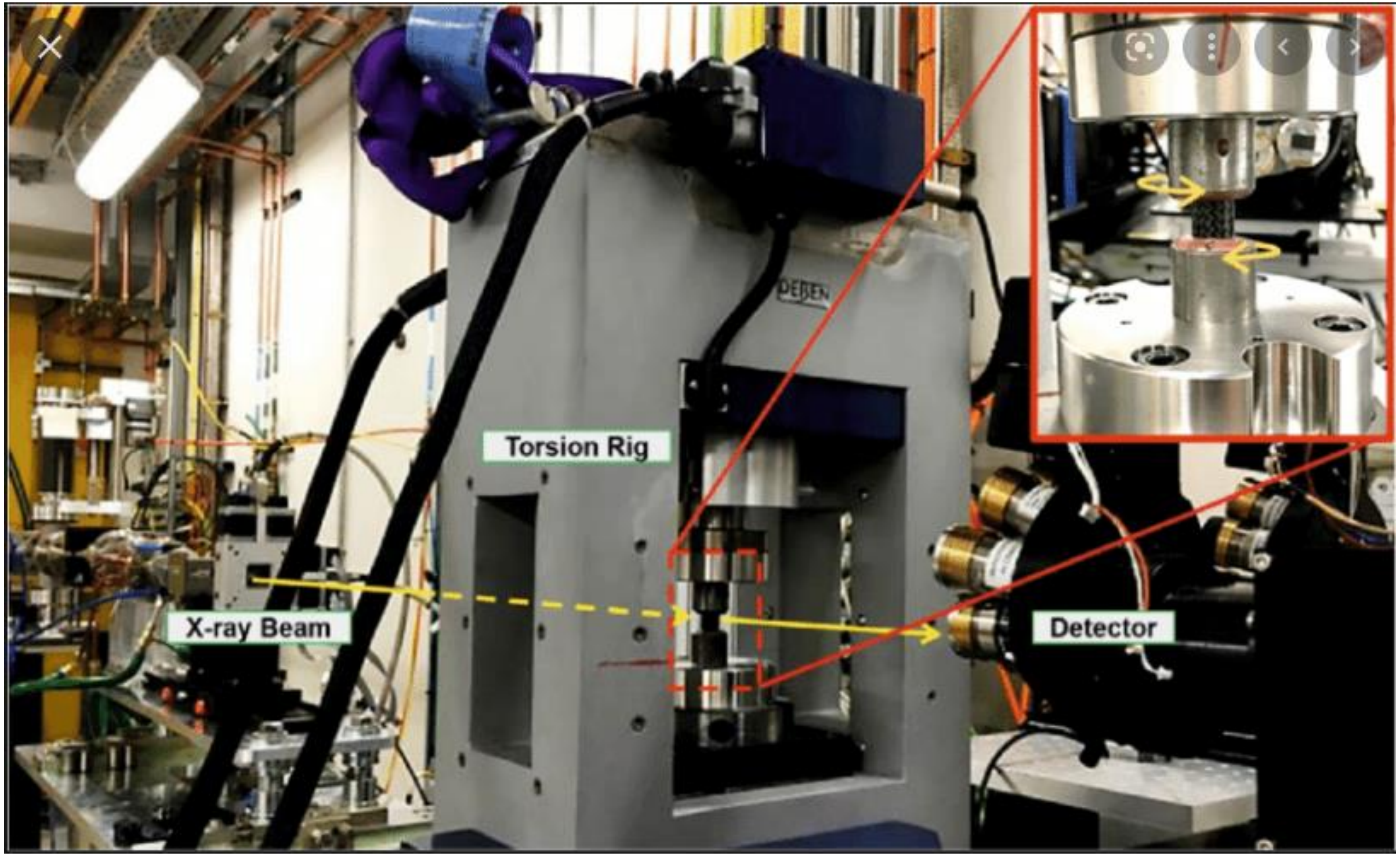

beatriz.moreno@lightsource.ca

In-situ synchrotron x-ray evaluation of strain-induced martensite in AISI 201 austenitic stainless steel during tensile testing

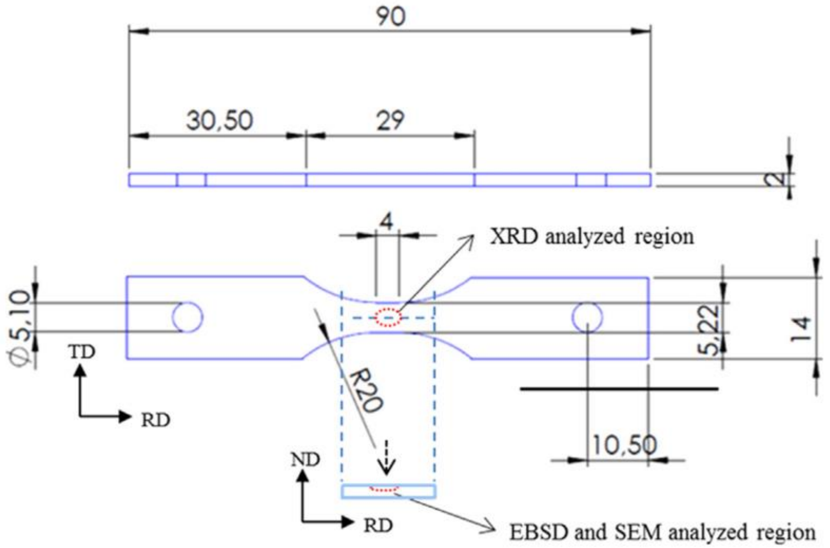

Goal:

- To understand the changes in microstructure of AISI 201 by applying a tensile stress using in-situ XRD.
- To track phase transformation and strain partitioning among the phases

Chemical composition of the austenitic stainless steel AISI 201 used in this work. Values expressed in wt%.

C	Mn	Si	P	S	Cr	Ni	Mo	Al
0.0237	7.018	0.382	0.037	0.0014	17.06	4.07	0.0429	0.0047
Cu	**Co**	**V**	**Nb**	**Ti**	**Sn**	**W**	**N**	**O**
0.0717	0.0616	0.0408	0.0038	0.0041	0.0064	0.0147	0.1640	0.0029

Gauss, C. et al. Materials Science & Engineering A **651**, 507, 2016

In-situ synchrotron x-ray evaluation of strain-induced martensite in AISI 201 austenitic stainless steel during tensile testing

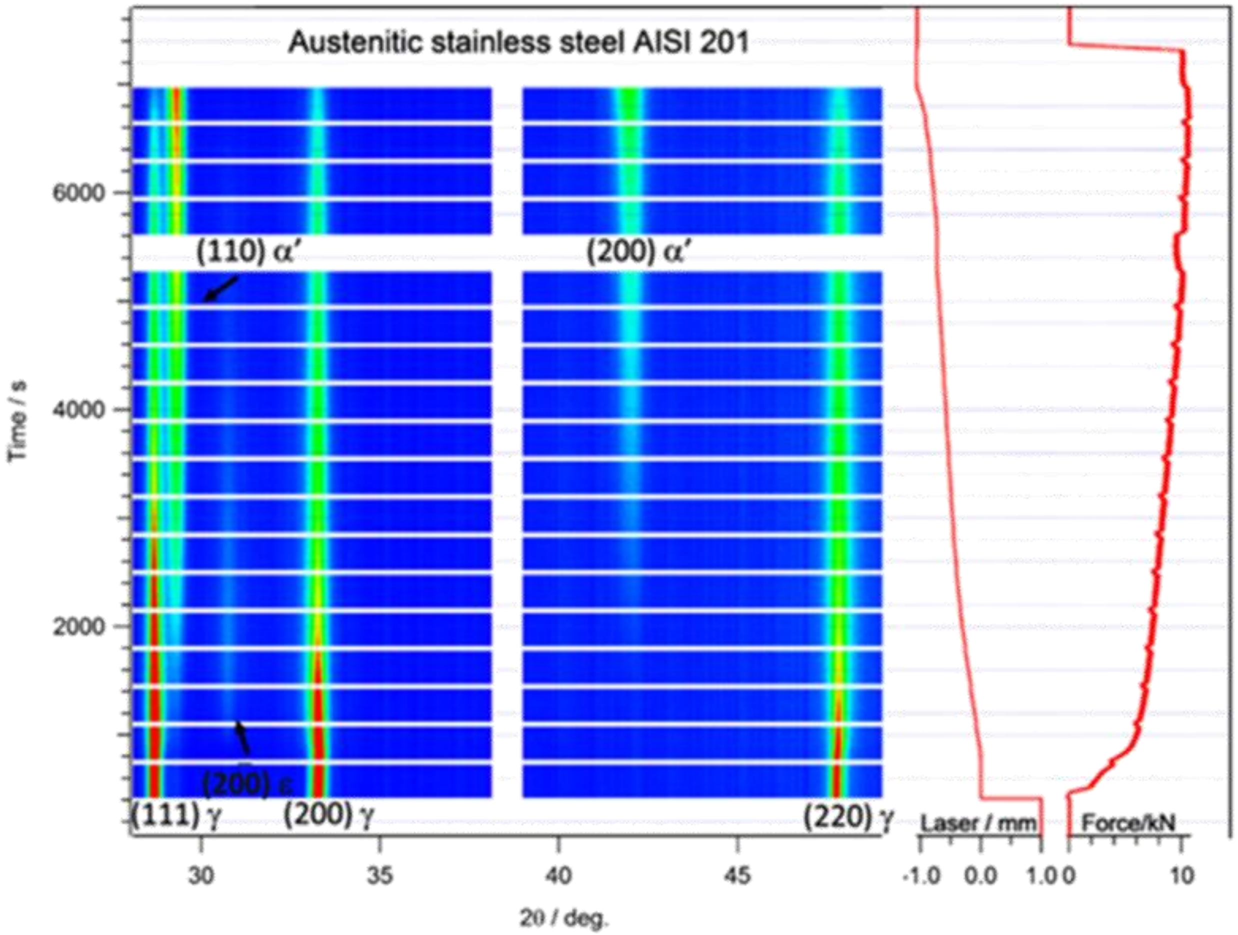

Metastable austenite (γ) decomposes into

- hcp-ε-martensite and
- bcc-α'-martensite

Gauss, C. et al. Materials Science & Engineering A **651**, 507, 2016

In-situ synchrotron x-ray evaluation of strain-induced martensite in AISI 201 austenitic stainless steel during tensile testing

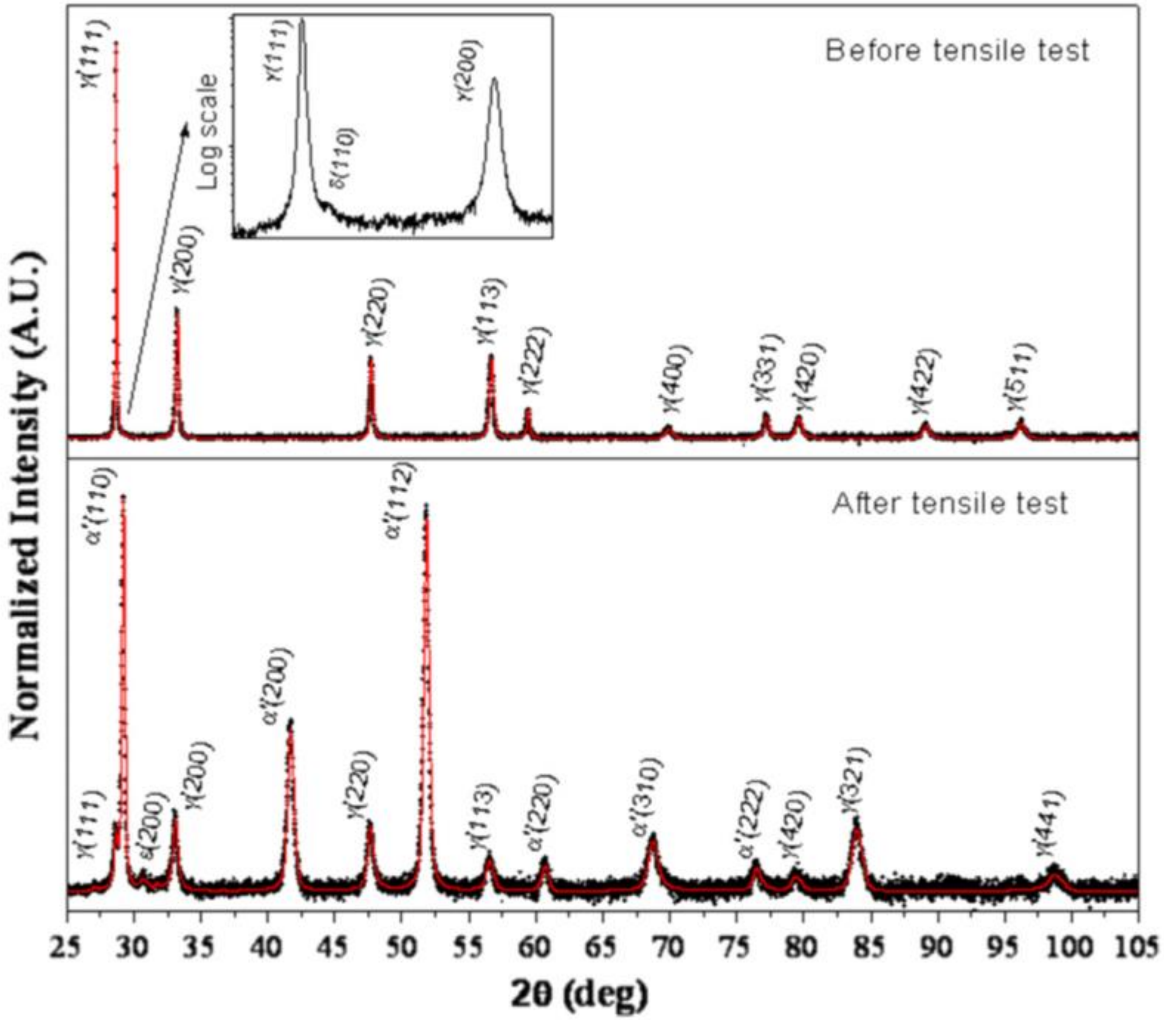

Metastable austenite (γ) decomposes into

- hcp-ε-martensite and
- bcc-α'-martensite

Gauss, C. et al. Materials Science & Engineering A **651**, 507, 2016

In-situ synchrotron x-ray evaluation of strain-induced martensite in AISI 201 austenitic stainless steel during tensile testing

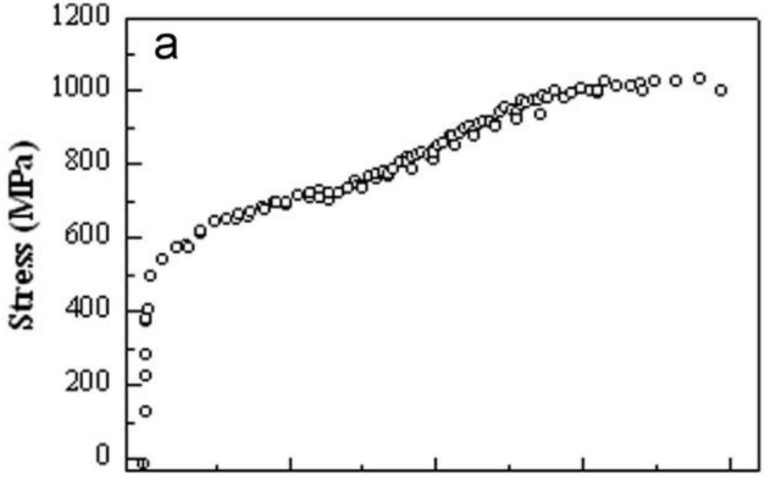

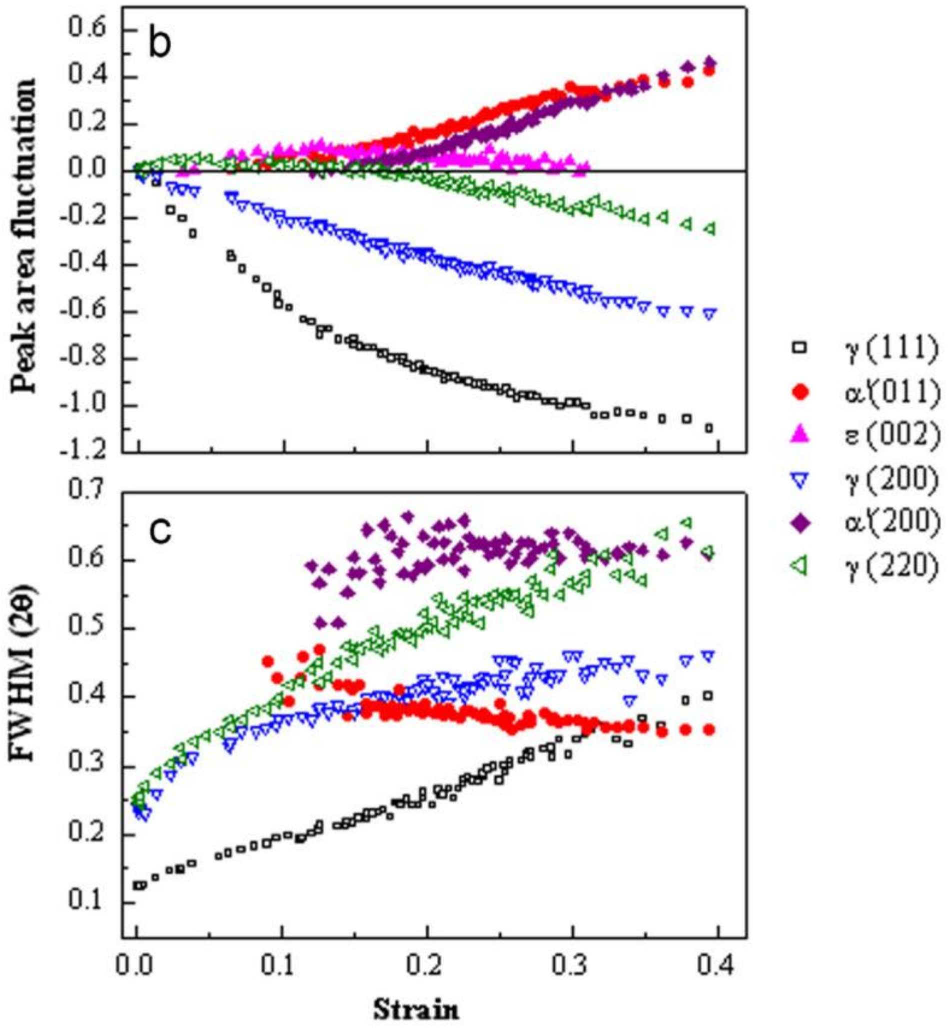

Data analysis:

- ✓ Phase identification
- ✓ Integrated intensity
- ✓ Peak position
- ✓ FWHM

Gauss, C. et al. Materials Science & Engineering A **651**, 507, 2016

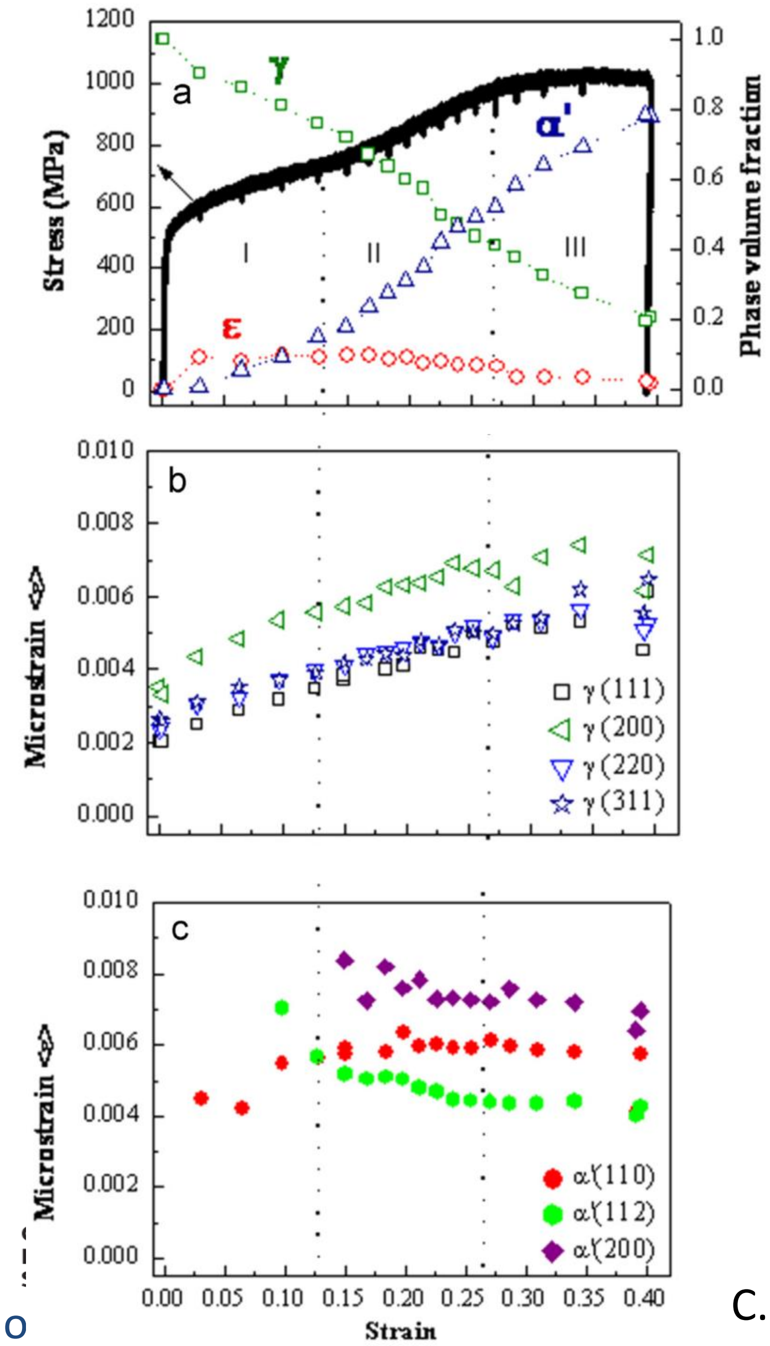

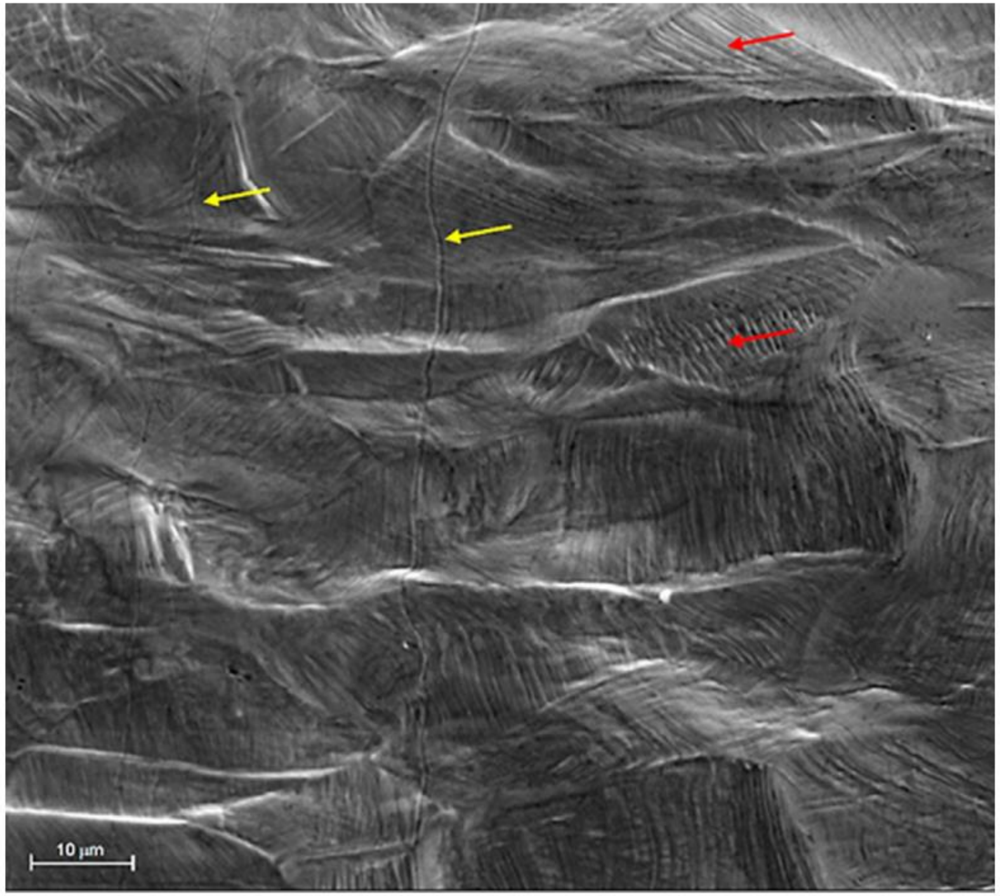

C. Gauss. Materials Science & Engineering A **651**, 507, 2016

In-situ synchrotron x-ray evaluation of strain-induced martensite in AISI 201 austenitic stainless steel during tensile testing

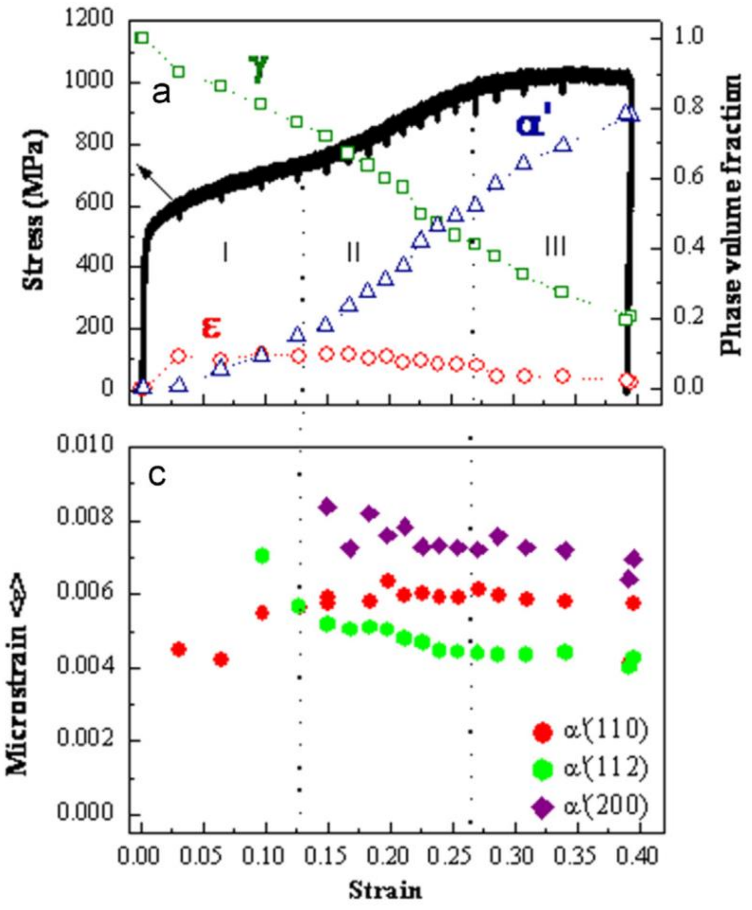

- ✓ The strain induced transformation of metastable gamma austenite(fcc structure) was followed in real time.
- ✓ ε-martensite is the first phase to appear followed by α' – martensite.
- ✓ Got information about the phase volume fractions and microstrain.
- ✓ FWHM of peaks is related to macroscopic mechanical properties. FWHM remains constant in the elastic regime and increases at the yield strength with the onset of plastic flow.

Gauss, C. et al. Materials Science & Engineering A **651**, 507, 2016

In-situ observation of bulk 3D grain evolution during plastic deformation in polycrystalline Cu

Reeju Pokharel [a,c,*], Jonathan Lind [a,b], Shiu Fai Li [b], Peter Kenesei [d], Ricardo A. Lebensohn [c], Robert M. Suter [a], Anthony D. Rollett [a]

99.995% pure polycrystalline copper during tensile loading

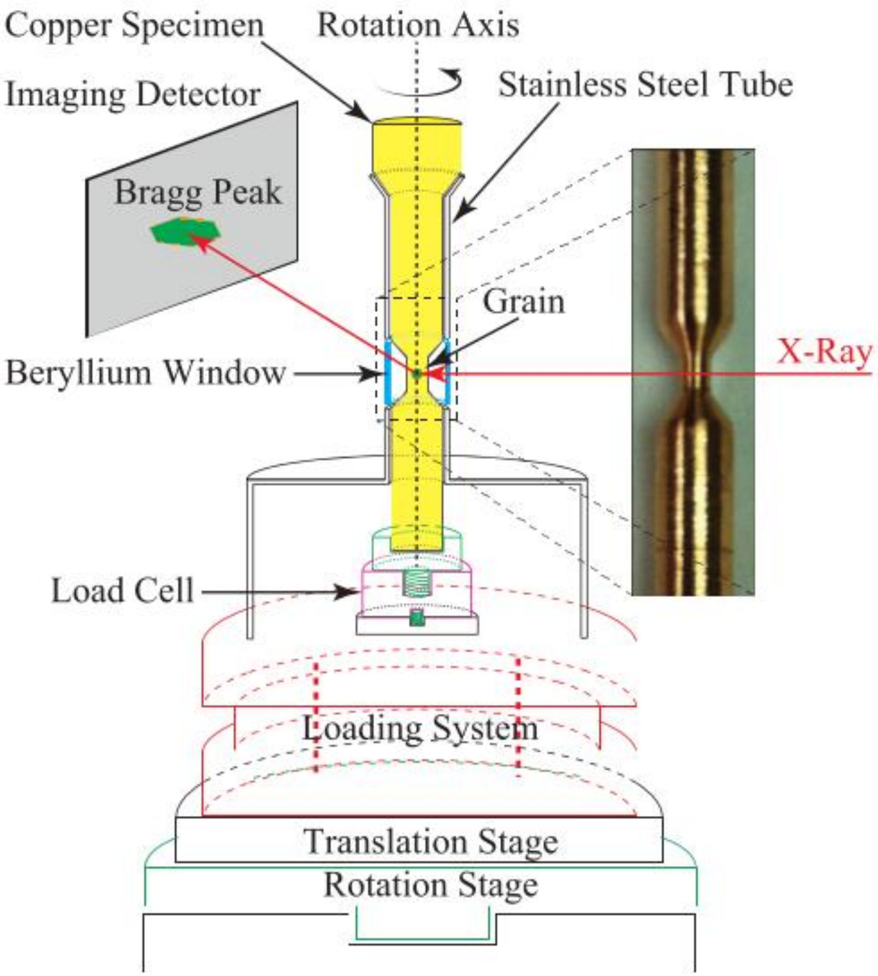

R. Pokharel et al. / International Journal of Plasticity 67 (2015) 217–234

In-situ observation of bulk 3D grain evolution during plastic deformation in polycrystalline Cu

CrossMark

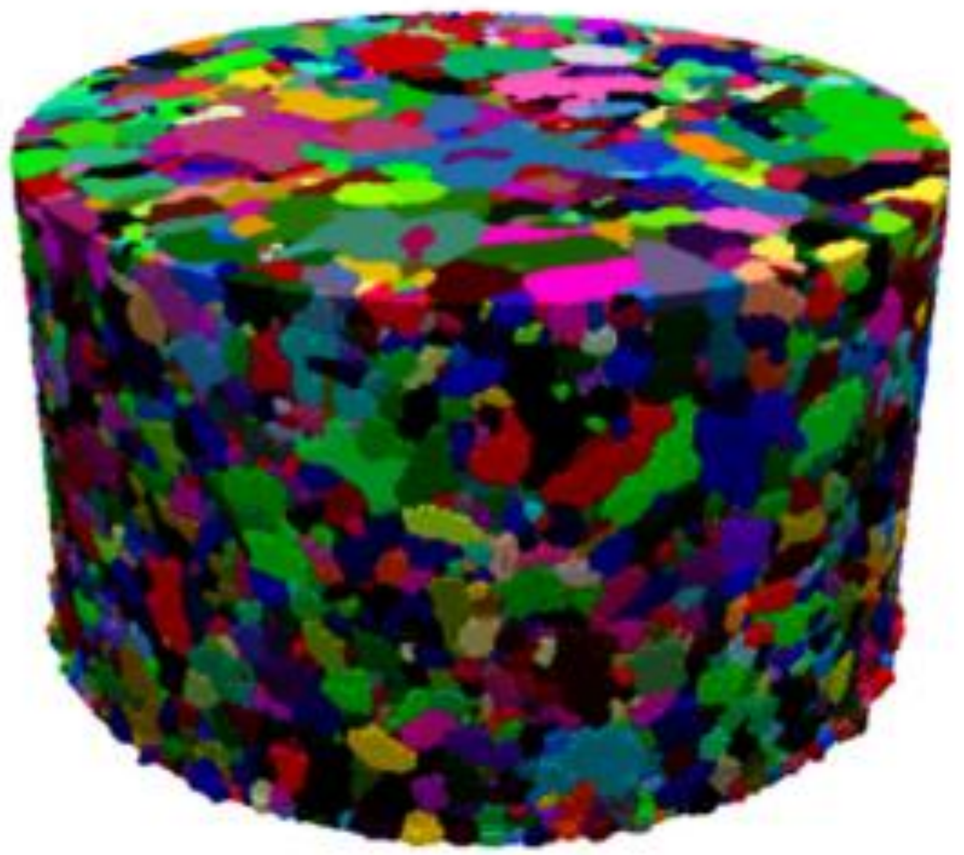

99.995%pure polycrystalline copper during tensile loading

beatriz.moreno@lightsource.ca

In-situ observation of bulk 3D grain evolution during plastic deformation in polycrystalline Cu

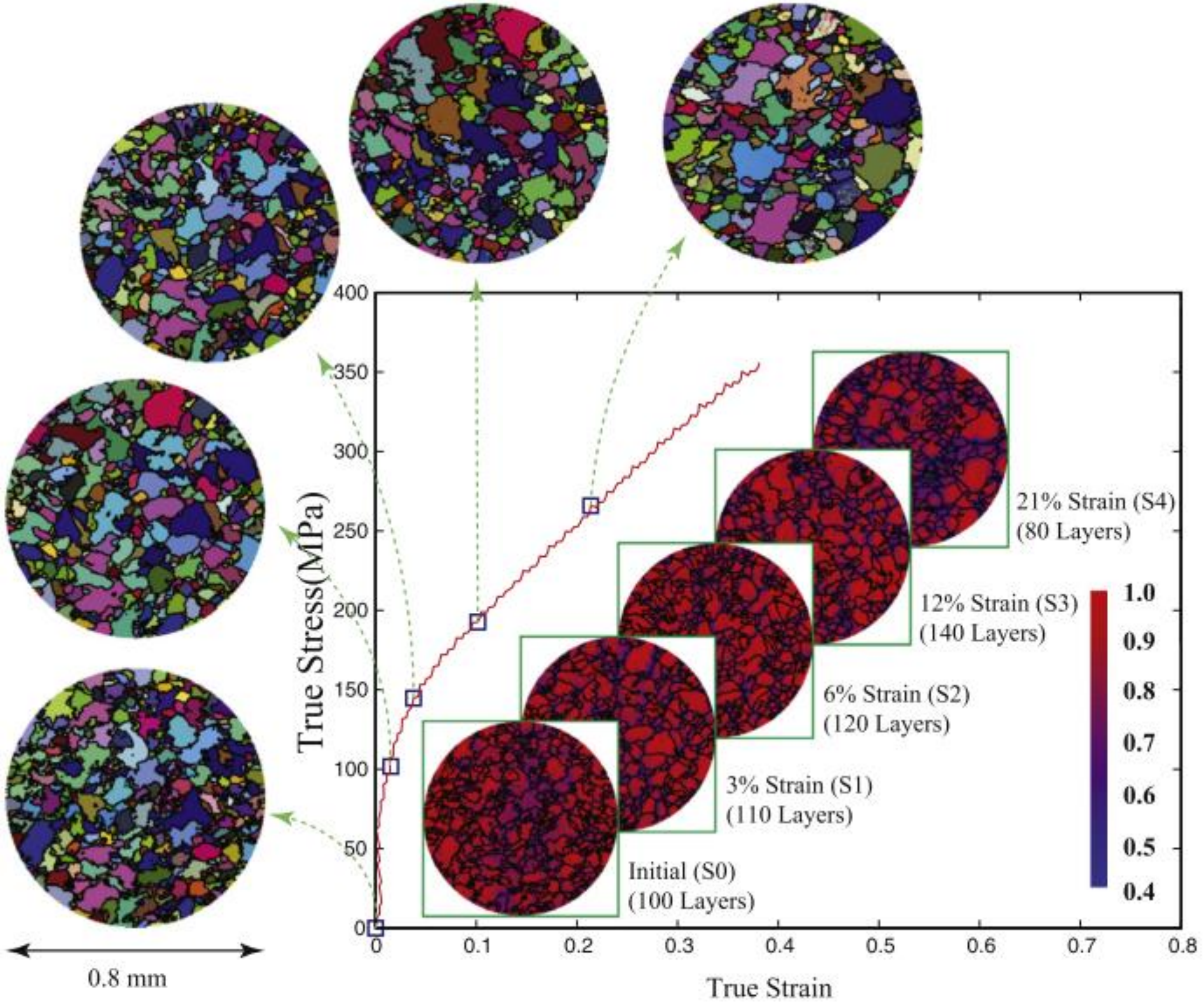

R. Pokharel et al. / International Journal of Plasticity 67 (2015) 217–234

Catalysts

Oil refinery catalytic reactor

beatriz.moreno@lightsource.ca

Catalysis

Catalysts play an important part in many chemical processes.
More than 85% of chemicals come from catalytic reactions

Catalysts:

- increase the rate of reaction
- are not consumed by the reaction
- are only needed in very small amounts

In-situ and operando catalytic experiments include

- Temperature and pressure control
- Structural characterization of intermediate compounds
- Gases in/out, flow control, analysis of gases out of the catalytic reaction

In-situ catalytic experiments

A versatile sample-environment cell for non-ambient X-ray scattering experiments

Peter J. Chupas,[a]* Karena W. Chapman,[a] Charles Kurtz,[a] Jonathan C. Hanson,[b] Peter L. Lee[a] and Clare P. Grey[c]

J. Appl. Cryst. (2008). **41**, 822–824

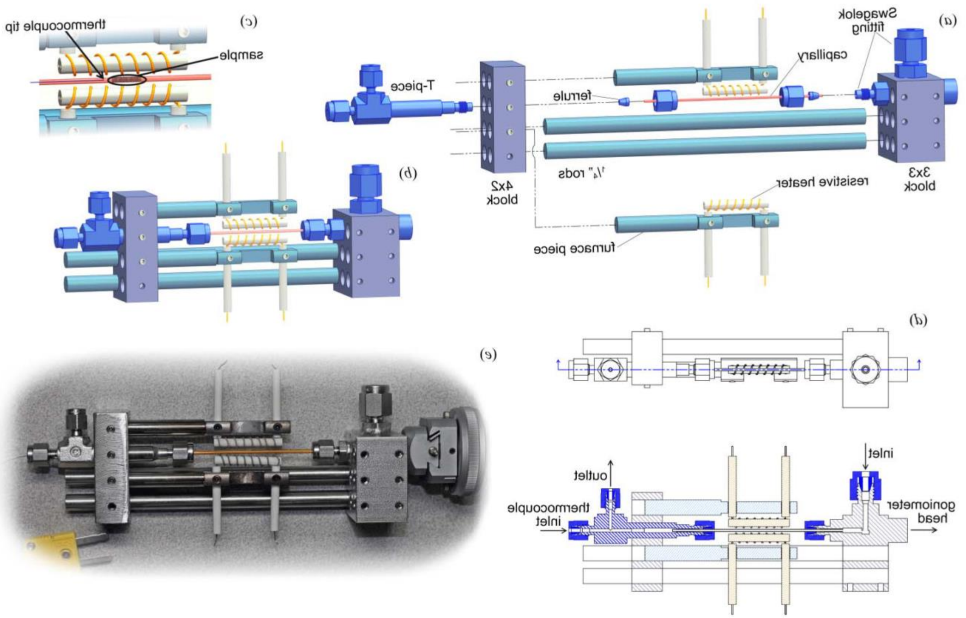

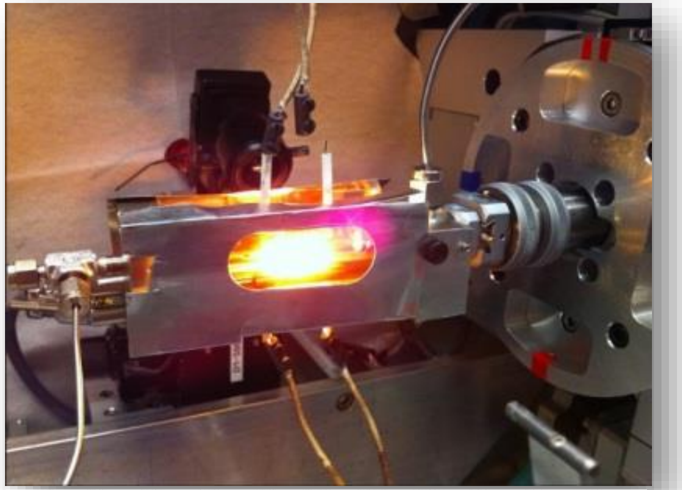

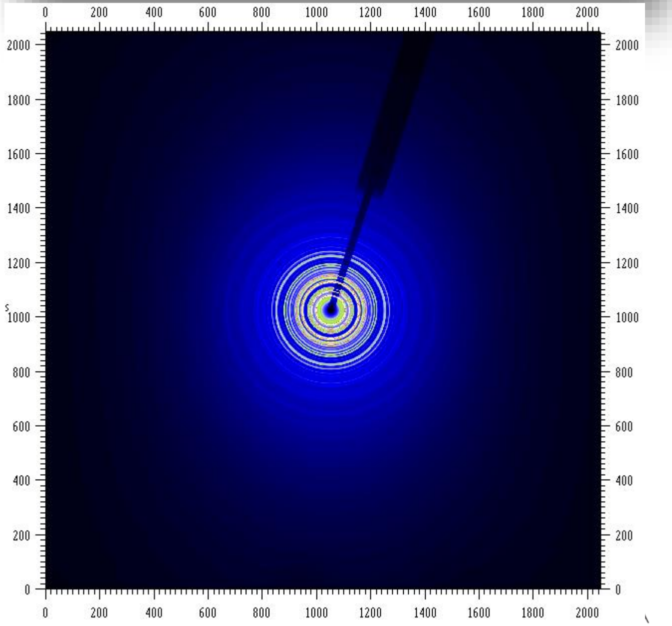

In-situ catalysis

Commercial catalyst Aurolite® (1% Au-P25)

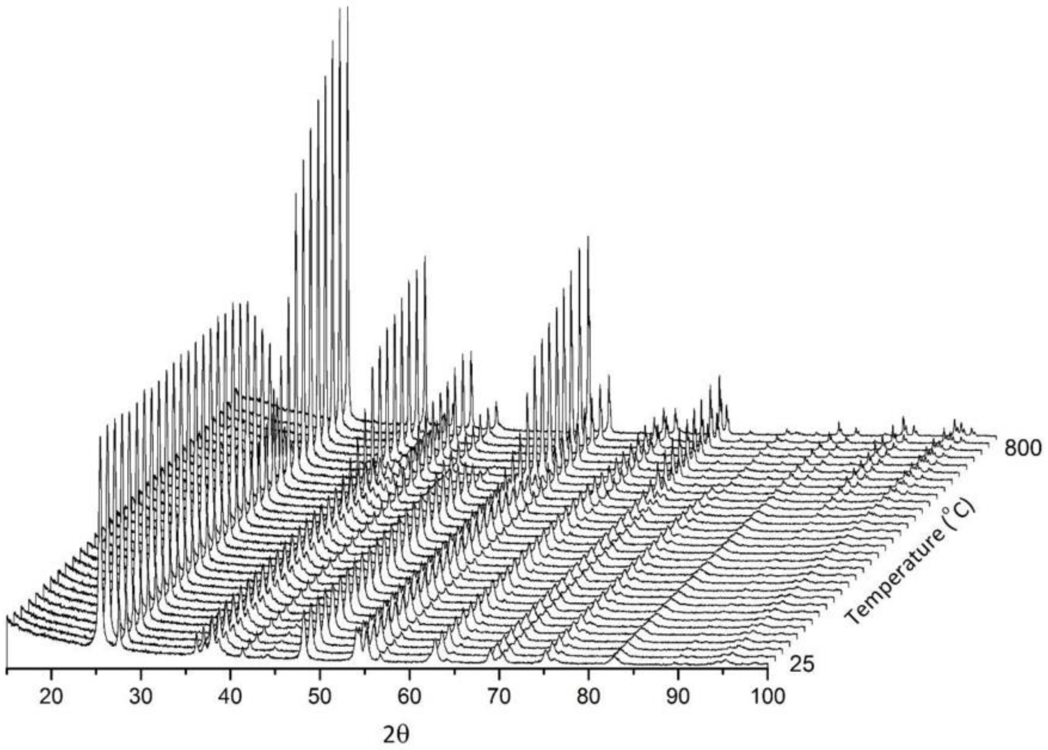

Phase change from anatase to the thermodynamically stable rutile phase

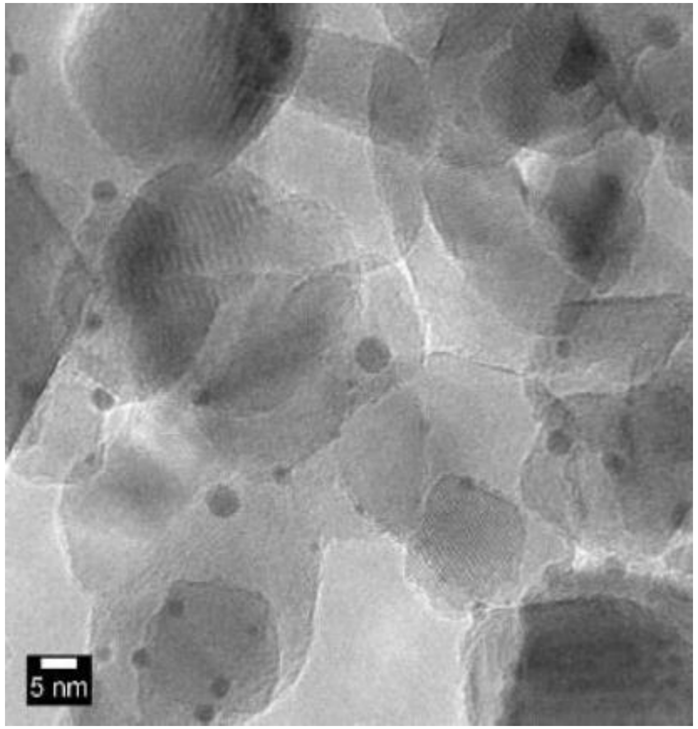

Achieving nano-gold stability through rational design† D. Barret et al.

In-situ catalysis

Commercial catalyst Aurolite® (1% Au-P25)

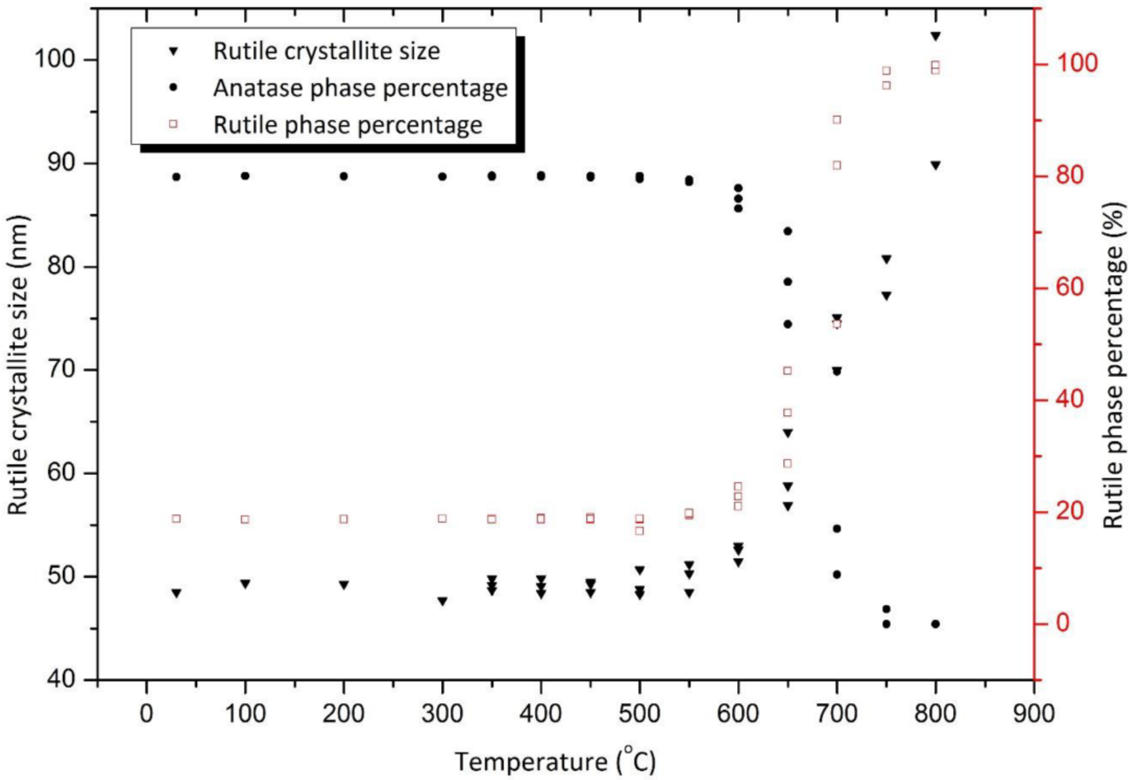

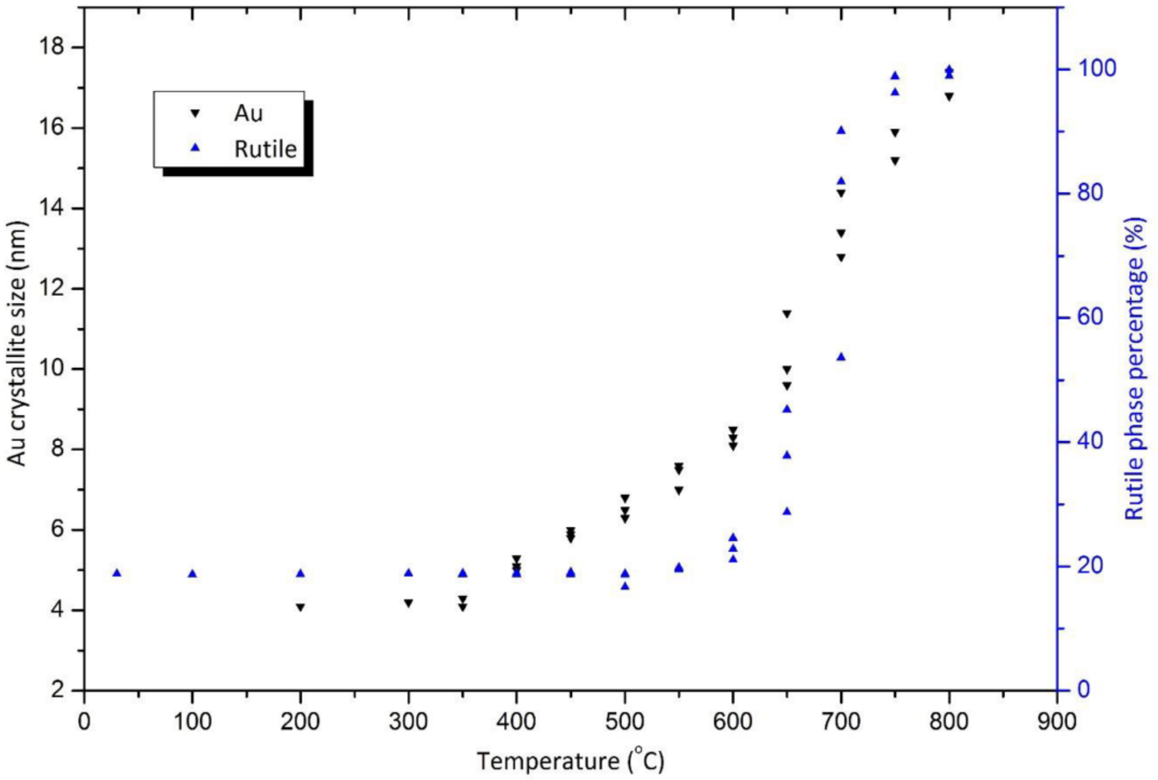

Structural instability of the support is a major factor in Au-nanoparticle growth
→ catalytic activity decreases

Achieving nano-gold stability through rational design† D. Barret et al. 2016

In-situ catalysis

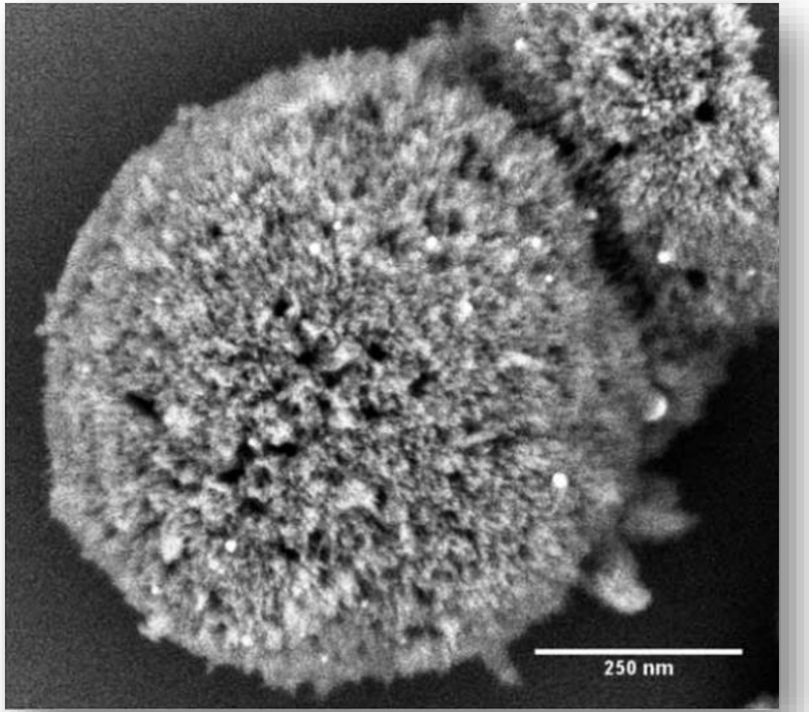

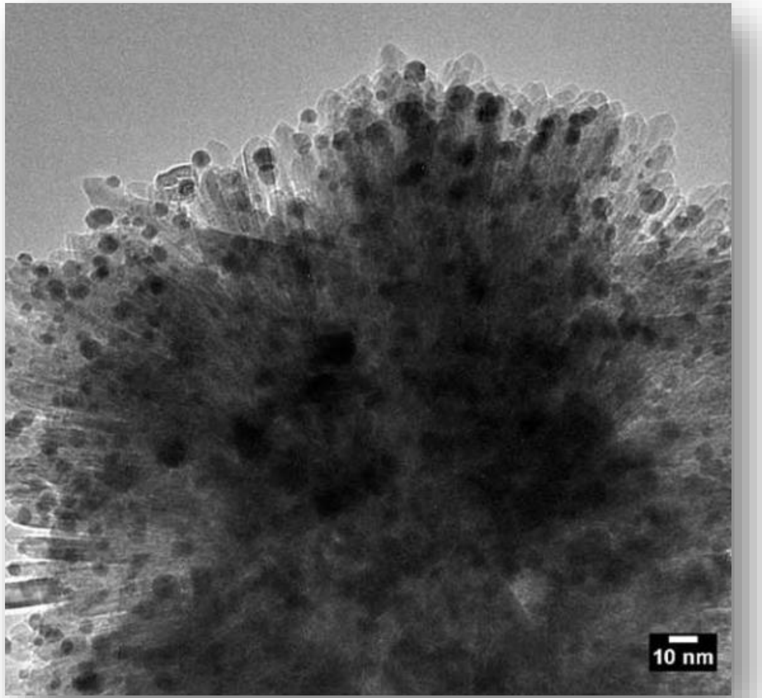

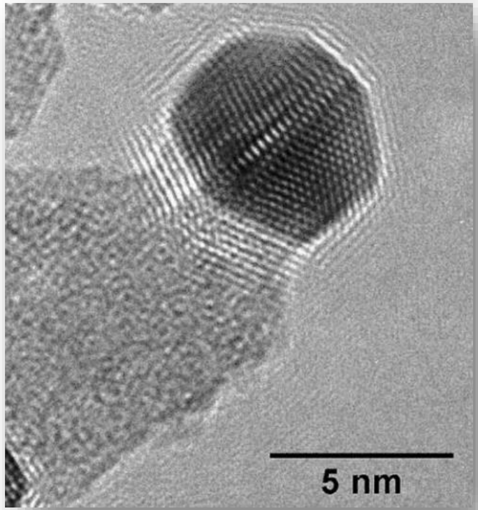

Achieving nano-gold stability through rational design† D. Barret et al. 2016

In-situ catalysis

The presence of Au resulted in a stabilizing effect with regards to the growth of the support structure.

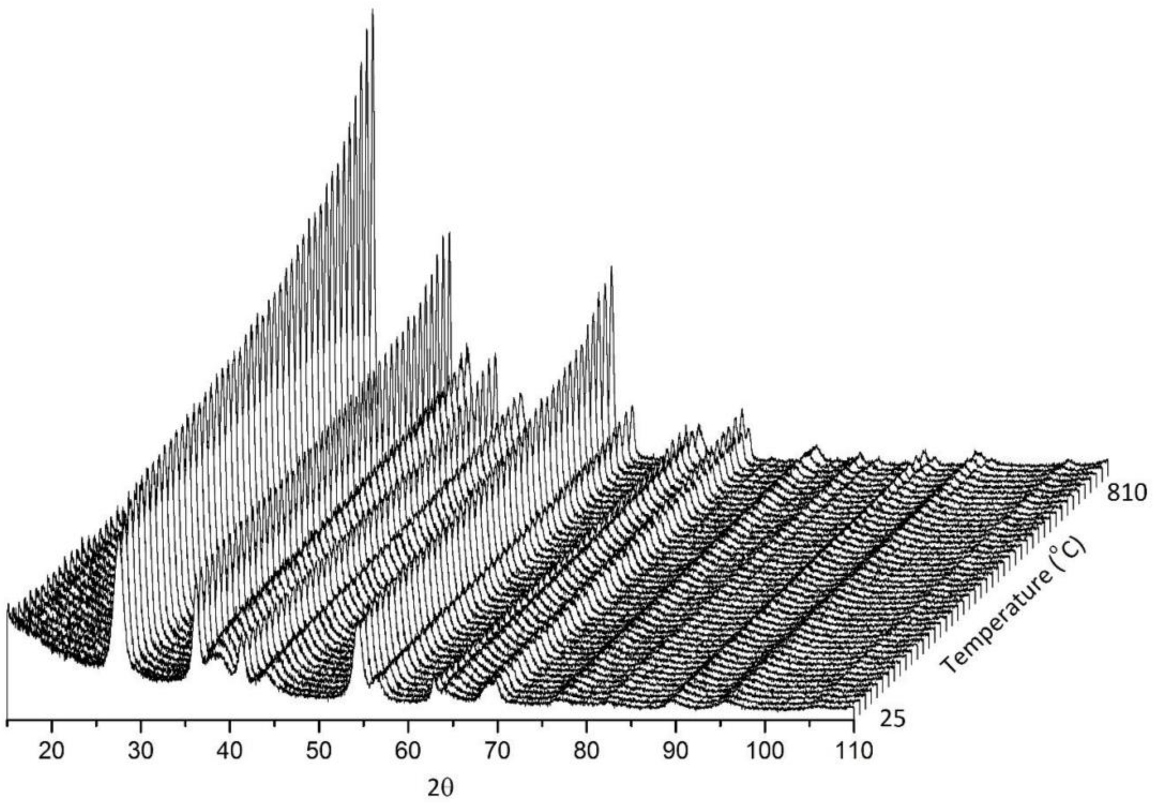

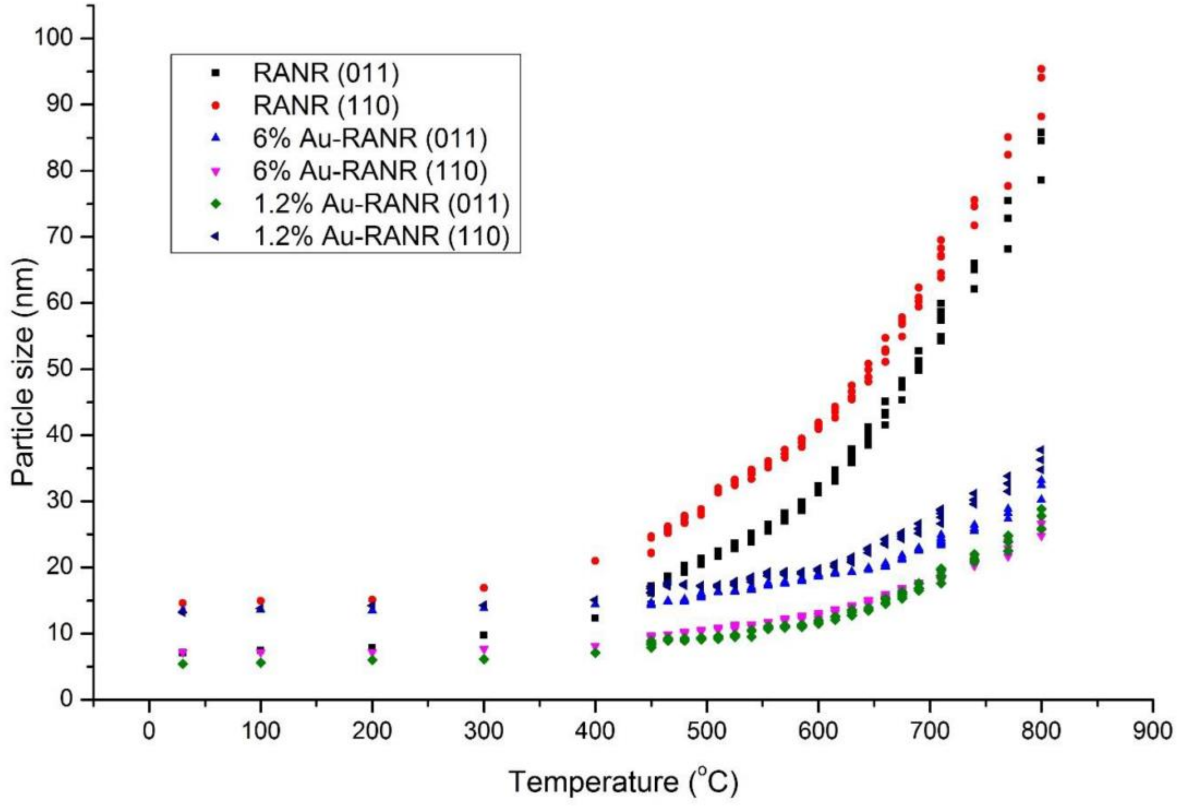

Achieving nano-gold stability through rational design† D. Barret et al. 2016

In-situ catalysis

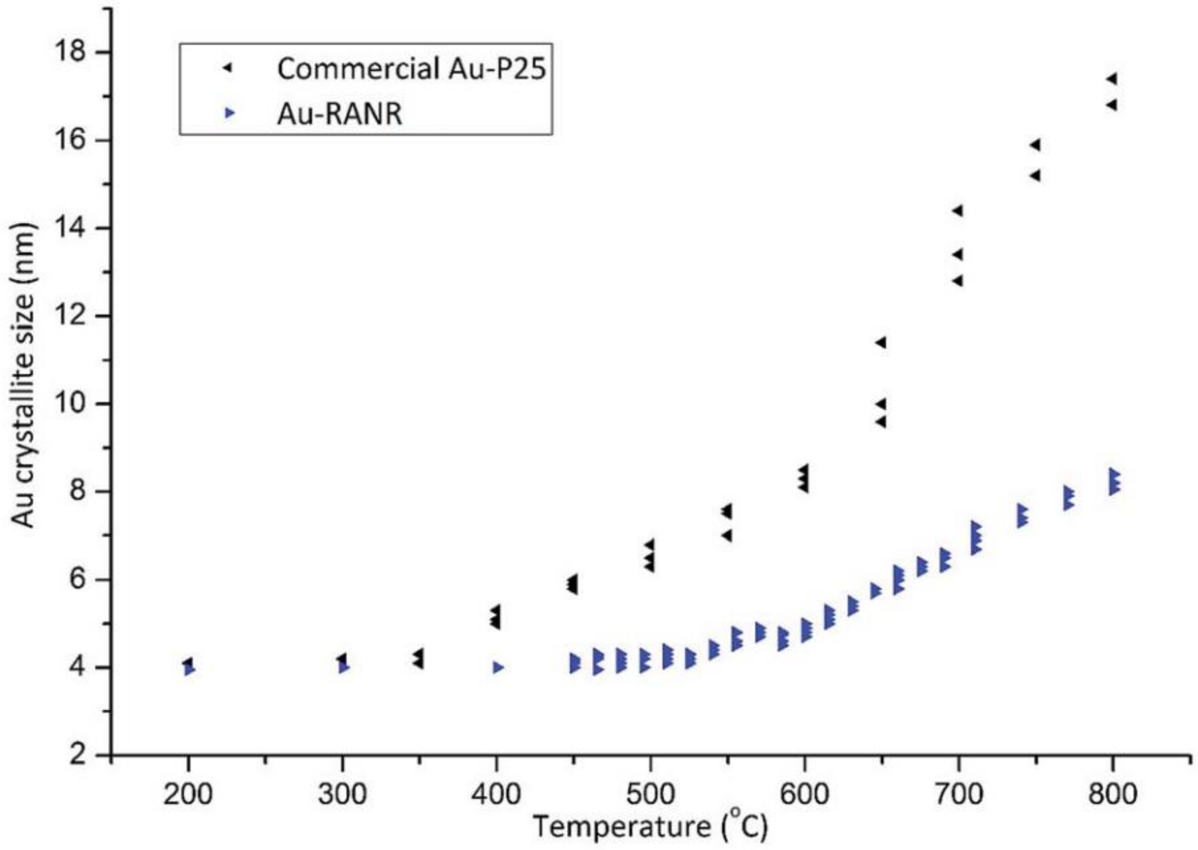

Fig. 3 Au crystallite sizes of the commercial Au–TiO_2 and Au-RANR catalysts determined from Rietveld refinement from *in situ* PXRD.

Achieving nano-gold stability through rational design† D. Barret et al. 2016

In-situ catalysis

- ✓ Thermodynamically stable support material
- ✓ Improved morphology
- ✓ Au nanoparticles sit isolated on the rod tips -> reduced mobility and coalescence
- ✓ Remarkable catalytic stability tested with CO oxidation

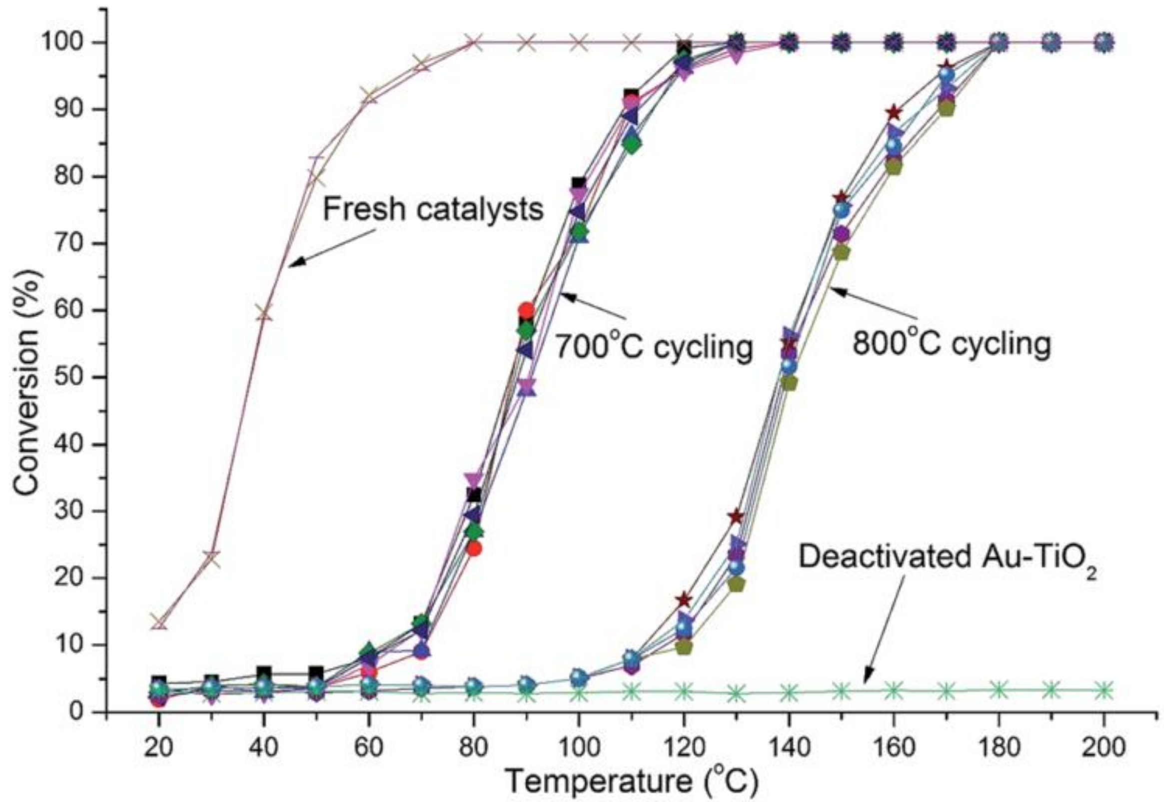

Fig. 4 Light-off curves for catalysts with 1.2% Au-RANR and commercial Au–TiO_2 after multiple 700 and 800 °C heating cycles (10 cycles in total).

Achieving nano-gold stability through rational design† D. Barret et al. 2016

Application of high-energy X-rays and Pair-Distribution-Function analysis to nano-scale structural studies in catalysis

Peter J. Chupas [a,*], Karena W. Chapman [a], Hailong Chen [b], Clare P. Grey [b]

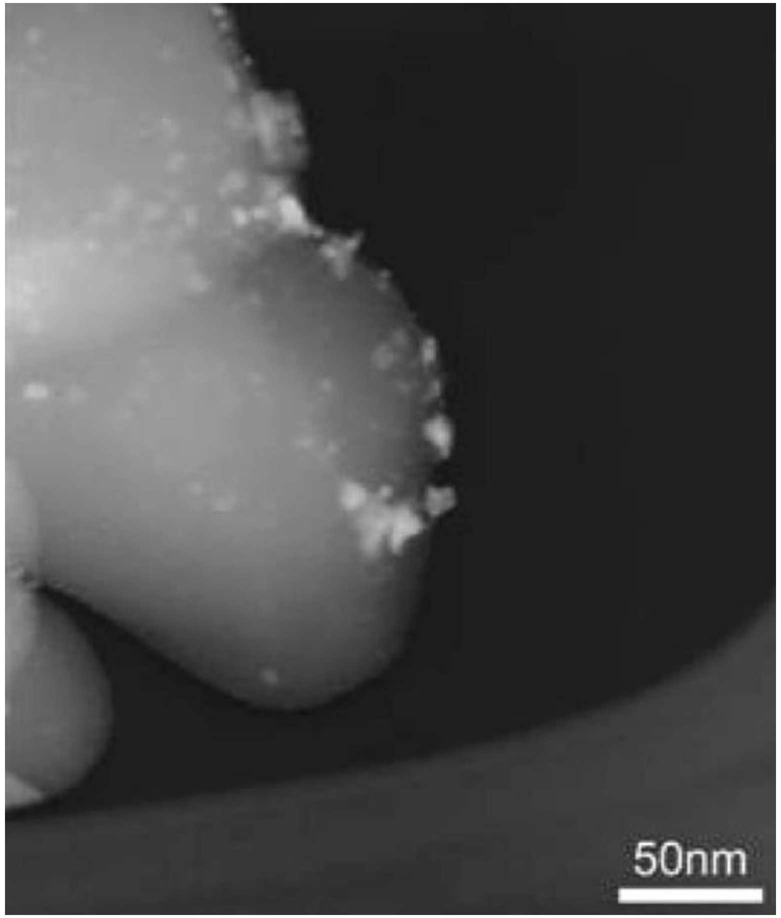

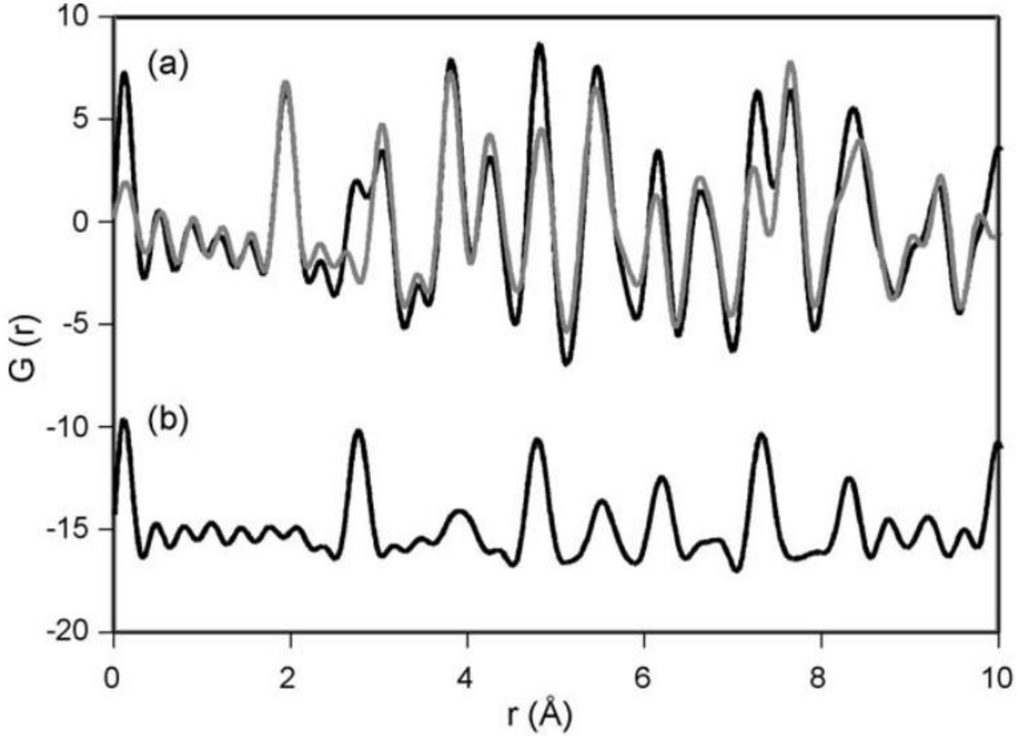

(a) Grey line: G(r) for TiO2 support
Black line: G(r) for 2.5% Pt on TiO_2 calcined under H_2 flow
(b) Differential PDF

Application of high-energy X-rays and Pair-Distribution-Function analysis to nano-scale structural studies in catalysis

Peter J. Chupas [a,*], Karena W. Chapman [a], Hailong Chen [b], Clare P. Grey [b]

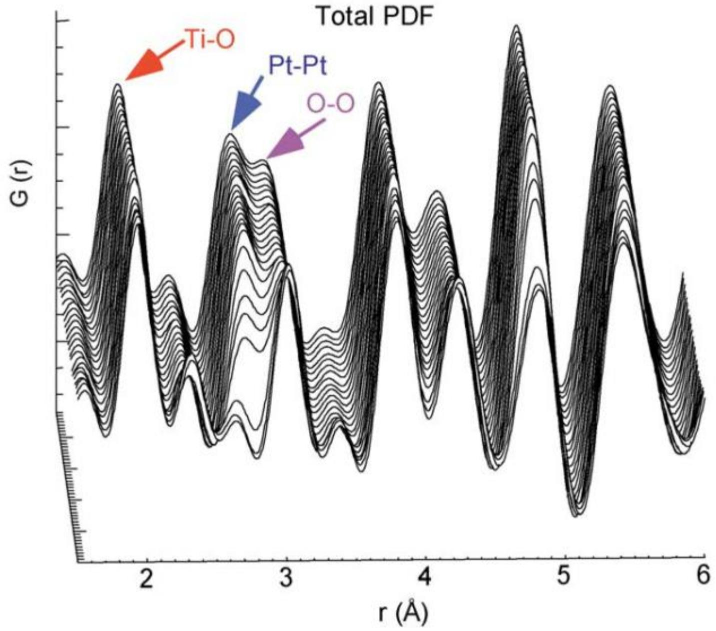

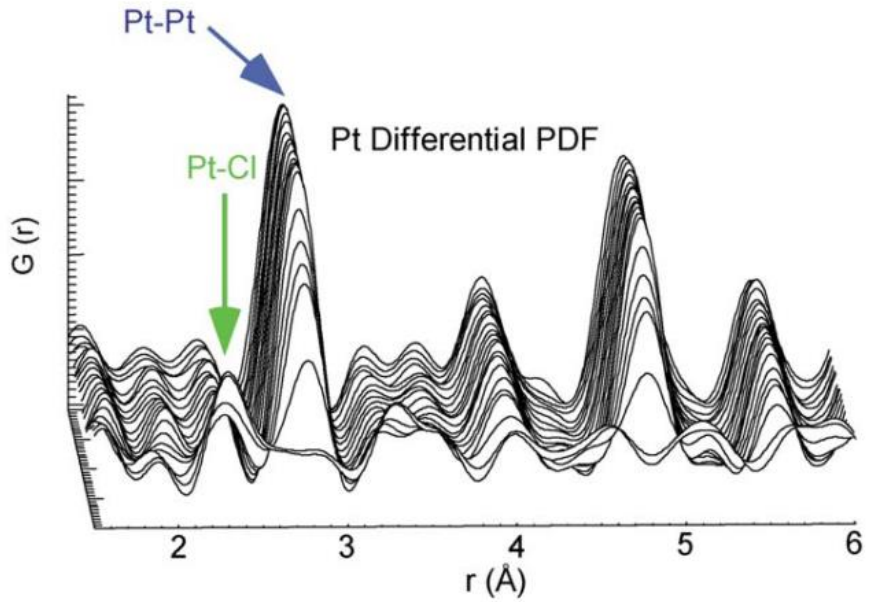

1. Pt nano-particles examined with atomic resolution
2. In-situ transformation of Pt^{4+}_ in $PtCl_6^{2-}$
3. Pt^{4+} reduced in situ with H_2 forming metallic fcc Pt nano particles
4. Observation of the Pt-O bond yields insight about catalyst interaction with TiO_2 support
5. Initial nano-particles are ~1nm, while by 200 ^{o}C they are larger and more crystalline
6. Suggests agglomeration of smaller particles to form larger particles

High pressure studies

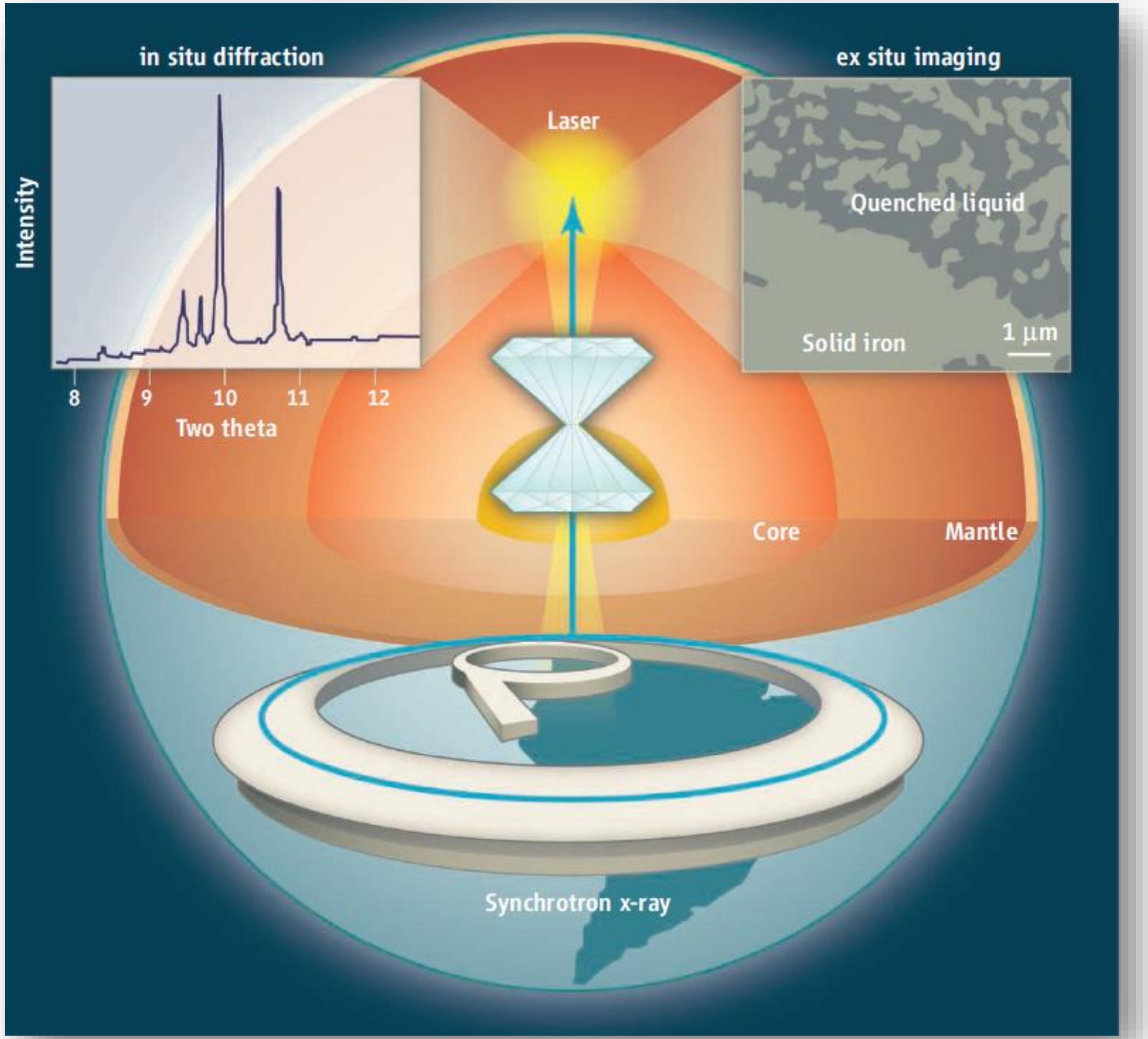

Probing extremes:

Melting Earth's core …

in the laboratory

Science **340**, 442 2013
Yingwei Fei

High pressure studies

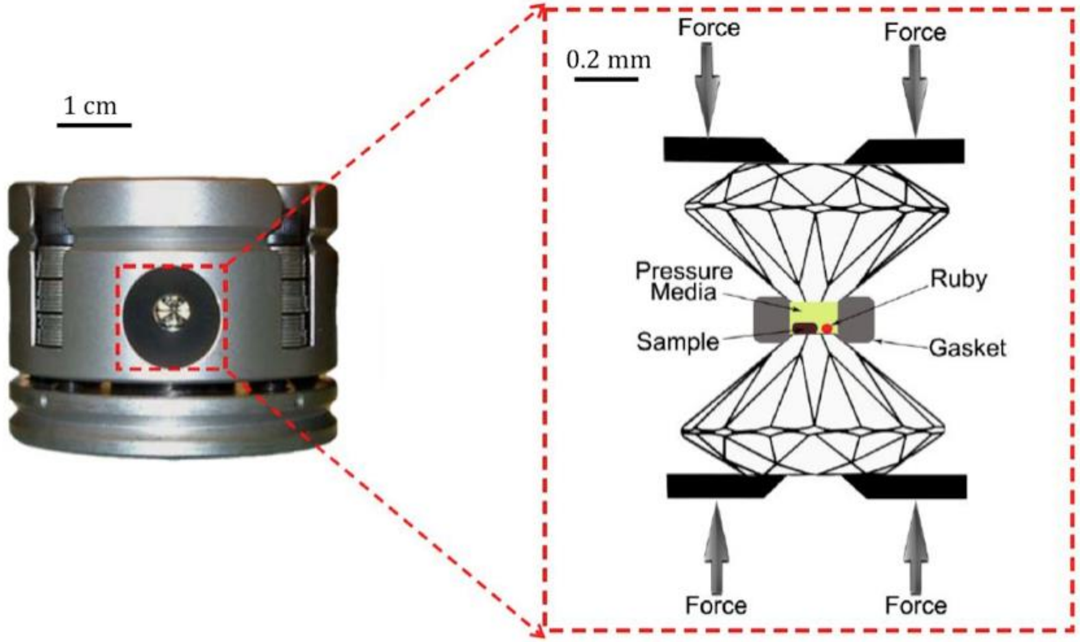

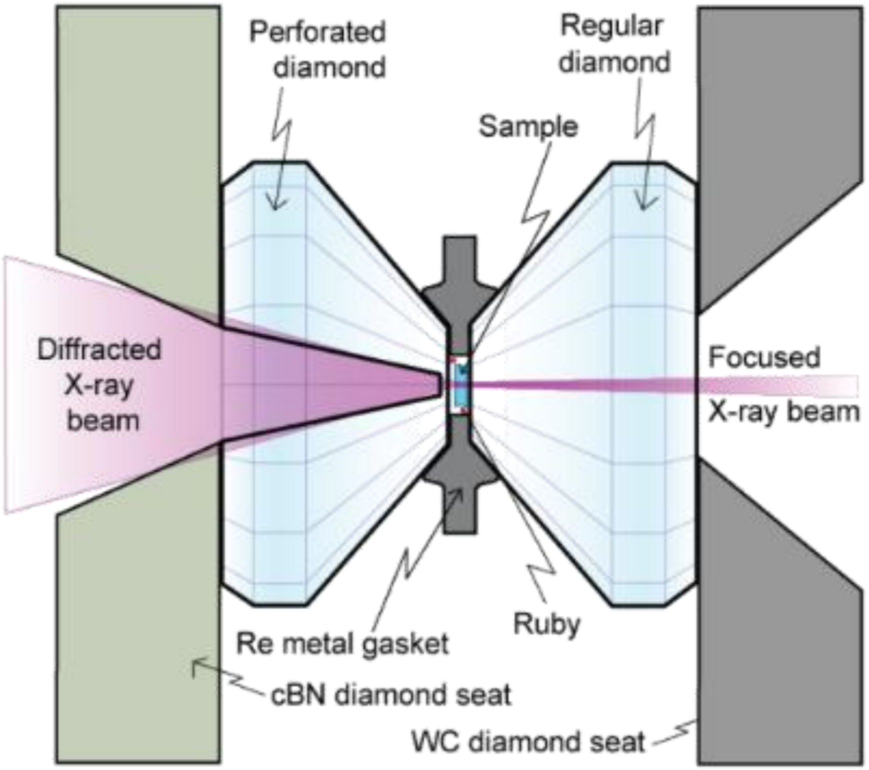

Earth's core is structured in a solid inner core, mainly composed of iron, and a liquid outer core.

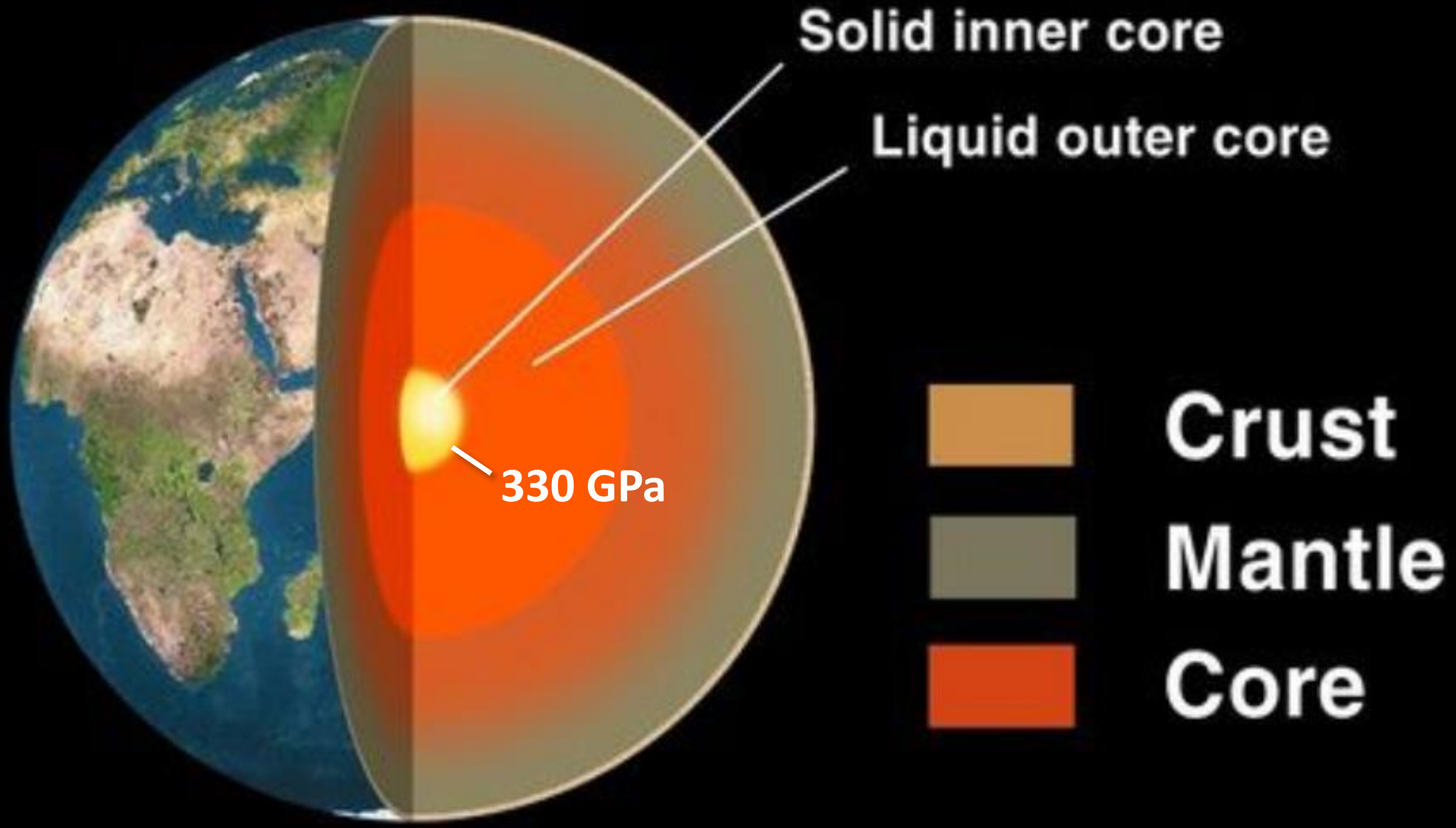

How does iron behave at these extreme temperatures and pressures?

Anzellini, Science 340, 464, 2013

Melting of Iron at Earth's Inner core Boundary based on Fast X-ray Diffraction

Static laser-heated diamond anvil cell experiments up to 200 GPa

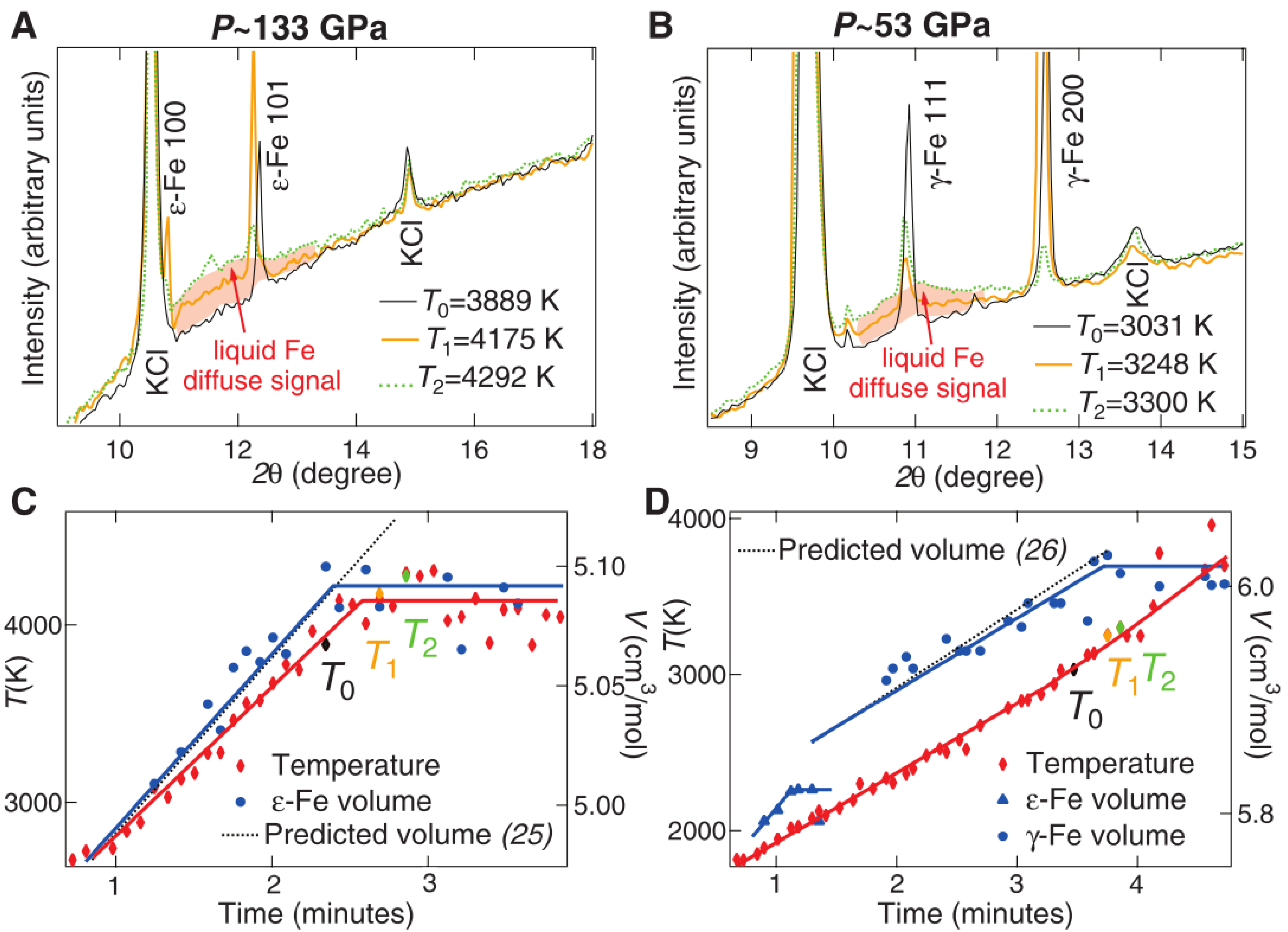

4000 K = 3727 °Celsius

1 GPa = 9869 atm

Science **340**, 464, 2013. Anzellini et al.

Melting of Iron at Earth's Inner core Boundary based on Fast X-ray Diffraction

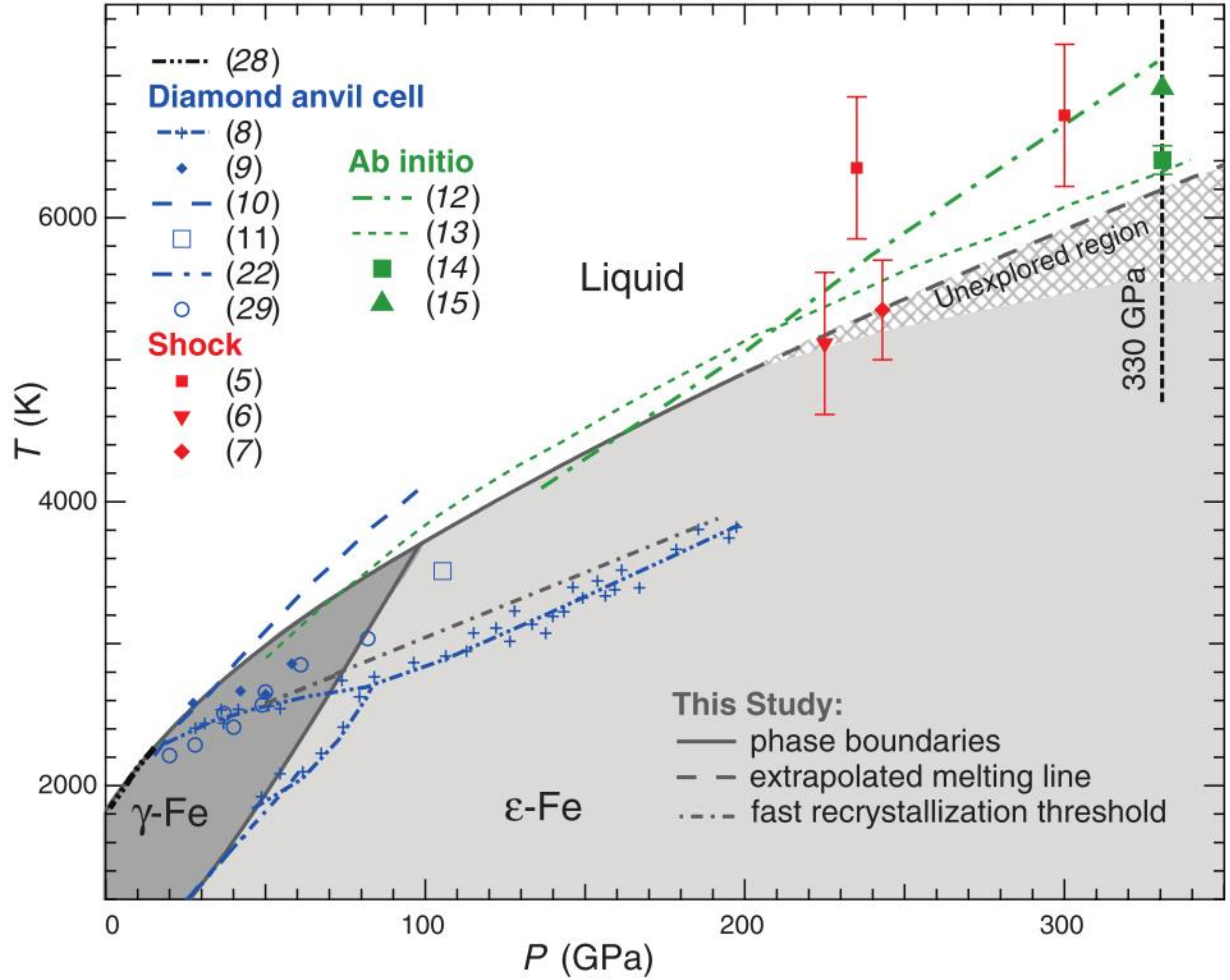

Fig. 3. Phase stability domains for Fe obtained in the literature and in this study. The stability field for ε-Fe is based on the current study data and data from (*19*).

Science **340**, 464, 2013. Anzellini et al.

Earth's core is structured in a solid inner core, mainly composed of iron, and a liquid outer core.

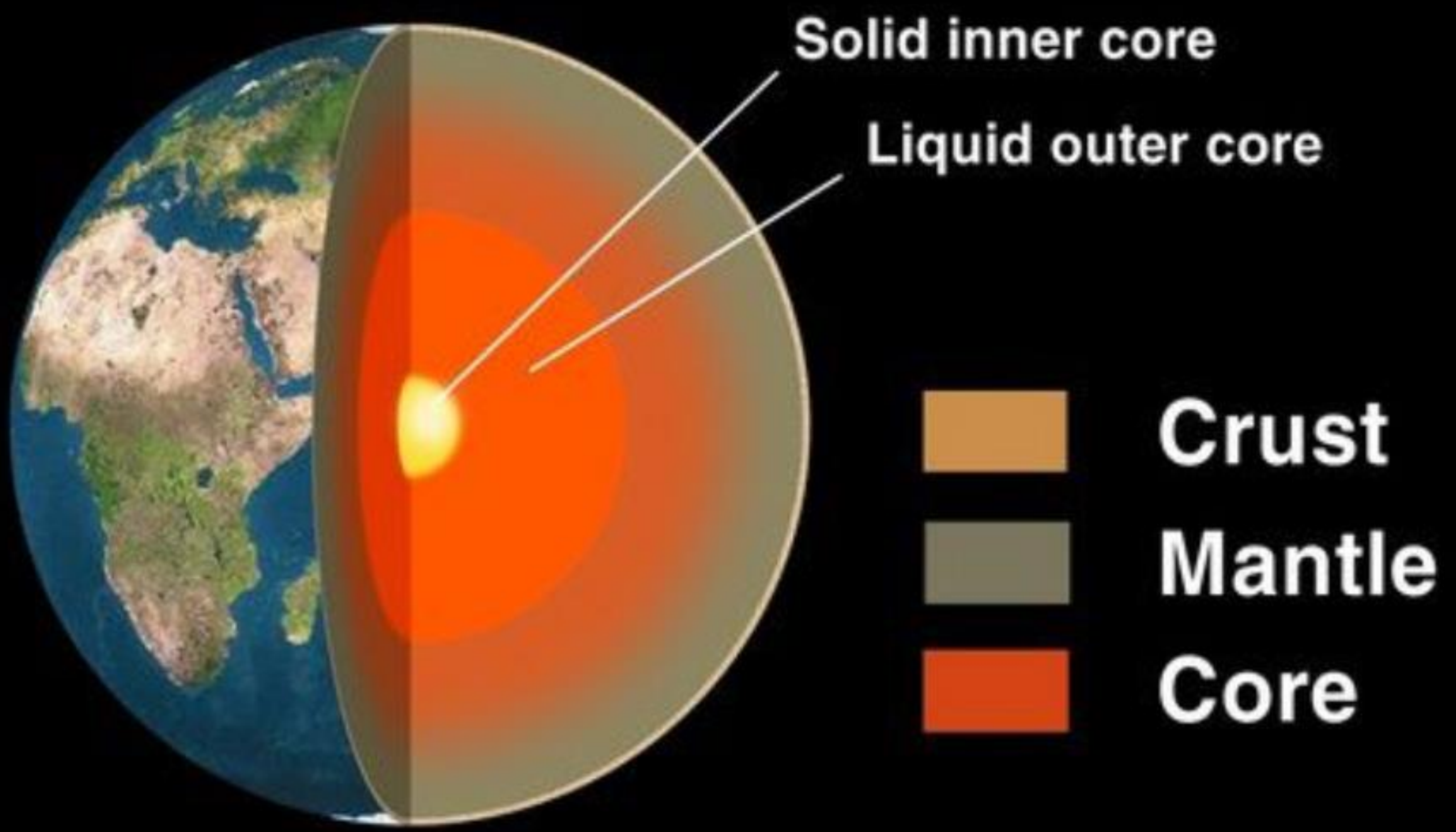

we conclude that the melting temperature of iron at the inner core boundary is 6230 ± 500 kelvin. This estimation favors a high heat flux at the core-mantle boundary with a possible partial melting of the mantle.

1811 K
at 1 bar

Anzellini, Science 340, 464, 2013

Externally controlled pressure and temperature microreactor for *in situ* x-ray diffraction, visual and spectroscopic reaction investigations under supercritical and subcritical conditions

Micro-reactor for pressure and temperature control

- In-Situ XRD and XAS experiments
- From ambient to up to 400 ^{o}C and 310 bar (external control)

✓ Structural studies

✓ in situ reaction processes

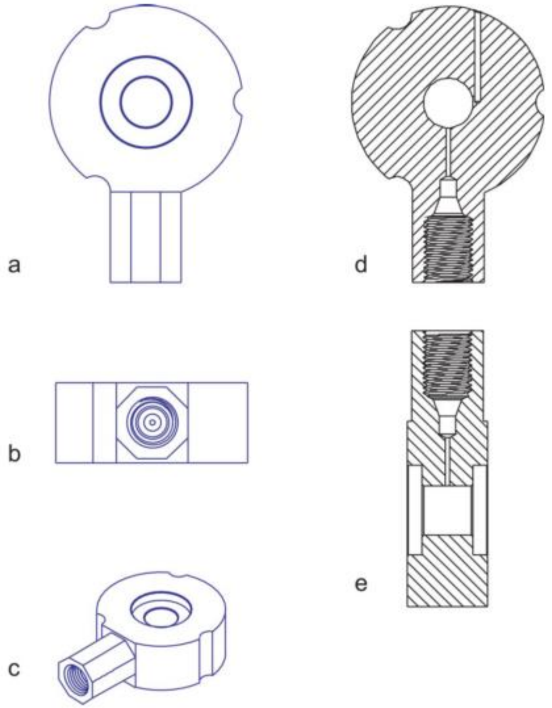

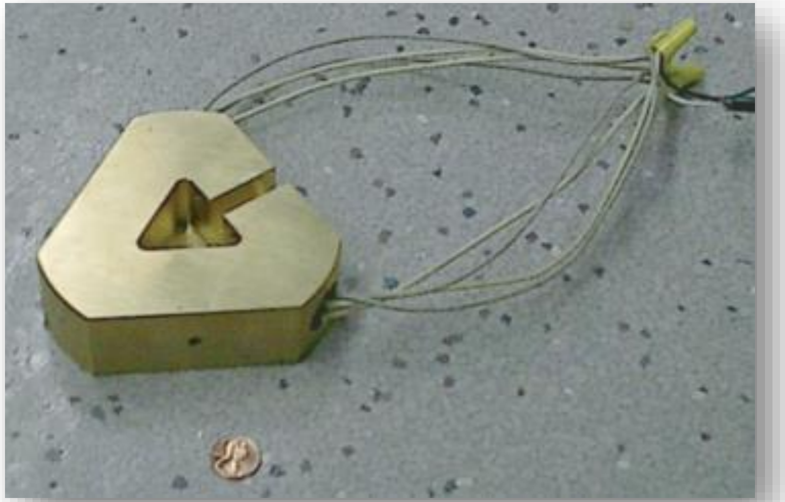

Jason Diefenbacher, Rev. Sci. Instrum. **76**, 015103 (2005)

beatriz.moreno@lightsource.ca

Externally controlled pressure and temperature microreactor for *in situ* x-ray diffraction, visual and spectroscopic reaction investigations under supercritical and subcritical conditions

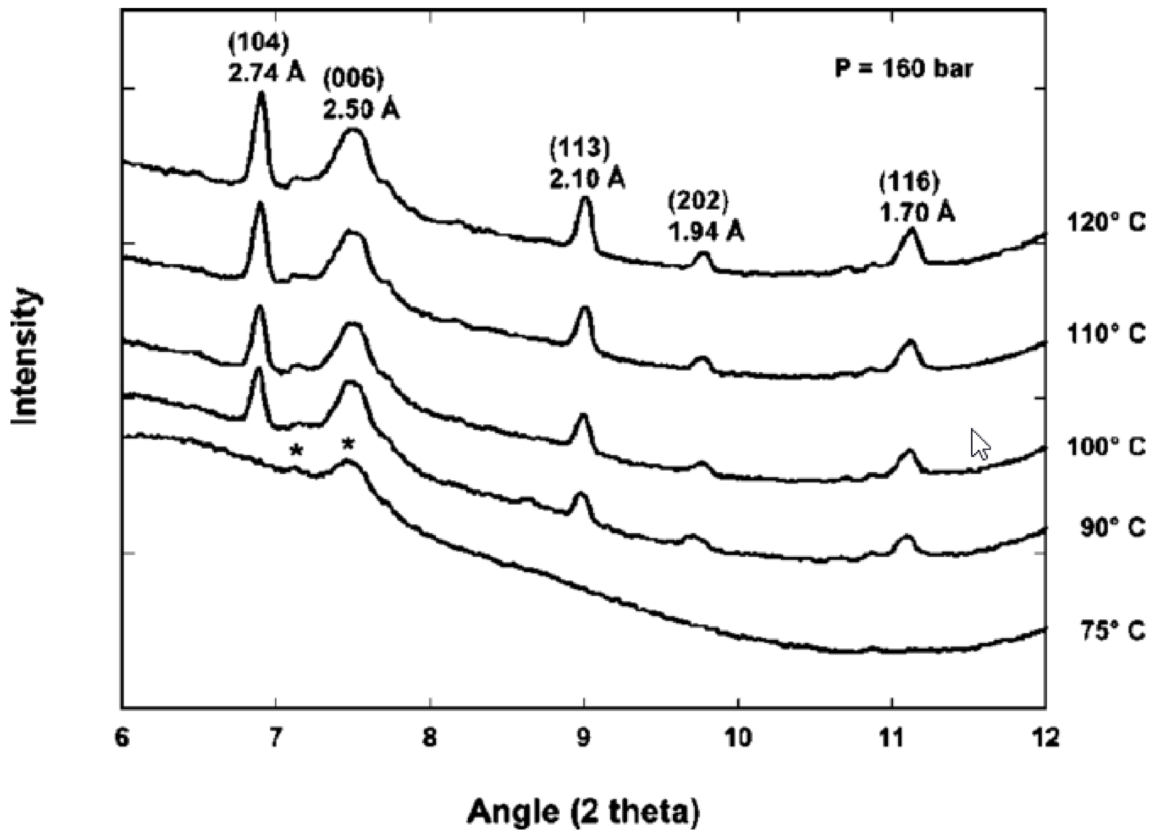

Conversion of a meta-serpentine to magnesite under high pressure and temperature:

$$Mg_3Si_2O_{6.32}(OH)_{1.36} + 3CO_2 \\ -> 3MgCO_3 + 2SiO_2 + 0.68H_2O$$

Carbonation of serpentine:

- 100,000 years for nature
- 1h with this high P/T setup

Jason Diefenbacher, Rev. Sci. Instrum. **76**, 015103 (2005)

Conclusions

- In-situ experiments allow to study the materials and components under working conditions
- They yield very important information about the processes, facilitating the improvement of the materials and devices
- Many options exist both for in-house diffractometers and synchrotrons
- Synchrotrons are very flexible and well suited for in-situ experiments.

beatriz.moreno@lightsource.ca

brockhouse.lightsource.ca

Brockhouse Diffraction Sector Beamlines

Home | Beamlines | User Guide | Contact Us | CPDW13

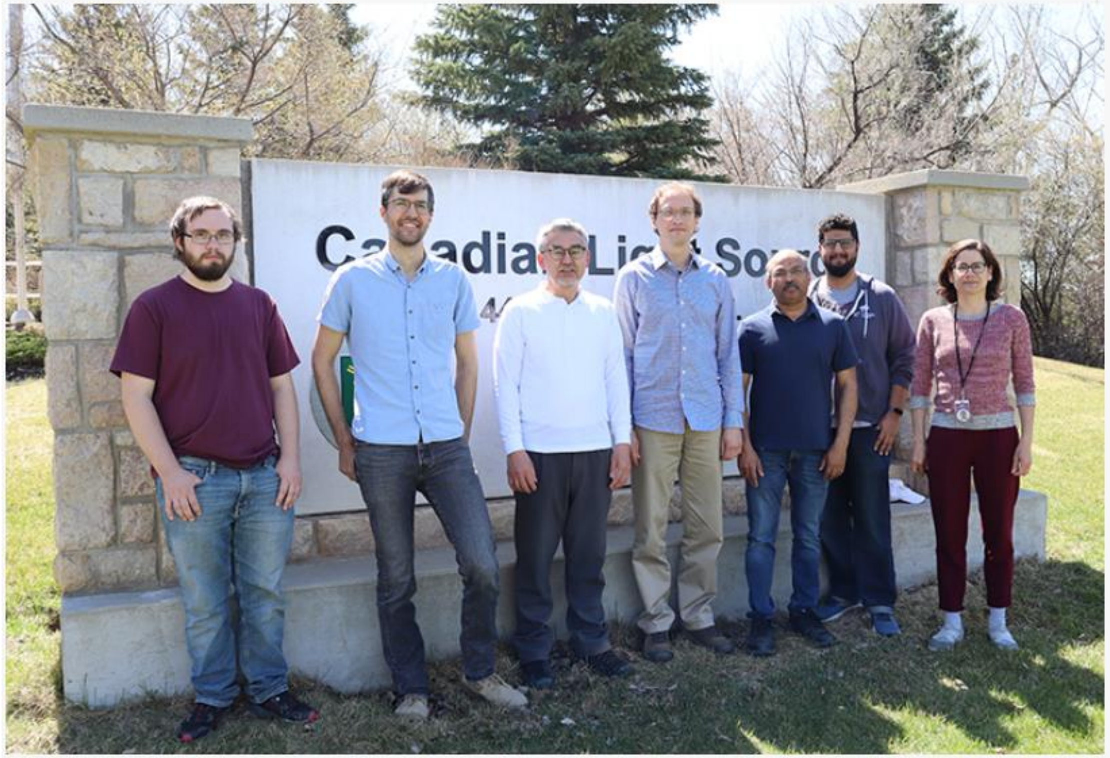

Welcome to the Brockhouse homepage. We provide a wide range of complementary diffraction and scattering techniques to fully characterize your materials.

- High resolution powder diffraction
- Pair distribution function (PDF)
- High energy diffraction for in-situ studies
- Reciprocal space mapping
- Small/wide angle X-ray scattering (SAXS/WAXS)
- High pressure crystallography
- X-ray reflectivity
- Grazing incidence diffraction (GID)
- Anomalous diffraction and magnetic diffraction

All 3 beamlines are now part of the general user program!

beatriz.moreno@lightsource.ca

Acknowledgments

beatriz.moreno@lightsource.ca